

5-2020

**ESTABLISHMENT OF ORGANOIDS FROM GASTRIC STEM CELLS
AND THEIR USE TO STUDY THE ROLE OF ARYL-HYDROCARBON
RECEPTORS**

Shakila Afroz Taleb

Follow this and additional works at: https://scholarworks.uaeu.ac.ae/all_dissertations

 Part of the [Medicine and Health Sciences Commons](#)

United Arab Emirates University

College of Medicine and Health Sciences

ESTABLISHMENT OF ORGANOIDS FROM GASTRIC STEM
CELLS AND THEIR USE TO STUDY THE ROLE OF
ARYL-HYDROCARBON RECEPTORS

Shakila Afroz Taleb

This dissertation is submitted in partial fulfilment of the requirements for the degree
of Doctor of Philosophy

Under the Supervision of Professor Sherif Karam

May 2020

Declaration of Original Work

I, Shakila Afroz Taleb, the undersigned, a graduate student at the United Arab Emirates University (UAEU), and the author of this dissertation entitled “*Establishment of Organoids from Gastric Stem Cells and their Use to Study the Role of Aryl-Hydrocarbon Receptors*”, hereby, solemnly declare that this dissertation is my own original research work that has been done and prepared by me under the supervision of Professor Sherif Karam, in the College of Medicine and Health Sciences at UAEU. This work has not previously been presented or published, or formed the basis for the award of any academic degree, diploma or a similar title at this or any other university. Any materials borrowed from other sources (whether published or unpublished) and relied upon or included in my dissertation have been properly cited and acknowledged in accordance with appropriate academic conventions. I further declare that there is no potential conflict of interest with respect to the research, data collection, authorship, presentation and/or publication of this dissertation.

Student's Signature: _____



Date: 3rd May, 2020

Copyright © 2020 Shakila Afroz Taleb
All Rights Reserved

Advisory Committee

1) Advisor (Committee Chair): Sherif M. Karam

Title: Professor

Department of Anatomy

College of Medicine and Health Sciences

2) Co-advisor: Asma Al-Menhali

Title: Associate Professor and Vice Dean

Department of Biology

College of Science

3) Member: Ernest Adeghate

Title: Professor and Chair

Department of Anatomy

College of Medicine and Health Sciences

Approval of the Doctorate Dissertation


This Doctorate Dissertation is approved by the following Examining Committee Members:

- 1) Advisor (Committee Chair): Sherif M. Karam

Title: Professor

Department of Anatomy

College of Medicine and Health Sciences

Signature 

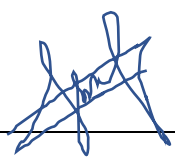
Date May 14, 2020

- 2) Member: Asma Al-Menhali

Title: Associate Professor and Vice Dean

Department of Biology

College of Science

Signature 

Date 18 May 2020

- 3) Member: Ernest Adeghate

Title: Professor and Chair

Department of Anatomy

College of Medicine and Health Sciences

Signature 

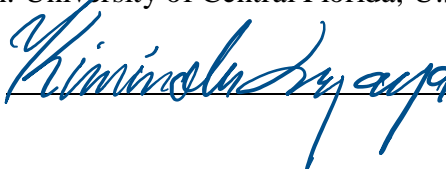
Date 14 May 2020

- 4) Member (External Examiner): Kiminobu Sugaya

Title: Professor of Medicine and Head of Neuroscience

Burnett School of Biomedical Sciences, College of Medicine

Institution: University of Central Florida, U.S.A.

Signature 

Date 5-14-2020

This Doctorate Dissertation is accepted by:

Dean of the College of Medicine and Health Sciences: Professor Juma Alkaabi

Signature _____



Date 19 August 2020

Dean of the College of Graduate Studies: Professor Ali Al-Marzouqi

Signature _____



Date 19/08/2020

Copy ____ of ____

Abstract

Stem cells are powerful tools in different aspects of biomedical and translational research, including disease modeling, drug testing, and tissue engineering for regenerative medicine. However, isolation and culture of organ-specific stem cells are challenging tasks. Therefore, the biological features of many adult stem cells are not well studied and their involvement in the development of cancer is still controversial. Some immortal stem cell lines have been established and used as an alternative to study features of organ-specific stem cells. The ability to grow cells in a scaffold-free, three-dimensional (3D) model system that mimics *in vivo* conditions would help in revealing more and more properties of stem cells.

In this study, two types of 3D culture models were established to define specific properties of gastric stem cells. In the first model, the hanging drop method was used to grow an immortalized mouse gastric epithelial progenitor/stem (mGS) cells with molecular and morphological features similar to those of stomach stem cells. Within a day, mGS cells hanging in RPMI media containing 10% serum without adding any growth factors formed a small cluster. By day 2, when transferred onto the surface of agarose using same media, each cell cluster developed into a small spherical organoid with a central lumen, characterized by electron microscopy. Due to cell proliferation, these organoids progressively grew in size and were maintained for six months. The second type of organoids was developed from incipient gastric glands freshly isolated from neonatal mouse stomach using the matrigel method. Organoids were developed within a day and were maintained for up to 10 days. The stem cell contribution and cellular dynamics during formation of these organoids were investigated using bromodeoxyuridine labeling. Organoids were further characterized at different time points by using calcein-propidium iodide labeling, electron microscopy, lectin histochemistry, immunohistochemistry and quantitative reverse-transcription polymerase chain reactions. Evidences of differentiation into gastric mucus-producing epithelial cells were detected.

To use the gastric organoids as a model for investigating the role of aryl-hydrocarbon receptors (AhR), one of the important factors involved in stem cell control as well as in the pathogenesis of cancer. Their expression levels were first

tested using immunohistochemistry. Data revealed the localization of AhR in mGS cells and cells forming the gastric primary organoids. These findings correlated with the cellular expression of AhR in gastric mucosa of mice, rats and humans. Immunolabeled cells were located in the middle of gastric glands where dividing stem cells are located. To test the consequences of AhR activation, two-day-old organoids were incubated with 0.1 and 1.0 nM of dioxin for two days. Upregulation of cytochrome P450 indicated activation of AhR. This was associated with upregulation of Oct-4 expression which suggested enhancement of self-renewal of gastric stem cells. Similar findings were observed in human gastric precancerous and cancer tissues.

In conclusion, gastric organoids are useful models to study regulation of gastric stem cells. Activation of AhR plays an important role in gastric stem cell self-renewal via Oct-4 upregulation. This could also explain a role for AhR in gastric cancer development. This study provides new insights into gastric stem cells which help in better understanding of their roles in tissue engineering and gastric cancer.

Keywords: Stem cells, Cell proliferation, Cell differentiation, Stomach, 3D culture, Organoids, Aryl-hydrocarbon receptors.

Title and Abstract (in Arabic)

إنشاء عضيات من الخلايا الجذعية المعدية واستخدامها لدراسة دور مستقبلات أريل الهيدروكربونية

الملخص

تعتبر الخلايا الجذعية أدوات قوية في جوانب مختلفة من البحوث الطبية الحيوية والتطبيقية، بما في ذلك نمذجة المرض، واختبار الأدوية، وهندسة الأنسجة للطب التجديدي. ومع ذلك، فإن فصل وزراعة الخلايا الجذعية الخاصة بالأعضاء هي مهمة صعبة. لذلك، لم يتم دراسة السمات البيولوجية للعديد من الخلايا الجذعية البالغة بشكل جيد ولا يزال دورها في تطور السرطان مثير للجدل. تم إنشاء بعض خطوط الخلايا الجذعية الخالدة في معملنا وتم أيضاً استخدامها كبديل لدراسة صفات الخلايا الجذعية الخاصة بالأعضاء. إن القدرة على نمو الخلايا في نظام نموذج ثلاثي الأبعاد 3D الذي يشابه ظروف الجسم الحي من شأنها أن تساعد في الكشف عن المزيد والمزيد من خصائص الخلايا الجذعية.

في هذه الدراسة، تم إنشاء نوعين من نماذج ثلاثية الأبعاد لدراسة خصائص الخلايا الجذعية المعدية. في النموذج الأول، تم استخدام طريقة القطرة المعلقة لنمو الخلايا الجذعية المخدلة المشابهة لتلك الموجودة في الخلايا الجذعية في معدة الفئران. في غضون يوم، شكلت الخلايا كتلة مستديرة صغيرة في وجود RPMI التي تحتوي على 10٪ من مصل الدم دون إضافة أي عوامل نمو أخرى. بعد نقلها إلى سطح مادة الأجاروز، تطورت كل كتلة من الخلايا إلى شكل كروي ينمو يوماً بعد يوم بسبب تكاثر الخلايا ويمكن الحفاظ عليها لعدة أشهر و تم فحص هذه العضيات بالمجهر الإلكتروني. أما النوع الثاني من العضيات فقد تم إنشاؤها من غدد المعدة الأولية المفصولة من معدة الفأر حديثاً الولادة باستخدام مادة الماتريجل. تم تكوين العضيات في غضون يوم واحد وإستمر نموها لمدة تصل إلى 10 أيام. تم تحديد مساهمة الخلايا الجذعية و ديناميكياتها أثناء تكوين هذه العضيات باستخدام طرق معملية عديدة، و تم الكشف عن أدلة لتمايز هذه الخلايا لتصبح منتجة لمخاط المعدة.

لاستخدام نموذج عضيات المعدة لدراسة دور مستقبلات أريل الهيدروكربونية (AhR)، وهي أحد العوامل الهامة التي تسيطر على الخلايا الجذعية وكذلك تشارك في التسبب في سرطان المعدة تم اختبار مستويات التعبير عنها أولاً باستخدام الكيمياء المناعية على الأنسجة. كشفت النتائج أن بعض خلايا أعضاء المعدة تحتوي على AhR، و تم تأكيد هذه النتائج أيضاً

بواسطة qRT-PCR في أنسجة المعدة لدى الفئران والجرذان والإنسان. توجد هذه الخلايا التي تحتوي على AhR في منتصف الغدد المعدية حيث توجد الخلايا الجذعية وأظهرت التعبير السيتوبلازمي والنووي. لتنشيط AhR، تمت معالجة عضيات بعمر يومين مع 0.1 و 1.0 نانومولر من الديوكسين لمدة يومين. كشفت النتائج عن زيادة تنظيم السيتوكروم P450 الذي يؤكد نجاح تنشيط AhR. كان هناك أيضًا زيادة في Oct-4 الذي يعزز التجديد الذاتي للخلايا الجذعية المعدية. تم دعم وتطبيق هذه النتائج من خلال دراسة كل من AhR و Oct-4 في أنسجة السرطان في المعدة.

في الختام، هذه الدراسة ساعدت على إنشاء عضيات المعدة وتم استخدامها لدراسة الصفات البيولوجية للخلايا الجذعية في المعدة و للتعرف على دور AhR في التجديد الذاتي للخلايا الجذعية وبالتالي يمكن استخدامها في المستقبل في هندسة و زراعة أنسجة المعدة و يمكن تطبيقها على أبحاث لهدف تشخيصي و/أو علاجي لمرضى سرطان المعدة.

مفاهيم البحث الرئيسية: الخلايا الجذعية، تكاثر الخلايا، تمايز الخلايا، المعدة، زراعة الخلايا ثلاثية الأبعاد، مستقبلات أريل الهيدروكربونية.

Acknowledgements

Firstly, I would like to thank ALLAH, the Almighty ("indeed we belong to Allah, and indeed to Him we shall return"), for blessing me with good health, knowledge, strength and this opportunity to get into PhD degree and completing it successfully. Alhamdulillah.

I am grateful to UAE and the UAE University for accepting me and giving me this golden opportunity to be a PhD student, providing the fellowships and also for the funding that supported my project. Heartfelt appreciation to College of Medicine and Health Sciences and Department of Anatomy, for all lab facilities and services I used throughout my PhD. Thanks to all the faculty members and special heartfelt appreciation to Dr. Rami Beiram for his time and kind support whenever I needed for any matters.

I would like to express my sincere gratitude to my supervisor Prof. Sherif Karam for all his continuous support, guidance, patience and motivations. Throughout my PhD journey, in my supervisor, I found an inspiring teacher, a caring father and an idol to follow to become a beautiful human being. I am really proud and honored to be his student.

I would like to thank my thesis committee members, Dr. Asma Al-Menhali, and Dr. Ernest Adeghate, for their time, valuable suggestions and encouragement.

I thank my fellow lab mates, Subi Sugathan, Neethu Vins, Reem Shouk, Prashanth Saseedharan for all the support, suggestions and motivations either at work or in personal matters throughout. I extend my gratitude to the animal house staffs, especially Dr. Mohammed Ali and Mr. Shafi for all the support provided for my

research. Also, special thanks to Dr. Saeed Tariq for his patience and support while using the confocal microscope.

Then, my love and prayers to all my dear friends, specially Mehwish Iqbal, Shama Parween, Asma Hassani, Mariam Naeem, Tasmin Nazim, Vidyanath Chaudhary for cherishing the good times and standing beside at tough times along this journey. Special prayers and love to my princess Hoorain Fathima, for being the most needed happiness especially during the struggling phases.

Finally, I would like to extend my deepest acknowledgement to my beloved family, my parents (abbu, ammu), my brother, sisters and my nephew (Zain Hussain Shah) for all their love, care, and support, without them it would not have been possible.

Dedication

To my beloved parents, brother and my second baba

Table of Contents

Title	i
Declaration of Original Work	ii
Copyright	iii
Advisory Committee	iv
Approval of the Doctorate Dissertation	v
Abstract	vii
Title and Abstract (in Arabic)	ix
Acknowledgements	xi
Dedication	xiii
Table of Contents	xiv
List of Tables.....	xvi
List of Figures	xvii
List of Abbreviations.....	xix
Chapter 1: Introduction	1
1.1 Overview	1
1.2 Statement of the problem	1
1.3 Relevant literature	2
1.3.1 Anatomy and histology of the stomach.....	2
1.3.2 Regulation of gastric stem cell proliferation and differentiation	14
1.3.3 AhR	17
1.3.4 Gastric cancer	23
1.3.5 Mouse gastric stem cell line.....	24
1.3.6 Two-dimensional (2D) cell culture VS Three-dimensional (3D) cell culture.....	27
1.3.7 3D Organoids	28
1.4 Aims of this study	36
Chapter 2: Methods	37
2.1 Development of 3D organoids from mGS cells.....	37
2.1.1 Mouse gastric stem cell culture	37
2.1.2 Formation of organoids by hanging drop method followed by force-floating technique.....	37
2.2 Development of 3D organoids from neonatal mouse gastric glands	40
2.2.1 Animals	40
2.2.2 Isolation of neonatal mouse stomach glands.....	40
2.2.3 Development of gastric organoids from gastric glands.....	41

2.2.4 Bromodeoxyuridine (BrdU) labelling of organoids	41
2.2.5 Histological characterization of the organoids	43
2.2.6 Reverse Transcription Quantitative Polymerase Chain Reaction (RT qPCR).....	46
2.3 Testing effects of dioxin-treated AhR activation in 3D primary organoids	49
2.4 Testing effects of dioxin-treated AhR activation <i>in vivo</i>	50
2.4.1 Dioxin treatment on mice	50
2.4.2 Tissue processing for light microscopy.....	50
2.4.3 Immuno-staining on stomach tissues	51
2.4.4 Lectin histochemistry	51
2.4.5 Quantitative analysis of labelling intensity	52
2.4.6 Statistical Analysis	53
Chapter 3: Results	54
3.1 Generation of mGS cell-derived organoids	54
3.2 Generation of organoids from neonatal mouse gastric glands.....	59
3.2.1 Tracking BrdU-labelled proliferating cells in the organoids	60
3.2.2 Cellular characterization of primary organoids.....	61
3.3 Use of organoid models to study role of AhR activation on stem cells	68
3.3.1 AhR expression in mGS cells.....	68
3.3.2 AhR expression in neonatal mouse stomach.....	68
3.3.3 AhR expression in gastric organoids.....	71
3.3.4 Effects of dioxin treatment on primary gastric organoids.....	71
3.3.5 Effects of dioxin treatment on gene expression patterns of primary gastric organoids	75
3.4 Effects of dioxin treatment on gastric mucosa.....	78
3.4.1 Characterization of AhR expression in stomach tissues	80
3.4.2 Effects of dioxin activated AhR <i>in vivo</i>	80
Chapter 4: Discussion	88
4.1 Gastric organoids from mGS cells	88
4.2 Gastric organoids from neonatal mouse gastric glands.....	90
4.3 Effects of AhR activation on gastric stem cells and gastric cancer <i>in vivo</i> and <i>in vitro</i>	92
4.3.1 Effects of AhR activation on gastric organoids	94
4.3.2 Role of AhR activation <i>in vivo</i>	97
Chapter 5: Conclusion.....	99
Chapter 6: Future Prospective.....	101
References	103

List of Tables

Table 1: Gastric stem cell markers and their corresponding references	11
Table 2: Gastric epithelial cell types	13
Table 3: List of primers used for RT-qPCR.....	49

List of Figures

Figure 1: Anatomy of the stomach and structural features of oxyntic and pyloric glands	7
Figure 2: Gastric stem cell differentiation.	16
Figure 3: AhR signaling pathway.	19
Figure 4: Mouse gastric stem cell line	26
Figure 5: Illustration of 2D and 3D cell culture	28
Figure 6: Hanging drop technique followed by force-floating method.	39
Figure 7: Generation of organoids from neonatal gastric glands	42
Figure 8: Processing of organoids using histogel for microscopic analysis	44
Figure 9: Phase contrast images of mGS cells forming organoids by hanging drop	55
Figure 10: Phase contrast images of mGS cell-derived organoids on non-adherent surface.	56
Figure 11: Phase contrast and confocal images of live and dead cells present in mGS cell-derived organoids.....	58
Figure 12: Electron microscopic images of a 4 weeks old organoid derived from mGS cells	59
Figure 13: Phase contrast images of organoids from neonatal gastric glands	63
Figure 14: Tracking BrdU labelled cells in the organoids	64
Figure 15: PAS staining and lectin histochemistry images of gastric organoids	65
Figure 16: Immunohistochemical and lectin histochemical analysis of gastric organoids	66
Figure 17: RT-qPCR analysis of gastric epithelial cell lineage specific genes at different stages of gastric organoid development (days 2, 4 and 10)	67
Figure 18: AhR expression in mGS cells.....	69
Figure 19: AhR expression in neonatal gastric glands.....	70
Figure 20: Comparison between cellular localization of BrdU and AhR expressions in two adjacent tissue sections obtained from neonatal stomach.....	70
Figure 21: AhR expression in gastric organoids	71
Figure 22: Phase contrast images of dioxin-treated gastric organoids at different treatment days.....	72
Figure 23: Celcein/PI staining images of dioxin-treated organoids.....	73
Figure 24: Lectin histochemical images of dioxin-treated organoids.....	74
Figure 25: HK-ATPase staining images of dioxin-treated organoids.....	76
Figure 26: Effects of dioxin-activated AhR on mRNA expressions of gastric cell specific markers and gastric stem cell markers	79
Figure 27: AhR expression in adult mouse stomach.....	82

Figure 28: Immuno-labelling images of BrdU and AhR expression in rat stomach.	83
Figure 29: Dioxin-treated AhR activation in mouse liver.....	84
Figure 30: Dioxin-treated AhR activation in mouse stomach.....	84
Figure 31: Effects of dioxin treatment on mucous cells.	86
Figure 32: Effects of dioxin treatment on parietal cells.....	87
Figure 33: AhR expression in human tissues (normal, gastritis and tumor).....	94
Figure 34: Illustration of overall findings on role of AhR on gastric organoids	100

List of Abbreviations

AhR	Aryl-Hydrocarbon Receptor
ARNT	Aryl Hydrocarbon Receptor Nuclear Translocator
BMP	Bone Morphogenetic Protein
BrdU	Bromodeoxyuridine
DAB	3,3'-Diaminobenzine
DAPI	4', 6-Diamidino-2-Phenylindole
DMEM/F-12	Dulbecco's Modified Essential Medium and Ham's F-12
ESCs	Embryonic Stem Cells
EGF	Epidermal Growth Factor
FBS	Fetal Bovine Serum
GSC	Gastric Stem Cells
GSII	<i>Griffonia Simplicifolia</i> II
<i>H. pylori</i>	<i>Helicobacter pylori</i>
HSCs	Hematopoietic Stem Cells
H,K-ATPase	Hydrogen Potassium ATPase
Ihh	Indian Hedgehog
Lgr5	Leucine-rich repeat-containing G-protein Coupled Receptor
Lrig1	Leucine Rich Repeats and Immunoglobulin Like Domain 1
mGS cells	Mouse Gastric Stem Cells
Oct-4	Octamer-Binding Transcription Factor 4
PAS	Periodic Acid–Schiff
PBS	Phosphate Buffer Saline

PSCs	Pluripotent Stem Cells
RT-qPCR	Quantitative Reverse Transcription Polymerase Chain Reaction
RPMI	Roswell Park Memorial Institute Medium
RUNX1	Runt-related Transcription Factor 1
Sox2	(Sex determining region Y)-box 2
TCDD	2,3,7,8-Tetrachlorodibenzo-p-Dioxin
3D	Three Dimensional
TFF	Trefoil Factor
TEM	Transmission Electron Microscopy
2D	Two Dimentional
UEA-1	<i>Ulex Europaeus</i> Agglutinin I
V-GSCs	Villin promoter-marked Gastric Stem Cells
WGA	Wheat Germ Agglutinin

Chapter 1: Introduction

1.1 Overview

Stem cells are undifferentiated cells with unique capacity to self-renew and differentiate into specialized cell types in the body. There are two main types of stem cell, embryonic stem cells and adult stem cells. Embryonic stem cells are known as pluripotent stem cells as they can give rise to any type of somatic cells in the body. Adult stem cells are found in adult tissues and usually used to repair and replace any damaged cells in the tissues. Stem cell research is one of the most fascinating areas in biomedical field because of their potential to proliferate and regenerate to produce different adult cell types. Current therapies, such as regenerative medicine, are already making use of the regenerative property stem cells. Apart from regenerating or repairing, stem cells are also believed to be involved in cancer development. However, this hypothesis is still under debate due to difficulties in stem cell research. One of the major difficulties is isolating and culturing the cells *in vitro*. Therefore, it is always preferable to use other representative models such as immortal cell lines or 3D-cell cultures which will help better understand the functional characteristic features of the stem cells.

1.2 Statement of the problem

Gastric cancer is the second most fatal cancer worldwide (Ang & Fock, 2014). Though many genetic and environmental factors are associated with the gastric cancer, the detailed mechanism of its development is still unclear. Some studies suggested that the adult epithelial cells are the ones that are transdifferentiated back to its proliferative state to become cancer stem cells and develop gastric cancer (Han & Oh, 2013). However, recent studies suggested that adult stem cells transform into cancer stem

cells and proliferate to develop cancer (Vaidya, Bacchus, & Sugaya, 2018; Zhu et al., 2009). Stem cells in the stomach may also cause cancer due to chronic inflammation resulting in genetic and epigenetic alterations in the stem cell niche (Hayakawa, Fox, & Wang, 2017). However, due to lack of sufficient understanding of molecular control of gastric stem cells, their involvement in gastric cancer is still remaining controversial. Some of the stem cell regulatory proteins may also have major effects on the gastric cancer progression. Therefore, mimicking *in vivo* conditions in the 3D organoid models might help to dissect the functional features of stem cells and their mechanistic role during cancer progression. These 3D models are better than the usual 2D culture where cells lose their physiological characteristics and do not mimic the *in vivo* condition.

1.3 Relevant literature

Stomach, a muscular organ which is located on the left side of the upper abdomen and receives food from the esophagus through lower esophageal sphincter. It secretes acid and enzymes used to digest food. The stomach muscles contract occasionally, churning food to improve digestion. The pyloric sphincter is a muscular valve that opens to allow the food from the stomach to move towards the small intestine.

1.3.1 Anatomy and histology of the stomach

The stomach is the main food processing organ of the digestive tract, which secretes a mixture of acid, mucus, and enzymes required for digestion. It is also the source of various hormones that control cell functions. It is a hollow, J-shaped organ located in the upper abdomen connecting the esophagus with the intestine. Anatomically, the stomach includes four regions: cardia, fundus, corpus and the

pyloric region. The stomach wall is made up of four layers. The outermost is the visceral peritoneal layer or the serosa, which is followed by the muscularis layer made of smooth muscle fibers, the submucosal connective tissue layer, and the innermost mucosal layer.

The gastric mucosa in humans and mice is very similar and divided into 4 parts fundus, cardia, corpus and pylorus. While in humans, the cardia is continuous with the esophagus, in mice, the fundus is continuous with the esophagus and the cardia forms a thin small area between the forestomach and the corpus. The gastric mucosa includes the lining cells that are organized in a monolayer of simple columnar epithelium with deep invaginations forming millions of tubular glands (Figure 1) (Bjerknes & Cheng, 2002; Karam & Leblond, 1993). The corpus glands are divided into four parts: pit, isthmus, neck, and base. The types of cells present in the glands in the corpus region are pepsinogen-secreting zymogenic cells, mucus-secreting cells which helps to protect the lining epithelium, acid secreting parietal cells which in human also produce intrinsic factor, hormone-secreting endocrine cells, and mucous neck cells. The percentage of these cells estimated in tissue sections were represented as 35%, 19%, 13%, 7%, and 6%, respectively (Karam & Leblond, 1992). The glands in the cardiac and pyloric regions are smaller than those of the corpus and composed mostly of two types of mucous cells and endocrine cells.

1.3.1.1 Gastric stem cells

Unlike the differentiated body cells, stem cells are undifferentiated with the ability to proliferate to self-renew and to differentiate in specialized cell types. Basically, there are two major kinds of stem cells: embryonic stem cells that can give rise to any cell types; adult stem cells which are normally present in body tissues, helps

organs in replacing damaged and dead cells due to some injury or usual cell renewal process.

All the gastric epithelial cells mentioned above originate from the gastric stem cells which divide to maintain themselves and replace the old degenerating cells. These stem cells are present in the isthmus region of the gastric gland and were detected in mice using ³H-thymidine radiography and electron microscopy techniques. ³H-thymidine radiography was used to label and detect the dividing cells and electron microscopy was used to characterize the ultrastructural features of the undifferentiated cells (Karam & Leblond, 1993). While the stem cells differentiate, they migrate in two directions: 1) toward the luminal surface to become surface mucous cells, and 2) towards the bottom of the gland to become mucous neck cells and then zymogenic cells. Both endocrine and parietal cells-complete their differentiation in the isthmus region and then migrate not only toward the gland bottom, but also a few migrate toward the luminal surface. This epithelial turnover is necessary to maintain healthy epithelial glands and to replace the dead or damaged cells due to harsh acidic environment in the stomach. The gastric stem cells are also called granule-free cells. They are the most proliferating cells and give rise to pre-parietal cells, pre-pit cells, pre-neck cells, pre-endocrine cells and pre-tuft cells. The granule-free cells can be found anywhere in the isthmus region, while pre-pit cells are located near the isthmus-pit edge and pre-neck cells at the isthmus-neck edge. The gastric stem cells are undifferentiated cells with no secretory granules, but there are few small granules in pre-pit and pre-neck cells (progenitor cells). Electron microscopic studies of these stem/progenitor cells have demonstrated that they have larger nucleoli (2.0-2.5 μm^2) with higher nucleus to cytoplasm ratio and smaller mitochondrial diameter (300-375 nm) than the mature cells. Moreover, the stem cells are of three subtypes, two of these

subtypes contain few small prosecretory granules near to the trans-face of the Golgi apparatus. This is an indication to the secretory activity of the Golgi apparatus to form secretory granules. In pre-pit and pre-neck cells, the content in the prosecretory vesicles are similar to the pit and neck cells respectively but with difference in the stages of condensation of secretory granules. The stem cells are characterized by the presence of immature Golgi, no prosecretory vesicles, therefore they are not involved in any secretion process (Karam & Leblond, 1993). Moreover, these cells also have characteristic features similar to primitive undifferentiated embryonic cells that are: 1) large nucleus containing reticulated nucleoli with diffuse chromatin and 2) the cytoplasm contains many free ribosomes along with very few numbers of small mitochondria and rough endoplasmic reticulum (Mizuno & Ishizuya, 1982). These undifferentiated and highly proliferative stem cells further differentiate and mature towards parietal cells, pit cells, neck cells, endocrine cells and tuft cells in the gland (Karam, 1993; Karam & Leblond, 1993) (Figure 2).

In addition, lineage tracing experiments done to study gastric stem cell dynamics helped in identification of other stem cells other than the stem cells present in the isthmus region. These experiments were also helpful to find various molecular markers expressed in those progenitor cells. The first proliferating cell marker identified was villin, an actin-binding protein, expressed in specific type of epithelial cells, rarely found in the pyloric region. It was discovered from transgenic mice that express Villin promoter-driven LacZ or GFP reporter. These long-lived cells known as Villin promoter-marked gastric stem cells (V-GSCs) are inactive in proliferation and have the capability to differentiate to multiple cell types (Braunstein et al., 2002; Qiao et al., 2007)

Another highly-proliferative progenitor cell type was identified by Hans Clevers lab, that expresses G protein-coupled receptor Lgr5 (Gpr49) found in the antral region of the stomach gland. These cells were identified using lineage-tracing experiment in mice. They also claimed that the Lgr5+ cells are located at the base of the corpus and pylorus in neonatal stomach as well (Barker et al., 2010).

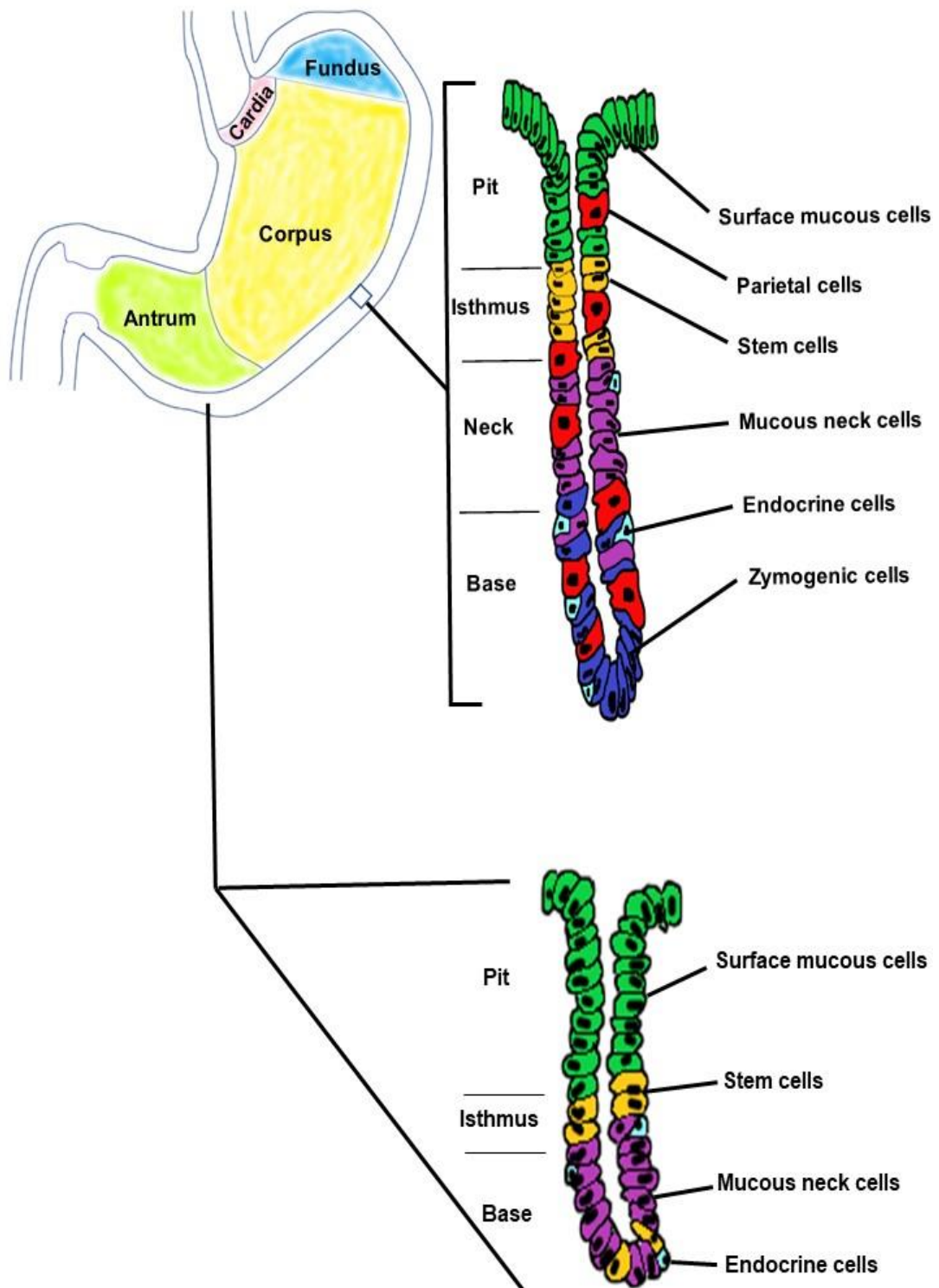


Figure 1: Anatomy of the stomach and structural features of oxyntic and pyloric glands. The stomach is made of four regions: cardia, fundus, corpus and pylorus. Oxyntic or corpus glands are divided into four parts: pit, isthmus, neck and base and populated by pit cells, parietal cells, stem cells, mucous cells, endocrine cells and zymogenic cells. The glands in pylorus contain pit cells, mucous cells, endocrine cells and stem cells.

Moreover, using Troy-CreERT mice, a subpopulation of zymogenic cells expressing Troy (member of tumor necrosis factor receptor family) was identified, located at the base of the corpus also have the ability to differentiate towards all the mature cell types in the corpus gland (Stange et al., 2013). These cells were found to be activated to differentiate during tissue injury caused by cytotoxic drugs (Hashimoto, Schlessinger, & Cui, 2008).

SRY (sex determining region Y)-box 2, also known as Sox2 is highly expressed in foregut region during the stomach development process. Sox2 is a member of the Sox family of transcription factors and it is essential for maintaining self-renewal and pluripotency of undifferentiated embryonic stem cells. It has also a crucial role in maintenance of neural stem cells (Rizzino, 2009). Using genetic lineage tracing and transplantation experiments in mice, some Sox2+ cells were also identified as proliferating cells, located in both the corpus and antral region of the stomach glands. These cells were capable to mature into all the cell types in the gland and necessary for the tissue renewal (Arnold et al., 2011; Que et al., 2007).

Many previous studies have attempted to find specific markers for gastric stem cells. A group of scientists discovered expression of Runt-related transcription factor 1 (RUNX1) in the stem cells in isthmus region of both corpus and pylorus using in-situ hybridization and immunohistochemistry techniques. 86% of proliferating cells in the isthmus region were found to be RUNX1-positive (Matsuo et al., 2017). RUNX1 is a protein encoded by RUNX1 gene. It belongs to the Runt-related transcription factor family of genes which also named as core binding factor- α (Avramopoulos, Cox, Blaschak, Chakravarti, & Antonarakis, 1992). RUNX1 is a key regulatory

transcription factor of hematopoiesis and involved in the generation and maintenance of hematopoietic stem cells (Chen, Yokomizo, Zeigler, Dzierzak, & Speck, 2009).

Another marker known as Lrig1 (Leucine Rich Repeats and Immunoglobulin Like Domains 1), was detected using a Lrig1 knock-in mouse model in the non-proliferating cells in the basal layer of the forestomach and the lower part of glands of both corpus and pylorus. In humans, it is encoded by the LRIG1 gene (Nilsson et al., 2001). Lrig1 was firstly identified as a marker of stem cells in the epidermis. Later some studies showed that Lrig1 also marked inactive stem cells in intestinal and colonic epithelium and were found to be highly proliferative and contribute actively to the maintenance of the tissues (Jensen & Watt, 2006; Powell et al., 2012). In the stomach, though Lrig1+ cells were found to be non-proliferating, fate-mapping experiments using a Rosa26-*loxP*-STOP-*loxP*-tdTomato mouse model suggested that these cells contributed to the long-term maintenance of the gastric epithelium. (Schweiger et al., 2018).

Moreover, one recent study suggested that stem cells self-renewal transcription factor, octamer-binding transcription factor 4 (Oct-4) was found to be expressed in the proliferative zone of the pylorus in normal human stomach (Al-Marzoqee et al., 2012). Oct-4 was first discovered as an ESC-specific and germline-specific transcription factor in mice. In humans, Oct-4 is the product of the POU5F1 gene (Okamoto et al., 1990; Rosner et al., 1990; Schöler et al., 1990). Oct-4 belongs to the POU (Pit-Oct-Unc) family of proteins and it is a crucial factor involved in the self-renewal of undifferentiated embryonic stem cells (Boyer et al., 2005). Further studies revealed that it is also expressed in adult stem cells (adult human breast, pancreas, liver, kidney, mesenchymal and gastric stem cells) (Tai et al., 2005). Using immunoperoxidase and

immunofluorescence staining on human gastric tissues, it was shown that Oct-4 was expressed in the dividing mucus-producing pre-pit and differentiating pit cells located in the isthmus region of the pit-gland units. This evidence suggested that Oct-4 was essential for the self-renewal of pre-pit cells and also involved in maintenance of cell division in differentiating pit cells which progressively decreases with migration. This was concluded based on decreasing gradient of Oct-4 expression towards the luminal surface (Al-Marzoqee et al., 2012).

Adding to the above-mentioned markers, cluster-of-differentiation (CD44) was also identified as a gastric stem cell marker. CD44 is a cell-surface glycoprotein that is involved in many biological processes including cell adhesion, cell–cell interactions and migration (Spring et al., 1988). Some studies also characterized its expression in the normal antral epithelium (Takaishi et al., 2009) and at the squamous-corporis junction of the mouse stomach (Ishimoto et al., 2010). Using immunohistochemical analysis, previous studies revealed that CD44 was expressed throughout the scant inter-glandular mesenchymal cells as well as epithelial cells within the isthmus and also in the pit region of the glands. CD44⁺ epithelial cells in isthmus, were found to be small in size and undifferentiated as they did not co-stain with markers specific for differentiated cells (pit-specific lectin *anguilla* agglutinin and neck mucous cell specific lectin GSII). In addition, the stem cell proliferation was found to be decreased in CD44 knockout mice, which also showed defect in the number of pit cells, due to fast turnover of the cells leading to a shortage in the gland. These altogether suggested a crucial role of CD44 signaling in normal gastric stem cell homeostasis (Khurana et al., 2013). Different gastric stem cell markers and their corresponding references are provided in Table 1.

Table 1: Gastric stem cell markers and their corresponding references

Gastric stem cell markers	References
Villin	(Braunstein et al., 2002; Qiao et al., 2007)
Lgr5	(Barker et al., 2010)
Troy	(Stange et al., 2013)
Sox2	(Arnold et al., 2011; Que et al., 2007)
RUNX1	(Matsuo et al., 2017)
Lrig1	(Schweiger et al., 2018)
Oct-4	(Al-Marzoqee et al., 2012)
CD44	(Khurana et al., 2013)

1.3.1.2 Gastric cell lineages

Different types of cells present in the gastric epithelium are described below.

- *Parietal cells*

Parietal cells are acid-secreting cells and are developed from pre-parietal cells in the isthmus region. Pre-parietal cells are generally characterized by long numerous microvilli, tubulovesicles with hydrogen potassium ATPase (H,K-ATPase), increased number of large mitochondria and few immature canaliculi. These pre-parietal cells undergo maturation by developing increasing number of tubulovesicles, mitochondria and gradually developing canaliculi to give rise to parietal cells within 2 to 3 days. Parietal cells usually migrate towards both upward and downward from the isthmus and distributed throughout the corpus glands, and the turnover time for these cells is approximately 54 days (Karam, 1993).

- *Pit cells or surface mucous cells*

Stem cells in the isthmus divide and differentiate towards pre-pit cells. These pre-pit cells then further migrate up towards the lumen and become pit cells. This migration takes around 60 hrs. Pit cells are characterized by increased sized of secretory granules near the Golgi apparatus, approximately double the size of the ones present in the pre-pit cells (Karam & Leblond, 1993). The turn-over time for the pit cells is around 3 days. Trefoil factor 1 (TFF1), a small trefoil protein co-expressed with the gastric mucin Muc5AC in the surface mucous cells and secreted into gastric mucus (Hanby et al., 1993; Lefebvre et al., 1993).

- *Mucous neck cells*

Some stem cells differentiate to pre-neck cells and migrate downwards from the isthmus to become mucous neck cells. Matured neck cells are characterized by larger (approximately 700 nm) and higher number of mucous granules, compared to pre-neck cells. These granules are located throughout the cytoplasm of the cells. The turn-over time for these cells is 1 to 2 weeks (Karam & Leblond, 1993; Sato & Spicer, 1980). TFF2, another member of the trefoil factor family, holding two TFF domains, is expressed along with the mucin MUC6 in the mucous neck cells (Hanby et al., 1993; Jørgensen, Diamant, Jørgensen, & Thim, 1982; Lefebvre et al., 1993)

- *Zymogenic cells*

Zymogenic cells are well known for pepsinogen secretion. They develop by trans-differentiation of mucous neck cells when they migrate down towards the base of the glands. The secretory granules of the mucous neck cells become larger in size (approximately 1070 nm) and more pepsinogenic during the maturation towards the zymogenic cells. Zymogenic cells also accumulate large amount of rough endoplasmic

reticulum and enlarged nucleolus. The estimated turn-over time for the zymogenic cells is 194 days (Karam & Leblond, 1993).

- *Endocrine cells*

Endocrine cells are hormone-releasing cells. Many different types of endocrine cells are present in the stomach glands including histamine-releasing enterochromaffin-like cells, gastrin-secreting G cells, somatostatin-secreting D cells and glucagon-secreting A cells and ghrelin-secreting cells. These cells scattered throughout the gland. Endocrine cells are derived from pre-endocrine cells, differentiated from the stem cells in isthmus (Karam & Leblond, 1992). One of the commonly used marker specific for endocrine cells is chromogranin A (Deftos, 1991). Details of gastric epithelial cells are presented in Table 2.

Table 2: Gastric epithelial cell types

Gastric epithelial cell types	Location	Turnover time	Specific markers
Parietal cells	Scattered all throughout corpus glands	Approximately 54 days	H,K-ATPase
Pit cells	Pit region	3 days	Muc5AC, TFF1
Mucous neck cells	Neck region	1-2 weeks	MUC6, TFF2
Zymogenic cells	Base	194 days	Pepsinogen
Endocrine cells	Scattered all throughout corpus glands	45-60 days	Chromogranin A

1.3.2 Regulation of gastric stem cell proliferation and differentiation

The gastric epithelium undergoes constant renewal process in order to maintain long-term tissue function. Different mechanisms and factors contribute to this renewal by regulating the gastric stem cells located in the isthmus, which actively undergo continuous proliferation and differentiation towards other matured gastric epithelial cells. Some of the important signaling pathways that are involved in the gastric stem cell renewal and differentiation are notch signaling, Wnt3 signaling, hedgehog signaling, epidermal growth factor (EGF) signaling and bone morphogenetic protein (BMP) signaling. Several important factors related to these signaling pathways were found to be expressed in the gastric epithelium and regulate the proliferation and differentiation of gastric stem cells. Surface mucous cells, located at the pit region, are generated from pre-pit cells, arise from gastric stem cells. This process is regulated by Indian hedgehog (Ihh) and EGF (Fukaya et al., 2006; Nomura et al., 2005). The generation and differentiation of zymogenic cells are regulated by the basic helix-loop-helix transcription factor Mist1 (Ramsey et al., 2007; Tian et al., 2010). Generation of parietal cells from pre-parietal cells derived from gastric stem cells is regulated by sonic hedgehog (Shh), gastrin, and BMP (Shinohara et al., 2010; Stepan et al., 2005; Wang et al., 1996).

Some previous studies have shown that the parietal cells play important role in the gastric stem cells proliferation and differentiation. Unlike other matured cells, parietal cells are differentiated and matured in the isthmus region without any migration. Inhibition of parietal cell differentiation and its secretion altered the stem cell proliferation and differentiation leading to increased number of progenitor cells (Helander, 1995; Karam, 1993; Karam & Alexander, 2001; Li, Karam, & Gordon,

1995, 1996). By using laser capture microdissection, it was possible to identify some genes expressed in parietal cells including growth hormone binding protein, vascular endothelial growth factor-B, parathyroid hormone-like peptide, insulin-like growth factor binding protein-2 and CD-36 are potential factors involved in the regulation of the stem cells (Mills et al., 2001).

There are some other factors effecting stem cell regulation such as gastrin, TFF1 and vitamin A. Previous studies have shown that gastrin, a hormone released by G cells, is involved in the development of stomach mucosa. Deficiency of this hormone leads to alteration in the stem cell proliferation and causes gastric adenocarcinoma in mice (Johnson, 1988; Zavros et al., 2005). TFF1, secreted by surface mucous cells, also affects the stem cell fate. In TFF1 knockout mice, some of the pre-parietal cells that were committed to differentiate to parietal cells, were driven towards the pit cell differentiation (Karam, Tomasetto, & Rio, 2004).

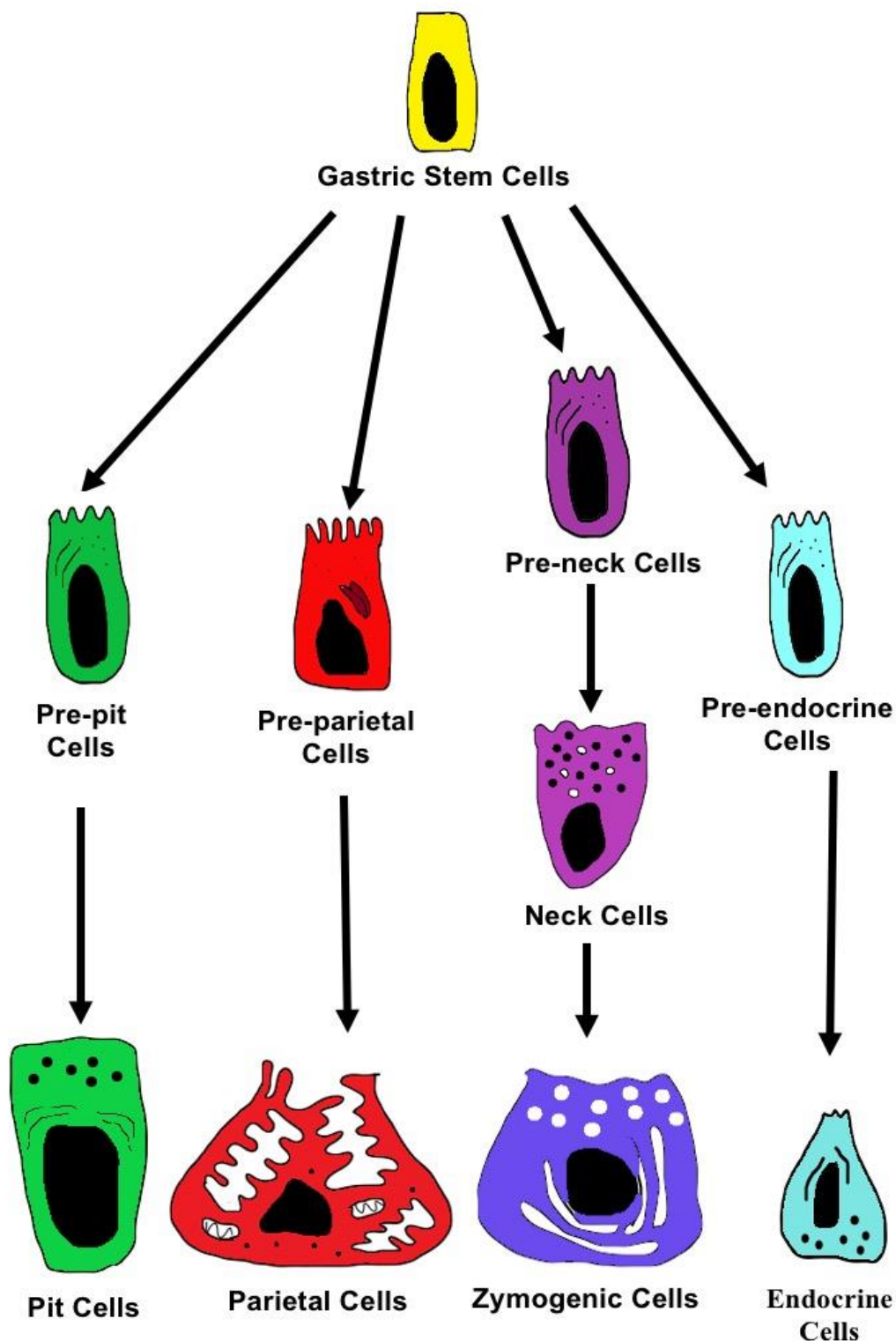


Figure 2: Gastric stem cell differentiation. Stem cells are first converted to progenitor cells which are pre-pits, pre-parietal cells, pre-neck cells and pre-endocrine cells. Then these cells will be converted to pit cells, parietal cells, neck cells, and endocrine cells respectively. Neck cells are further converted to zymogenic cells moving downwards towards the base of the gland.

Another important factor was found to have effects on the stem cell dynamics is retinoic acid (Vitamin A). This was due to the identification of the retinoic acid receptor in the gastric progenitor cells of mice, rabbits and human (Karam, Hassan, & John, 2005). In addition, retinol increases parietal cell differentiation in developing rabbits (Karam, Ansari, Al-Dhaheeri, & Alexander, 2004). Some studies also showed that retinoic acid administration increased number of S-phase progenitor cells and enhanced differentiation towards zymogenic cells (Karam et al., 2005).

Apart from the factors mentioned above, recently scientists are gaining interest to study effects of aryl-hydrocarbon receptor (AhR), a transcription factor expressed in almost all types of tissues. AhR is commonly known for its xenobiotic response. AhR was also found to be regulating stem cells in intestine (Metidji et al., 2018). Since most the of the stem cell regulatory control factors of intestine and stomach are interlinked through their development pathways, there might be a possibility that AhR may have a crucial role in the gastric stem cell regulation.

1.3.3 AhR

AhR is a ligand-activated transcription factor, first discovered by Poland et al. (1976) in mouse liver. AhR belongs to the superfamily of basic helix-loop-helix/Per-ARNT-Sim (Nebert, 2017), the only ligand-dependent receptor in the group. The structure of the AhR contains three domains: one DNA binding Per-Arnt-Sim domain, one N-terminal basic helix-loop-helix domain for ligand binding and C-terminal variable domain (Murray, Patterson, & Perdew, 2014; Stockinger, Di Meglio, Gialitakis, & Duarte, 2014). It binds to several ligands based on its functions and expressed in almost all types of tissues including liver, pancreas, lungs, spleen, and placenta. Moderate expression of Ahr is also found in the brain, skeletal muscles and heart (Jiang, Wang,

Fang, & Zheng, 2010; Spence et al., 2011). Many physiological AhR ligands such as raw or cooked dietary components derived from fruits and cruciferous vegetables (e.g. flavones, isoflavones, flavanones, carotenoids, glucobrassicin) and tryptophan metabolites (e.g. kynurenine, kynurenic acid, cinnabarinic acid, xanthurenic acid) contribute to the functions of AhR *in vivo* (Murray & Perdew, 2017). Numerous environmental toxicants including polycyclic and halogenated aromatic hydrocarbons also act as ligands that bind to AhR and facilitate transcription of target genes. Dioxin (2,3,7,8 -tetrachlorodibenzo-p-dioxin (TCDD)) having the higher affinity for AhR is involved in most of the AhR-mediated response (Denison & Nagy, 2003). Therefore, dioxin was chosen in this study as a ligand for AhR activation experiments.

1.3.3.1 AhR activation pathway

Inactive AhR, bound with a protein complex made of heat shock protein 90 (Hsp90), AhR-activated 9 (ARA9) and prostaglandin E synthase 3 (p23), usually resides in the cytoplasm of the cell. Upon binding to dioxin or other ligands, AhR is translocated to the nucleus and binds to aryl-hydrocarbon nuclear translocator (ARNT) to form a heterodimer protein. This heterodimer complex (AhR/ARNT) further interacts with dioxin response elements (DRE) and regulates transcription of target genes such as cytochromes P450s, p21^{Cip1} and interleukin 6 (Murray et al., 2014) (Figure 3).

1.3.3.2 AhR in stem cell regulation

Upon ligand-bound activation, AhR is involved in many biological processes including apoptosis, cell cycle regulation (Puga, Xia, & Elferink, 2002), response to xenobiotic stimulus and toxic substances (Ema et al., 1994), regulation of immune response (Quintana & Sherr, 2013) and cell proliferation (Allan & Sherr, 2005).

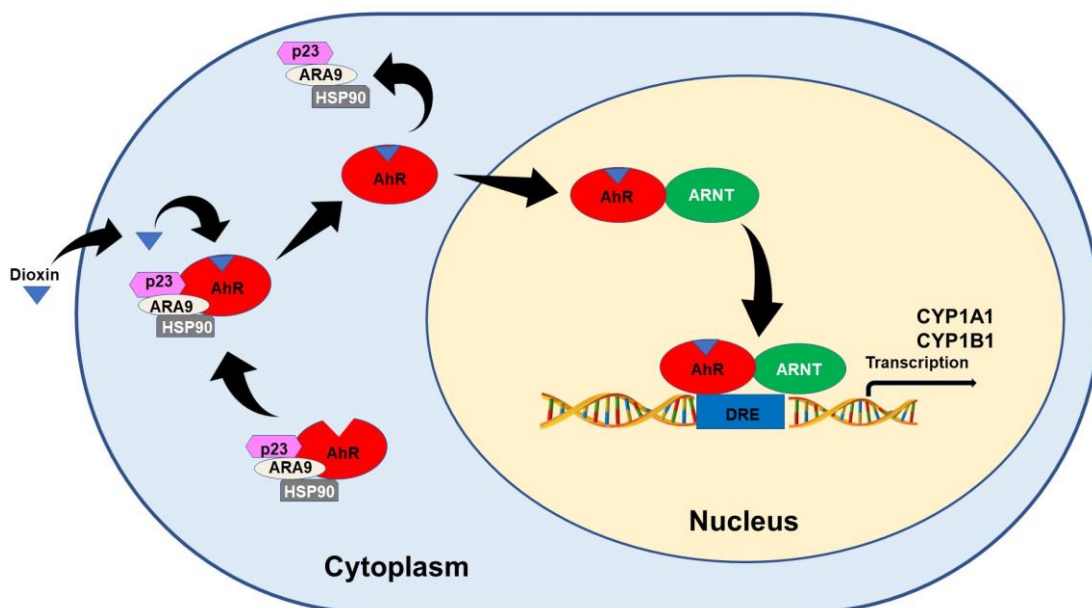


Figure 3: AhR signaling pathway. AhR bound to a protein complex (Hsp90/ARA9/p23) in the cytoplasm of the cell, binds to dioxin and translocated to the nucleus. The ligand-bound AhR further binds to aryl-hydrocarbon nuclear translocator (ARNT) to form a heterodimer protein. This heterodimer complex then interacts with dioxin response elements (DRE) and regulates transcription of target genes, most commonly cytochrome P450s (CYP1A1, CYP1B1).

Some studies showed that AhR was also involved in maintenance of stem cell homeostasis. First evidence of that was shown by studies on regulation of hematopoietic stem cells (HSC). Different studies on effects of AhR activation on HSC regulation were conducted: 1) use of xenobiotic AhR ligands, 2) phenotypic analysis of knockout AhR mice, 3) studying the presence and regulation of the AhR within HSCs, 4) examining genes regulated by the AhR pathway in conjunction with HSC regulatory factors and 5) investigations of hematopoietic disorders. All the above studies suggested that the AhR expression was essential for the proper maintenance of quiescence in HSCs and AhR down-regulation was vital for “escape” from quiescence state and subsequent proliferation of HSCs. Therefore, AhR act as a negative regulator

of hematopoiesis restricting excessive or unnecessary proliferation of these cells, preventing the premature exhaustion of HSCs and sensitivity to genetic alterations. Moreover, AhR dysregulation altered the ability of HSCs to sense proper signals in the bone marrow microenvironment leading to hematopoietic disease (Singh, Casado, Opanashuk, & Gasiewicz, 2009).

Previous reports proposed that AhR may also have possible regulatory role on skin stem cells. This was shown by testing effects of dioxin-activated AhR in skin of humans and mice. Activated AhR in skin stem cells altered differentiation and produced chloracne that led to alterations in the stimulation of stem cell into cell cycle, increased stem cell proliferation and differentiation towards the epidermal pathway instead of hair follicle and sebaceous gland cells (Arnold & Watt, 2001; Panteleyev & Bickers, 2006).

Some studies have also revealed that AhR was an important regulatory factor in neural development. These studies showed that both AHR and ARNT genes were expressed in the embryonic neuroepithelium (Abbott, Birnbaum, & Perdew, 1995; Abbott & Probst, 1995). AhR expression was also confirmed in neural stem cells isolated from developing forebrain and found to be expressed in activated form in granule neuron progenitors during neurogenesis. These data suggested that activation of AhR may altered the stability between proliferation, differentiation, and apoptosis in early postnatal period. Moreover, study using AhR-KO mice showed reduction in cell numbers in the developing and adult cerebellum along with decrease in GABA α 6 receptor expression in mature granule neurons, suggesting that AhR was important for development and/or maintenance of neuronal cell population. Together, these studies provided information in support of AhR contribution in neurogenesis

through regulation of neural stem and progenitor cells (Collins et al., 2008; Williamson, Gasiewicz, & Opanashuk, 2005).

A very recent study proposed that AhR play a significant role in intestinal homeostasis using different transgenic mouse models ($Ahr^{-/-}$ mice, $R26^{Cyp1a1}$, $Villin^{Cre}Ahr^{fl/fl}$, $Villin^{Cre}R26^{LSL-Cyp1a1}$ and $Lgr5^{Egfp-Ires-creErt2}$ mice), though the mechanism is still not known. The study found that AhR influenced the regeneration of intestinal epithelial cells upon injury by bacterial infection or chemical treatment. Deletion of AhR in intestinal epithelial cells resulted in failure to control the infection due to unlimited intestinal stem cells proliferation and reduced differentiation leading to malignant transformation. In contrast, AhR activation by dietary ligands restored altered intestinal homeostasis maintaining the stem cell niche and prevented tumorigenesis by controlling the inhibition of Wnt- β -catenin signaling and intestinal epithelial cells proliferation restriction (Metidji et al., 2018).

1.3.3.3 AhR in cancer

Recently, studies have also started focusing on the role of AhR in tumorigenesis and cancer development based on tumor mediating effects from exposure of dioxin, one of the industrial contaminants. Dioxin exposure was first reported to cause skin dermatitis (Tauchi et al., 2005), chloracne (Panteleyev & Bickers, 2006) and skin cancer (Ikuta, Namiki, Fujii-Kuriyama, & Kawajiri, 2009) through AhR activation. Moreover, AhR activation also enhanced tumorigenesis in the liver (Barouki, Coumoul, & Fernandez-Salguero, 2007) and other organs such as breast, lungs and prostate. Immunohistochemical studies showed that those tumors had significantly higher AhR expression than the normal tissues (Richmond et al., 2014; Saito et al., 2014; Su, Lin, & Chang, 2013).

Some of the previous studies have also suggested that AhR may be linked to gastrointestinal tumors. But this is still controversial whether it suppresses or enhances the tumor formation in the gut. Scientists tested various mouse models and cancer cell lines to study roles of AhR which are ligand dependent. In some colon cancer cell lines (Caco-2, LS174T, H508, MMP9 and SN7-C4), AhR increased the cell growth and helps in migration (Tompkins et al., 2010; Villard et al., 2007; Xie, Peng, & Raufman, 2012), whereas in others (LoVo, HCT116, DLD-1 and SW837), cell growth was inhibited by AhR (Ronnekleiv-Kelly et al., 2016; Yin et al., 2016). Furthermore, several studies have suggested that AhR null mice models developed increased colon tumors indicating tumor-suppressor activity of AhR (Diaz-Diaz et al., 2016). In addition, several stomach cancer cell lines were used to study the involvement of AhR in gastric cancer development in the stomach. In some cell lines (MNK5 and AGS cells), AhR promoted the growth and migration, whereas in SGC-7901 cells, it suppressed the cell growth (Kolluri, Jin & Safe, 2017). Moreover, a transgenic mouse model was developed with higher expression of constitutively active AhR, which demonstrated enhanced numbers of gastric tumors indicating towards possible oncogenic property of AhR (Andersson et al., 2002). However, it was not clear that the effects in the transgenic models were due to any genetic-error or activation of AhR pathway. These observations altogether raise questions on the role of AhR in the development of gastric cancer, whether it is involved in pathogenesis of the cancers or inhibiting it. Therefore, one of the focus of this study to investigate AhR role in stomach tissues, for which animals were injected with dioxin to activate AhR and examined to study the effects *in vivo*.

1.3.4 Gastric cancer

Gastritis is a common worldwide health problem which in severe cases give rise to gastric cancer, the second most fatal cancer around the globe (Ang & Fock, 2014). Gastric cancers are histologically categorized into two types: well-differentiated intestinal gastric cancer, which tend to occur more in aged people in the pyloric region of the stomach, and undifferentiated diffuse gastric cancer, which commonly observed in young people (Hohenberger & Gretschel, 2003). *Helicobacter pylori* (*H. pylori*) is the common causative agent for gastritis and gastric cancer (Nomura et al., 1991; Parsonnet et al., 1991).

Although adult stem cells are involved in the regeneration of the somatic cells, some studies have also shown that stem cells are the major cellular source of cancer. One of the important observations in the *H. pylori*-related gastric cancer is that it drives the migration of bone marrow stem cells to the gastric mucosa and turn them into cancer cells in the process of development of the gastric cancer (Houghton et al., 2004). Moreover, studies on transgenic mouse expressing regulatory elements of H,K-ATPase beta subunit diphtheria toxin 176 have revealed that *H. Pylori* infection also depended on the gastric progenitor cells in the stomach and *H. Pylori* can invade into the epithelial gastric progenitor cells and form colonies in the cytoplasm, further confirming the possible involvement of the stem cells in the gastric cancer development (Li et al., 1996; Karam, & Gordon, 2005; Syder et al., 1999).

Moreover, studies using transgenic mouse model for gastric cancer expressing simian virus 40 large T antigen demonstrated that inhibiting parietal cell differentiation leads to pre-parietal cell hyperplasia and also increase in the number of other gastric epithelial progenitors. Later at the age of 5-6 months, these mice developed gastric

cancer with highly invasive progenitor cells which further leads to neoplasia. This model was an indication that stem/progenitor cells contribute to cellular origin of the neuroendocrine cancer in the stomach (Karam, Li, & Gordon, 1997; Li et al., 1995; Modlin et al., 2005; Syder et al., 2004).

Some studies reported that the deletion of some transcription factors including APC and Klf drives the transformation of the Lgr5+ and villin+ progenitor cells towards cancer stem cells (Barker et al., 2010; Li et al., 2012) One of the important potential markers identified for cancer stem cells is CD44 (Tongtawee et al., 2017). However, previous study also suggested that even the adult cells are transdifferentiated back to its proliferative state and develop the stem cell properties during gastric cancer development (Guasch & Fuchs, 2005). Although, these evidences indicate possible links between the stem cells and the gastric cancer, the mechanism underlying this process is still not clear.

To understand these mechanisms better, scientists recently started focusing on the metabolic pathways and the genetic factors associated with the stem cell regulation as well as gastric cancer development. One of such important factors is the AhR. Some current studies reported that this receptor enhances formation of tumors in many organs including skin, liver, breast, and colon (Murray et al., 2014). Moreover, AhR is also known for its involvement in stem cell homeostasis (Singh et al., 2009). Further, detailed investigations on this receptor will provide insight information in understanding the mechanism of gastric cancer development.

1.3.5 Mouse gastric stem cell line

As mentioned above, studying the biological features of gastric stem cell is very crucial for understanding the mechanism of the gastric cancer development as

well as defining the factors involved in this process. However, these stem cells are relatively few and difficult to isolate, culture and maintain for biological investigations. Therefore, production of an immortalized cell line representing the cells will be useful. A cell line known as mouse gastric stem cells (mGS cells) (Figure 4) was established from a transgenic mouse expressing Simian Virus 40 large T antigen using H,K-ATPase promoter (Farook, Alkhalaf, & Karam, 2008). These cells resemble characteristic features of gastric stem cells (Karam & Leblond, 1993). These features include large nucleus-to-cytoplasm ratio, large reticulated nucleoli and diffuse chromatin, cytoplasm containing many free ribosomes and a few small elements of rough endoplasmic reticulum, mitochondria and Golgi saccules. In addition, these cells did not have the machinery for any functional characteristics similar to differentiated cells including secretion of acid, pepsinogen, mucus and hormones. Furthermore, immunohistochemical analysis revealed that mGS cells neither express any markers (H,K-ATPase, intrinsic factor, chromogranin A) specific for mature gastric cells nor bind to lectins *Griffonia simplicifolia* II (GSII) and *Ulex europaeus* agglutinin I (UEA-1) specific for mucous cells. However, these cells express stem cell markers such as Oct-4, notch3, DCLK1 similar to mouse gastric epithelial progenitor cells (Al-Marzoqee et al., 2012; Giannakis, Chen, Karam, Engstrand, & Gordon, 2008). Therefore, mGS cells can be used as alternative to mouse gastric stem cells and as a representative model to study features and roles in the formation of cancer. Moreover, these cells also have the ability to grow on 3D microfibrinous scaffolds (Pulikkot et al., 2014).

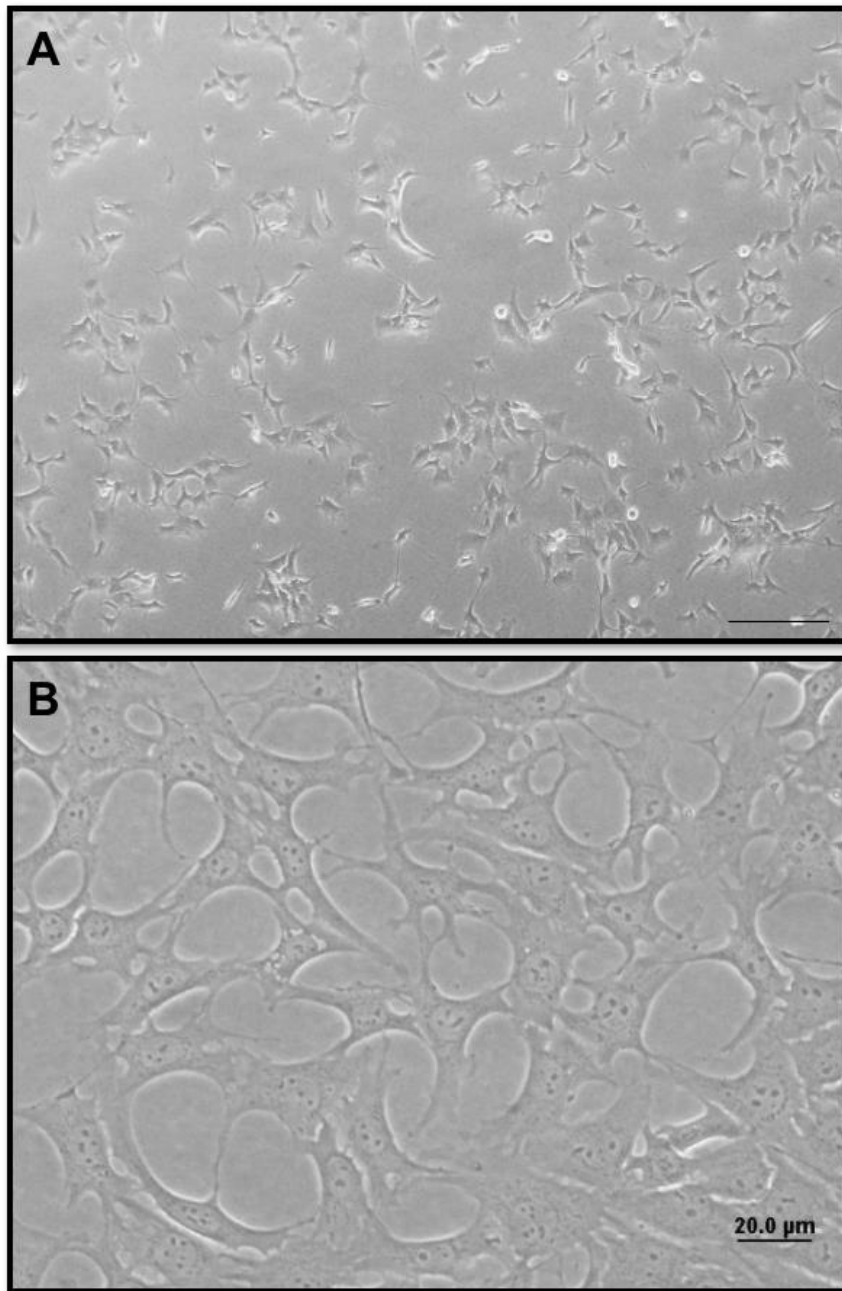


Figure 4: Mouse gastric stem cell line. A) Lower magnification phase contrast image. B) Higher magnification image. These cells consist of large nucleus with nucleoli and diffuse chromatin Bar=200 μm.

1.3.6 Two-dimensional (2D) cell culture VS Three-dimensional (3D) cell culture

2D cell culture is a commonly used *in vitro* technique in biomedical research. In this 2D system, cells are attached to a flat surface to form a monolayer of cells. However, culturing cells in 3D has been attracting researchers over the years and seemed to be closer to *in vivo* systems than 2D. These 3D culture systems have been used as biological model for testing drug activity and study several human diseases including cancer and microbial infections (Fatehullah, Tan, & Barker, 2016; Hill & Spence, 2017). Recently, 3D culture models, known as 3D spheroid/organoids, have become a major scientific progress and an important tool in biological and clinical studies (Figure 5).

Organoids are 3D structures that are generated from stem cells to mimic *in vivo* organs both structurally and functionally (Lancaster & Knoblich, 2014). In the term organoid, 'oid' came from the Latin 'oides' which means resemblance. Three types of cells that are commonly used to grow organoids are: embryonic stem cells, induced pluripotent stem cells and organ specific adult stem cells. This 3D model helps to study many *in vivo* biological processes including stem cell functions and effect of mutations (Fatehullah et al., 2016). This can also be applied for regenerative medicine studies. Different types of organoids have been developed from numerous cell types such as stomach cells, liver cells, neural cells, pancreatic cells, and intestinal cells.

1.3.7 3D Organoids

1.3.7.1 History of development of 3D organoids

Organoid cultures were evolved historically over many years. The first attempt to mimic tissues *in vivo* was done by Ross Harrison in 1906 through hanging drop method to study the origin of nerve fibers.

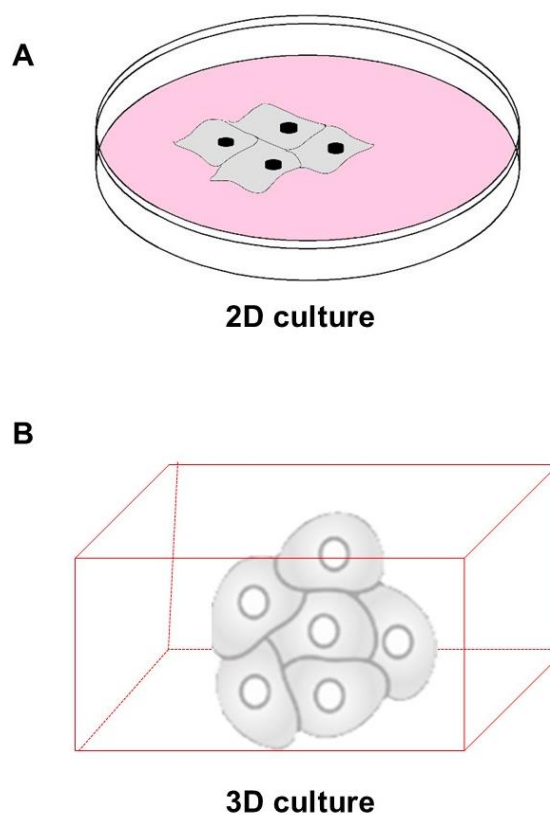


Figure 5: Illustration of 2D and 3D cell culture. A) In 2D culture, cells form a monolayer on the surface, growing and connecting to each other. B) In 3D culture, cells immersed in matrix, grow in its own dimensional way and start creating their own environment to achieve a structure mimicking the *in vivo* organs.

In this method, a piece of nerve cord from embryo was kept on a drop of lymph on coverslip and was then inverted and sealed over an excavated slide. This hanging drop

of lymph environment allowed the nerve fiber to grow (Horrison, 1906). In 1907, Wilson proved that the detached sponge cells can re-aggregate into a whole organism. Later, “tube culture method” (growing tissues in tubes) (Strangeways & Honor, 1926) was developed along with “watch glass method” (Fell & Robison, 1929) in which tissue fragment was cultured on plasma clot on concave glass surface placed in petri dish filled with wet cotton. Ehrmann and Gey in 1956 showed that cells grew and survived well on collagen (Ehrmann & Gey, 1956). Lasfargues in 1957 generated first mammary organoids using collagenase to dissociate adult mouse mammary gland tissue. Moscona in 1959 showed that cells growing in suspension form tissue like structures by clumping together (Moscona, 1959). In the meantime, Richard Swarm and group (1963) prepared a gel called Engelbreth-Holm-Swarm (EHS) sarcoma that mimicked the basement membrane which is nowadays frequently used and named as matrigel (Kleinman & Martin, 2005). Matrigel contains laminin (Timpl et al., 1979), collagen, fibronectin, and entactin. In 1988, Bissell and colleagues generated 3D ducts and ductules from breast epithelial cells on EHS sarcoma (Li et al., 1987). In 2008, Sasai and group used pluripotent stem cells to grow 3D cerebral cortex tissue by using serum-free culture of embryoid body-like aggregates method (Eiraku et al., 2008).

1.3.7.2 Methods to develop organoids

Different types of methods have been established for developing 3D organoids based on nature and architecture of cells or tissues to mimic the *in vivo* system as close as possible. Some of the common methods that we have used in this study are described below.

- *Hanging drop method*

Harrison (1906) first came up with the hanging drop method to grow nerve fibers on lymph drops (Harrison, 1906). This method was further modified by Kelm et al. (2003) to form 3D organoids through hanging a drop of cell-containing media. Kelm and group seeded cells in different densities on 60-well MicroWell MiniTray and inverted the tray to hang the drop of cell suspensions leading to gather at the bottom of the drops to form 3D structures (Kelm, Timmins, Brown, Fussenegger, & Nielsen, 2003). These drops stay at hanged position due to surface tension. This method was later done on 60-mm petri dishes. Moisture levels of the drop were maintained by filling the bottom lid with PBS. Nowadays there are 3D hanging drop plates that are commercially available such as gravity plus or 3D perfecta, for growing organoids for longer period of time, but they need to be transferred to non-adherent plates for analysis or to grow for further studies.

- *Force-floating method*

In this method, cells are forced to grow on suspension on a surface that is modified to prevent their attachment. As a result, cells aggregate to form spheres (Lin & Chang, 2008). Ivascu and Kubbies in 2006 used this method to grow organoids from both cancer and non-cancerous cells by coating the surface of 96-well plates (both round and conical) with 0.5% poly-2-hydroxymethyl methacrylate. This coating prevented the cells from attaching to the surface and helped them clump together to form 3D organoids (Ivascu & Kubbies, 2006). Although some organoids did not form compact structure, but this problem was resolved by adding 2.5% liquid reconstituted basement membrane to media. The well plates can also be coated with 1.5% agarose

to prevent cell adhesion to the surface. The non-adherent plates are now commercially available.

- *Matrigel technique*

Generally, epithelial cells communicate with nearby cells and extracellular matrices (ECM) to organize themselves into tissues. As ECMs along with basement membrane plays important role in cellular structure and function, its use in 3D culture showed better results mimicking *in vivo* conditions. Current well-known example is matrigel, which contains basement membrane proteins such as laminin, collagen IV, matrix metalloproteinase-2, perlecan, entactin, and some growth factors (Kleinman & Martin, 2005).

1.3.7.3 Types of organoids developed

So far different kinds of organoids have been derived from stem cells. Some of them are discussed below.

- *Brain organoids*

Brain organoids were grown from neural stem cell, induced pluripotent stem cells and also by using pluripotent stem cells (PSCs). Briefly, PSCs can be used to grow brain organoids with minimal media conditions. First the cells differentiate into neuroectoderm, then grown in 20% KSR media (Knockout serum replacement) give rise to neuroepithelium. These neuroepithelium are then transferred to matrigel and agitated in bioreactors for further growth and development into brain organoids (Lancaster & Knoblich, 2014). Watanabe et al. (2005) first showed that murine embryonic stem cells (mESCs) when grown on serum-free culture SFEB (serum-free, floating culture of embryoid body-like aggregates) aggregate and differentiate into

telencephalic precursors (Watanabe et al., 2005). Altering growth factors of the media may give rise to many other regions of the brains such as sub pallial patterning and adeno-hypophysis (Danjo et al., 2011; Suga et al., 2011). Scientists were also able to develop single brain organoid with multiple brain regions (Lancaster et al., 2013). During the ectoderm stage of organoid development, the differentiation can be diverted to retinal epithelium using 1.5% KSR and transferring them to 2% matrigel that will give rise to optic cup organoid (Lancaster & Knoblich, 2014).

- *Kidney organoids*

Throughout the past few years, different protocols have been tried to generate kidney organoids from embryonic stem cells, but those were not proved applicable for research purposes. Researchers later studied different growth factors including retinoic acid (RA), bone morphogenic protein (BMP), and fibroblast growth factor (FGF) that play major role in differentiation, development and repair of kidney, which were later used to establish an appropriate protocol for developing kidney organoids (Kim & Dressler, 2005). Briefly, kidney organoids were derived from PSCs in media containing various growth factors such as activin A which converts PSCs to mesendoderm. Mesendoderm was then differentiated towards kidney organoids with the addition of BMP, FGF9, and retinoic acid (Lancaster & Knoblich, 2014).

- *Liver and pancreas organoids*

Liver and pancreas organoids were generated from leucine-rich repeat-containing G-protein coupled receptor (Lgr5)⁺ hepatic and pancreatic stem cells respectively, which share genetic similarity with intestinal Lgr5⁺ stem cells. Thus using the R-spondin based culture system (media with R-spondin, FGF, Noggin etc.) established by Sato and Clevers for intestine organoids development (Sato & Clevers,

2013), researchers showed that the organoids can be differentiated into matured, functional hepatocytes (Huch et al., 2013). Later, liver organoids were finally generated on matrigel along R-spondin based media which have functional similarities to *in vivo* hepatocytes (Huch et al., 2015). Furthermore, previous studies showed that the Lgr5⁺ stem cells from both pancreas and liver are functionally and phenotypically similar (Dorrell et al., 2014). Therefore, these cells can be differentiated towards either pancreas or hepatocytes by altering culture conditions. Liver organoids were also generated from PSCs through activin A treatment which gave rise to hepatic cells. These cells combined with mesenchymal and endothelial cells formed 3D organoids (Takebe et al., 2013).

- *Intestinal organoids*

Intestinal mucosal epithelium is composed of glandular folding known as crypts (downward) and villus (upward) respectively that are made of single layer simple columnar cells. Intestinal homeostasis is preserved by the rapid self-renewal of stem cells that express Lgr5 (Barker et al., 2007) lying at the base of crypt capable of dividing and differentiating to renew cells in the intestinal tissue. Sato et al. first used a culture media cocktail consists of R-spondin-1, noggin, and FGF associated with matrigel to culture intestinal crypts or Lgr5⁺ stem cells (Sato et al., 2009). R-spondin-1 is the ligand for Lgr5 receptor which together enhance Wnt-signalling (pathway required for stem cell proliferation and maintenance) (de Lau et al., 2011; Pinto, Gregorieff, Begthel, & Clevers, 2003; Sato, Stange, et al., 2011). Following the same culture system, Sato and Clevers generated intestinal organoids from Lgr5⁺ stem cells derived from intestinal tissue (Sato & Clevers, 2013). However, Lgr5⁺ stem cells were quiescent, slowing the organoids formation. So, it was recommended to grow

organoids from whole crypt gland or co-culturing Lrg5⁺ stem cells with Paneth cells that express EGF and Wnt3, and thus forming organoids with all the differentiated matured intestinal cells (Sato et al., 2011; Sato et al., 2009). In case of colonic organoids, Wnt3 should be added to the media as colon crypts lacking the Paneth cells (Sato, Stange, et al., 2011). Furthermore, intestinal organoids were also generated from PSCs. First PSCs were treated with activin A to generate hindgut organoids and then the organoids were cultured in matrigel overlaid with R-spondin-conditioned media cocktail (Spence et al., 2011).

- *Stomach organoids*

Similar to intestinal stem cells, the pyloric stem cells of stomach express Lrg5. Thus, a similar protocol with some modifications was used to generate stomach organoids from Lrg5⁺ stem cells. Organoids were also developed from Troy⁺ zymogenic cells found at the base of corpus glands (Barker et al., 2010; Stange et al., 2013). For human gastric organoids, factors such as epidermal growth factor (EGF), Wnt, and R-spondin were added to the culture media (Bartfeld et al., 2015), while for mouse gastric organoids, Noggin, fibroblast growth factor (FGF10), and gastrin were used (Schumacher et al., 2015). Although these organoids were shown to have matured stomach cells such as mucous neck cells, endocrine cells, zymogenic cells, and pit cells, however they lack parietal cells indicating that there was still something missing in the culture system. Schumacher et al. tried co-culturing organoids with stomach mesenchymal stem cells and were able to differentiate towards all types of cells (Schumacher et al., 2015). Stomach organoids were also grown from PSCs. Briefly, PSCs were treated with Activin A to develop into definitive endoderm by day 3. This further was converted to posterior foregut organoid upon treatment with growth factors

such as Wnt, FGF4, Noggin, and retinoic acid (RA) by day 6, which was then further differentiated towards antral region with the withdrawal of Wnt up to day 9. Finally, the organoids were grown and differentiated up to 34 days with media containing only EGF (McCracken et al., 2014). All the previous protocols used to develop gastric organoids from PSCs were towards antral region missing the parietal cells. Recently, McCracken and his group showed that stem cells in the gastric organoids can also be differentiated towards parietal cells of the corpus region. After studying different signaling pathways including Wnt/ β catenin pathway and MEK-pathway that are involved in stomach growth and development during embryonic stages, this study tested if modifying any of these pathways have any effect on the growth of the stomach organoids. Then, it was suggested by the study that the activation of β catenin by GSK3 β inhibitor CHIR99021 (CHIR) and inhibiting MEK-pathway with PD0325901(PD03) drive the stem cell differentiation towards parietal cells (corpus) in the organoids (McCracken et al., 2017).

1.3.7.4 Applications of organoids

The fact that the cells in the organoids organize themselves to mimic *in vivo* organs, it makes them excellent models to be applied in the study of many important fields far better than using usual 2D cell culture. Organoids are used in many studies including tissue regeneration, disease modeling, drug testing, organ morphogenesis and development and host pathogen interactions.

Organoids can also be a useful model for stem cell research. Since, stem cells are the main source for organ development and nowadays it is also believed that stem cells are involved in pathogenesis of some diseases like cancer, it is a highly demanding research field, but it is very challenging because of difficulty in isolating

and culturing stem cells. Therefore, 3D organoids will help in better understanding in the stem cell functions and factors regulating them as these organoids mimic *in vivo* organs far better than the usual 2D cell cultures.

1.4 Aims of this study

The first aim of this study was to develop 3D organoids from mGS cells. mGS cells have typical epithelial cell appearance and also have characteristic features resembling the gastric stem cells. Therefore, in this study, the mGS cells were tested for the capacity to develop organoids as these cells somewhat morphologically resembles the gastric epithelial progenitor cells.

The second aim was to develop organoids from neonatal mouse gastric glands and label the dividing cells by bromodeoxyuridine. Then the organoids at different time points were followed to test whether the stem cells are involved in the development of the organoids. The organoids were characterized using, immunohistochemistry and electron microscopy and tested for differentiation towards the stomach cell lineages.

The fourth aim was to investigate the expression of AhR in gastric epithelial cells, tissues and organoids.

This fifth aim was to investigate effects of dioxin-activated AhR on mouse stomach tissues and organoids. Finally, AhR expression was investigated in human stomach tissues.

Chapter 2: Methods

2.1 Development of 3D organoids from mGS cells

In this experiment, the hanging drop method was used to grow organoids from mGS cells, followed by force-floating method. Then the cells in the organoids were characterized using cell viability assays and electron microscopy.

2.1.1 Mouse gastric stem cell culture

Mouse gastric stem cells were maintained in Roswell Park Memorial Institute (RPMI) media (Thermo Fisher Scientific, USA) containing 10% fetal bovine serum (FBS) (Thermo Fisher Scientific, USA) in a humidified chamber at 37°C with 5% carbon dioxide (CO₂). Cells were passaged every four days when 70-80% confluence. Briefly, media was removed, cells were washed with phosphate buffer saline (PBS) (Thermo Fisher Scientific, USA), cells were incubated in trypsin, collected in a 15 ml tube and centrifuged. Cells were transferred into new flask containing fresh media and incubated in CO₂ incubator. The media was changed every third day.

2.1.2 Formation of organoids by hanging drop method followed by force-floating technique

Cells were grown to 70-80% confluence and trypsinized, followed by centrifugation and removal of supernatant. Total live cells were counted using hemocytometer, and 500 or 1000 cells were used for each hanging drop experiment. In short, the 90 mm petri dish bottom was filled with 10 ml PBS and the upper lid was used for hanging drops, which contained 20 µl of cell suspensions in RPMI media, supplemented with 10% FBS. The whole set up was then incubated in humidified CO₂

incubator at 37°C. The drops were monitored daily and incubated until cell aggregates were formed. Once spherical organoids were formed, they were washed with fresh media and transferred to agarose (1.5%) coated 96-well plates for growth and development (Figure 6).

2.1.3 Cell Viability assay

Media from the organoid culture plates was removed following PBS wash. Organoids were incubated for 15 mins in calcein (3 μ M) (Molecular Probes, USA) and then for 15 mins in propidium iodide (2.5 μ M) (Molecular Probes, USA). Calcein was used for detecting live cells and propidium iodide (PI) for dead cells. Then the organoids were imaged by inverted phase contrast microscope (Olympus IX71, Japan) or confocal microscope (Nikon Eclipse Ti, Japan).

2.1.4 Transmission electron microscopy (TEM)

To detect ultra-structural features of cells forming organoids the electron microscopy was used. Organoids were fixed with Karnovsky's fixative with 0.2% tannic acid for 30 mins and washed with 0.1 M sodium cacodylate (3 times for 10 mins each) followed by 1-hour incubation with 1% osmium tetroxide. Organoids were then washed with distilled water for 3 times (2 mins each). Then the organoids were dehydrated with ascending grades of ethanol series (30%, 50%, 70%, 80%, 90%, 95%, and 100% for 15 mins each), and embedded using resin. Sample on resin blocks were sectioned (ultrathin approximately 100 nm) and stained with uranyl acetate followed by lead citrate. Finally, organoids were visualized using electron microscope (Tecnai G2 Bio Twin, Holland).

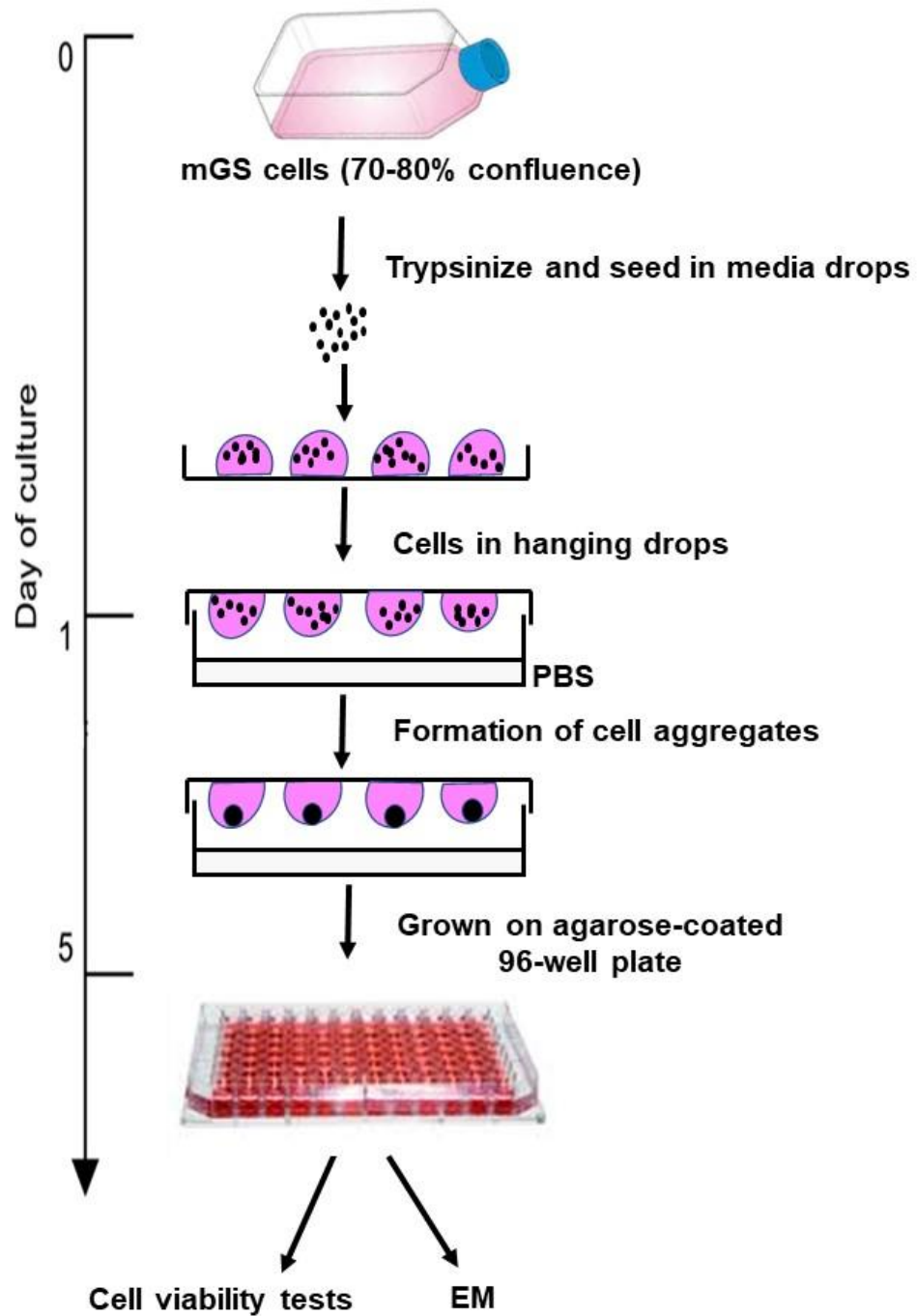


Figure 6: Hanging drop technique followed by force-floating method. mGS cells were cultured and extracted when approx. 80% confluence and seeded in RPMI media drops (8 μ l) hanging on the upper cover of the petri dish, the bottom was filled with PBS. After 5 days, organoids were transferred to agarose coated plates to grow and analyze them further by cell viability assays and electron microscopy.

2.2 Development of 3D organoids from neonatal mouse gastric glands

2.2.1 Animals

All the *in vivo* experiments in this study were carried out using C57BL/6J mouse strain provided by the animal house, United Arab Emirates University. Mice were kept and maintained under special germ-free conditions at a constant temperature of $22\pm 3^{\circ}\text{C}$, 55% relative humidity, on a 12-hours light/dark cycle and regular food and water supply.

2.2.2 Isolation of neonatal mouse stomach glands

C57BL/6 mice of 5 days old were used to isolate stomach glands. Mice were sacrificed and the stomach was quickly excised using scissor and cut along the greater curvature. Stomach was washed with cold PBS several times and cut into small pieces of approximately 1 mm. Tissue pieces were then washed with cold PBS and then washed with buffer containing 96.2 mM NaCl, 54.9 mM D-sorbitol, 8.0 mM KH_2PO_4 , 5.6 mM NaHPO_4 , 43.4 mM sucrose, 0.5 mM DL-dithiothreitol, in deionized water). Then the tissue pieces were incubated with chelating buffer containing EDTA (2 mM) for 30 mins at 4°C on a rotating platform. The buffer solution was removed, tissue pieces were placed in a petri dish and gently pressed with a glass slide to separate the gastric glands. Glands were then re-suspended in advanced Dulbecco's modified Eagle medium/F12 (DMEM/F12) (Thermo Fisher Scientific, USA) medium containing 10% FBS, collected in a 15 ml tube and large tissue pieces were allowed to settle at the bottom. Supernatant containing the isolated glands was transferred to a new tube and centrifuged ($250\times g$, 5 mins). The isolated glands were then used for the formation of organoids.

2.2.3 Development of gastric organoids from gastric glands

Matrigel was thawed at 4°C and 24-well plates were pre-warmed at 37°C. Isolated gastric glands were pelleted down and resuspended with ice-cold matrigel (growth factor reduced, phenol red free) purchased from Corning, USA and seeded in pre-warmed 24-well plates (50 µl per well). The matrigel containing glands was allowed to solidify for 15 mins at 37°C and then covered with 500 µl 10% DMEM/F12 medium supplemented with several growth factors: murine Wnt3A (Peprotech, UK), R-spondin 1 (R & D systems, USA), 2% B27 supplement without vitamin A (Thermo Fisher Scientific, USA), 1% N2 supplement (Thermo Fisher Scientific, USA), 50 ng/ml epidermal growth factor (Peprotech, UK), 150 ng/ml noggin (Peprotech, UK), 100 ng/ml fibroblast growth factor (Peprotech, UK), 1.25 mM N-acetyl-L-cystein (Sigma-Aldrich, USA), 10 nM gastrin (Sigma-Aldrich, USA) and 10 µM Y-27632 (Sigma-Aldrich, USA). Matrigel containing glands were maintained in a humidified incubator at 37°C, 5% CO₂. When the organoids were developed, media was changed every other day without Y-27632, it is only required at the initial days for saving the cells from dying when getting separated from extra cellular matrix (Figure 7).

2.2.4 Bromodeoxyuridine (BrdU) labelling of organoids

Neonatal mice were injected with BrdU (120 mg/kg) intra-peritoneally. After two hours of injection, mice were euthanized and some stomachs were used for organoid formation and few stomachs were processed for microscopic analysis. Organoids of different time points were processed for paraffin embedding and microscopic examination.

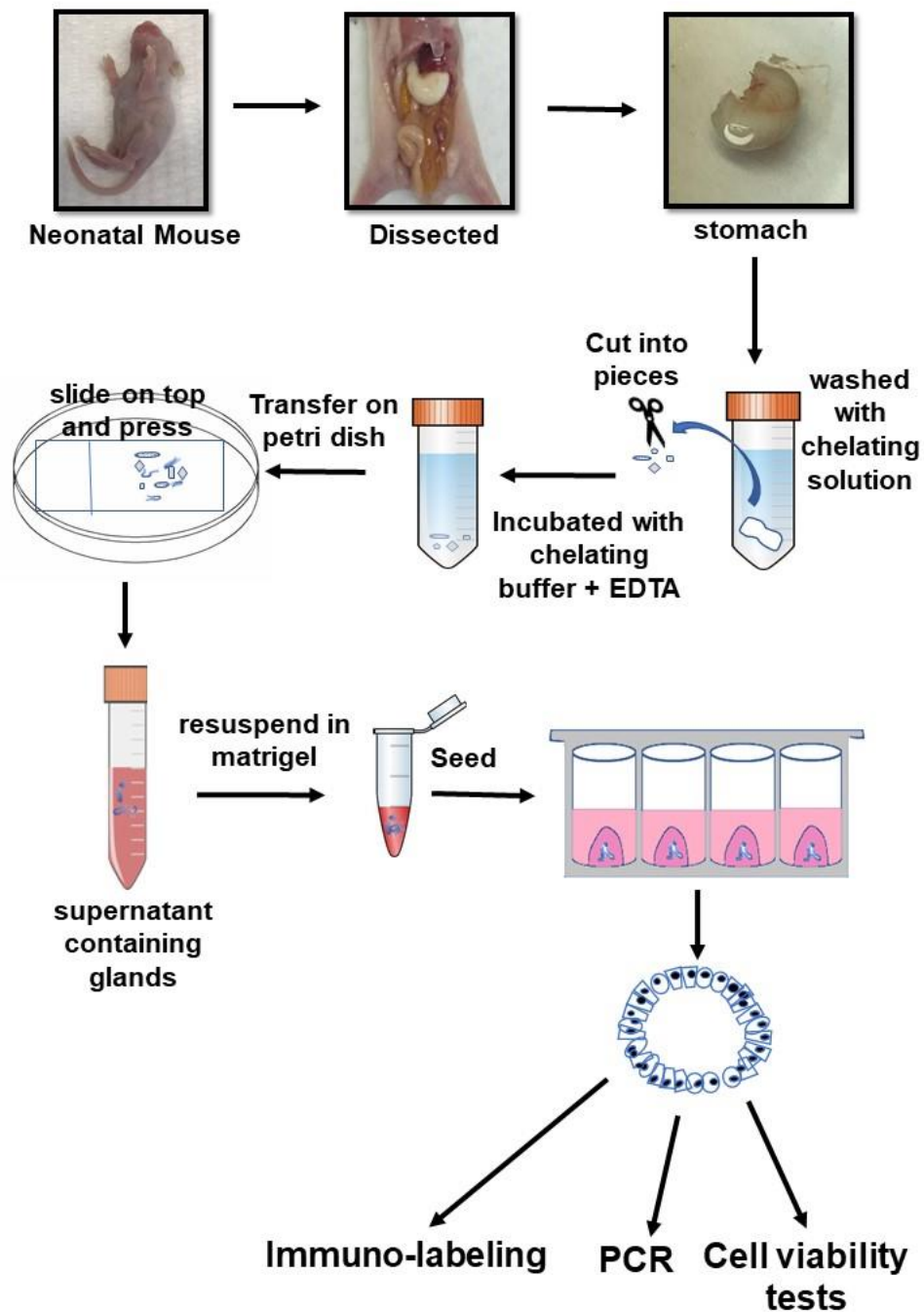


Figure 7: Generation of organoids from neonatal gastric glands. 4 days old mice were dissected, stomach was cut opened and cut into small pieces. Tissue pieces were washed, incubated in chelating buffer with EDTA, pressed between a slide and a petri dish and collected using DMEM/F12 media. The media was collected, centrifuged, supernatant containing glands were seeded in matrigel. Media was added after the matrigel was solidified and kept in humidified incubator at 37°C.

2.2.5 Histological characterization of the organoids

2.2.5.1 Processing of organoids for microscopic examination

The organoids in matrigel were fixed in 4% paraformaldehyde (PFA) in PBS at 4°C for 2 hours. Liquified matrigel was gently removed and organoids were transferred to a 1.5 ml centrifuge tube, pre-warmed histogel (Thermo Fisher Scientific, USA) at 60°C was added to the tube. The histogel with organoids was then solidified and rapped in a thin filter paper and transferred to tissue processing cassettes. The histogel containing organoids were then fixed in 10% formalin for 2 hours and dehydrated in ethanol series (50% for 30 mins, 70% for 30 mins, 80% for 30 mins, 90% for 1 hour, 100% for 2 hours), 1 hour incubation in isopropanol and 2 hours in acetone followed by overnight infiltration in paraffin at 54°C. Then they were embedded in paraffin, sectioned (5 µm) and mounted on gelatin-coated slides (Figure 8).

Histogel paraffin sections containing organoids were dewaxed by incubating at 60°C for 10 mins followed by incubation in xylene twice for 5 mins each. Then the sections were rehydrated with a descending series of alcohol 100% (twice for 3 mins), 95%, 90%, 70%, 50%, 30% (3 mins each) and further steps were followed according to staining procedure (Figure 8).

2.2.5.2 Periodic-acid Schiff and hematoxylin staining

Hydrated sections of organoids were incubated in periodic acid solution (Abcam, Cambridge, UK) for 5 mins following few washes with tap water, sections were incubated with Schiff reagent for 15 mins. Then hematoxylin solution (Thermo Fisher Scientific, USA) was added for 1 min and sections were washed with tap water and dehydrated with series of alcohol (70%, 90%, 100% twice, for 3 mins each) and

incubated in xylene twice for 5 mins each. The slide was finally mounted with DPX and covered with coverslips.

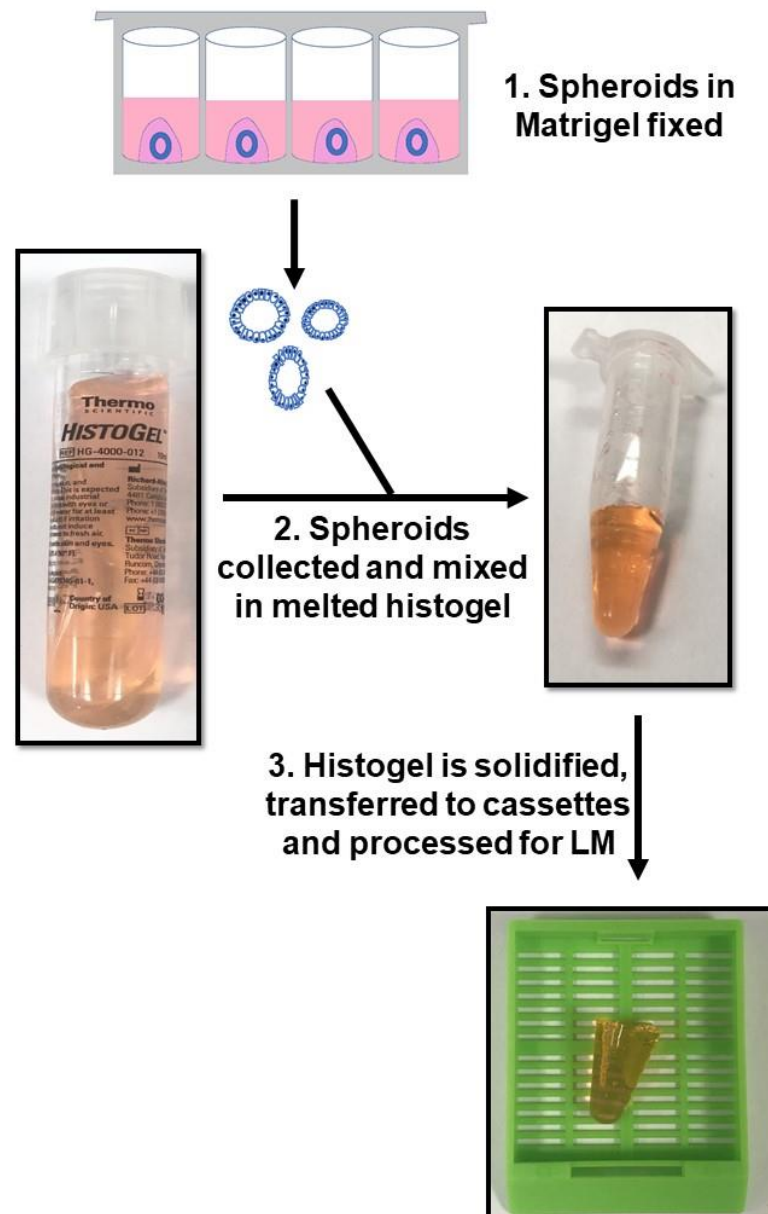


Figure 8: Processing of organoids using histogel for microscopic analysis. Organoids were fixed in 4% PFA, separated from matrigel and embedded in melted histogel. Then histogel containing organoids was placed in a cassette and whole set was then processed for microscopic analysis.

2.2.5.3 Immunostaining

Rehydrated sections of organoids were washed with PBS three times for 5 mins each. Sections were incubated in PBS containing 1% Bovine Serum Albumin and 0.5% Tween-20 to block the non-specific binding sites for 45 mins, followed by incubation with primary antibodies for 1 hour or overnight at 4°C. Primary antibodies used for organoids were mouse monoclonal anti H,K-ATPase β -subunit (Medical and Biological Laboratories Co. Woburn, MA, USA), E-cadherin, anti-pepsinogen C (Abcam, UK), Chromogranin A (Abcam, UK). Sections were then washed with PBS and incubated with secondary antibody, goat polyclonal anti-mouse (Alexa Fluor 488 conjugated) (Abcam, USA) for 1 hour (1:500). For nuclear staining, some of the sections were stained with propidium iodide prepared in PBS (1:10000) for 1 min. Sections were then washed several times with PBS for 5 mins each and mounted with mounting media. Florescent signals in the immune-stained sections, reflecting antigen-antibody binding sites were visualized by confocal microscope (Nikon Eclipse Ti, Japan).

2.2.5.4 Immuno-peroxidase staining

After dewaxing and rehydration, organoid sections were washed with PBS, and incubated with 3% hydrogen peroxide (H_2O_2) prepared in methanol for 30 mins to inhibit endogenous peroxidases. Sections were then washed with PBS, blocked by incubating in 1% BSA. Then the sections were incubated with primary antibody mouse monoclonal anti-BrdU antibodies (Medical and Biological Laboratories Co., Nagoya, Japan) or mouse monoclonal anti-AhR antibody (Santa Cruz Biotechnology, USA). Following, washing with PBS three times 5 mins each, sections were incubated with biotinylated polyclonal anti-mouse secondary antibody (1:500) (Jackson Immuno

Research Laboratories, USA) for 1 hour. The substrate Extravidine peroxidase conjugate (Sigma, St. Louis, MO, USA) prepared in 1% BSA (1:1000) was added for 1 hour and then washed with PBS. Antigen-antibody bindings were then visualized by adding 3'3'-diaminobenzidine (DAB) (Sigma, St. Louis, MO, USA). The section was then washed with distilled water. Then the sections were dehydrated through a series of increasing concentrations of alcohols, 70%, 90%, 100% twice for 3 mins each and immersed in xylene twice for 5 mins and finally mounted with Dibutylphthalate Polystyrene Xylene (DPX) mounting medium. The sections were finally visualized, and the images were captured by Olympus light microscope connected to DP70 digital camera.

2.2.5.5 Lectin histochemistry

The sections of organoids were deparaffinized, rehydrated and washed with PBS 3 times for 5 mins each. Then the sections were blocked in 1% BSA with 0.5% Tween-20 in PBS for 45 mins. Then sections were incubated with rhodamine-conjugated fucose-specific UEA-1 lectin (Vector Laboratories, USA) for 1 hour followed by washing with PBS three times for 5 mins each. Then the sections were incubated with Alexa Flour 488 conjugated Wheat germ agglutinin (WGA) (Thermo Fisher Scientific, USA) and washed with PBS 3 times (5 mins each). Some sections were stained with propidium iodide for nuclear staining. Finally, sections were dehydrated and mounted with mounting media and imaged by the confocal microscope.

2.2.6 Reverse Transcription Quantitative Polymerase Chain Reaction (RT qPCR)

Firstly, media from the organoids at different time points (2, 4, 10 days) was removed and washed with cold PBS. Matrigel was melted in cold PBS and removed.

The organoids were lysed with TRIZOL Reagent (Ambion) by repetitive pipetting and kept at room temperature for 5 min to allow dissociation of nucleoprotein complexes. Then, 200 μ l chloroform was added to the sample and shaken vigorously for 10 seconds. Samples were then incubated at room temperature for 5 mins and centrifuged at 13000 revolutions per minute (rpm) for 15 mins at 4°C. The aqueous phase approximately 200 μ l was removed using a micropipette and equal volume of isopropanol was added to precipitate the RNA. Tubes containing RNA solution were inverted until the solution was clear and incubated at room temperature for 10 mins and then the samples were centrifuged for 15 mins at 13000 rpm at 4°C. The supernatant was removed and washed with 1 ml of 75% ethanol prepared in nuclease-free water. Samples were centrifuged at 10000 rpm at 4°C (5 mins), the ethanol was poured off and the pellet was left to air dry. 20 μ l nuclease free water was added to each tube and incubated at 55-60°C for 10 mins in a water bath. RNA samples were then stored in -80°C for 24 hours.

The RNA was quantified using a Nanodrop 2000 spectrophotometer (Thermo scientific, USA). Firstly, 1 μ l of nuclease free water was added on the platform as blank and then 1 μ l of RNA samples were added. The concentration per 1 μ l of sample was noted. Total RNA purity was taken as a value from 1.9 to 2.00 at 260 nm/280 nm ratio.

Next, a High-Quality cDNA Reverse Transcription kit (Applied Biosystems, Ludhiana) was used for cDNA synthesis. Reverse transcriptase master mix was prepared by adding appropriate volume of 25x deoxyribonucleotide triphosphates (dNTPs), 10x reverse transcriptase (RT) buffer, Multiscribe™ reverse transcriptase, 10x Random Primers and RNAase inhibitor. Then nuclease free water and RNA templates were added to the master mix for each sample. These mixtures were then

centrifuged to spin down the contents and to remove any air bubbles formed. Then the samples were incubated at 25°C for 10 mins, 120 mins at 37°C and 5 secs at 85°C on a Thermocycler and the cDNA samples were stored at -20°C.

Synthesized cDNA was used as template in PCR. qPCR was performed using SyBR green master mix, which was prepared by adding forward and reverse primers, Nuclease free water and SYBER green (2X SYBER® Select Master Mix, Applied Biosystems, USA). The master mix was then added to the 96-well plate and 0.5 µl of cDNA (contains 25 ng cDNA) was added to each well (samples were duplicated). The plate was then sealed with adhesive cover and centrifuged to remove any air bubbles and spin down the DNA samples. The PCR machine (Quant Studio 7 Flex, Applied Biosystems, USA). PCR was conducted for 40 cycles each consists of 95°C denaturation and 60°C for annealing and extension. The Ct values obtained from the PCR machine (Quant Studio 7, Applied Biosystems) were used to analyze the respective mRNA expressions with respect to the house keeping gene Glyceraldehyde 3-phosphate dehydrogenase (GAPDH). For quantification, Delta Ct (threshold cycle) values were calculated by $CT_{\text{target}} - CT_{\text{GAPDH}}$. DATA were expressed as $100 \times 2^{\Delta Ct}$ in order to express the difference in cycles to cross the threshold as a percentage. The list of primers used are provided in Table 3.

Table 3: List of primers used for RT-qPCR

Gene	Primer	Sequence (5'-3')
Muc5	Forward	AGGGCCCAGTGAGCATCTCCTA
	Reverse	CATCATCGCAGCGCAGAGTCA
TFF1	Forward	CCCGGGAGAGGATAAATTGT
	Reverse	GCCAGTTCTCTCAGGATGGA
MUC6	Forward	CTCACCTTCTACCCCAGTATCA
	Reverse	GGCAACGAG TTAGAGTCACATT
TFF2	Forward	GCAGTGCTTTGATCTTGGATGC
	Reverse	TCAGGTTGGAAAAGCAGCAGTT
H,K-ATPase β	Forward	AACAGAATTGTCAAGTTCCTC
	Reverse	AGACTGAAGGTGCCATTG
CgA	Forward	GCAGCATCCAGTTCCTCACTTCC
	Reverse	TCCCCATCTTCCTCCTGCTGAG
AhR	Forward	CGCTGAAACATGAGCAAATTG G
	Reverse	ACAGCTTAGGTGCTGAGTCACAGG
Lrig 1	Forward	ACAGCTGCCCCACATACAAC
	Reverse	GGGATGGTAGGCTGTGTCA
RUNX1	Forward	GGCAACTAACTGCTGGA ACT
	Reverse	CTCATCTTGCCGGGGCTCAG
Troy	Forward	CAAGGTCCTACCTCTACACA
	Reverse	AAGGTTACCTTGCTGGTAC
Oct-4	Forward	GTTCTGCGGAGGGATGGCATA C
	Reverse	AAGGCCTCGAAGCGACAGATG
CD44	Forward	TCGATTTGAATGTAACCTGCCG
	Reverse	CAGTCCGGGAGATACTGTAGC
CYP1A1	Forward	TGTCAGATGATAAGGTCATCACG
	Reverse	TCTCCAGAATGAAGGCCTCCAG
GAPDH	Forward	TCAAGAAGGTGGTGAAGCAGG
	Reverse	TATTATGGGGGTCTGGGATGG

2.3 Testing effects of dioxin-treated AhR activation in 3D primary organoids

Gastric organoids from neonatal mouse were seeded in matrigel and grown for two days as mentioned before. At day 2, the old media containing growth factors was changed with fresh media containing dioxin (0.1 nM and 1 nM) along with all the growth factors and hormones needed for the organoid growth. Organoids were

monitored using phase contrast microscope (Olympus IX71, Japan). After two days of treatment organoid were collected at day 4 and processed for microscopic studies and also collected for PCR. Images were taken using confocal microscope.

2.4 Testing effects of dioxin-treated AhR activation *in vivo*

2.4.1 Dioxin treatment on mice

Recently weaned 21 days old male mice (n=3) were injected daily with dioxin (50 µg/kg), (prepared in dimethylsulfoxide (DMSO) and diluted in PBS) intraperitoneally for three consecutive days and sacrificed on day four. Control mice (n=3) received only vehicle. The mice were euthanized, and the stomachs were cut opened through greater curvature, washed with cold PBS. Small portion of the stomach was cut longitudinally and kept in the RNA later (Ambion, USA) for RT-qPCR. The samples were then kept at -80°C for further studies. Rest of the tissue portion was fixed and processed for light microscopy.

2.4.2 Tissue processing for light microscopy

The control and dioxin treated stomach tissues were fixed overnight in Bouin's solution, dehydrated in ethanol series (70% for half an hour, 90% for 1 hour, 100% for 2 hours twice). Then the tissues were taken under the fume hood and incubated in xylene: ethanol (1:1) and xylene (30 mins twice). Tissues were then embedded in melted paraffin (at 54°C) for 1hour. This step is done thrice using fresh paraffin each time to replace the xylene completely from the tissues. Then the tissues were placed in tissue processing molds filled with melted paraffin longitudinally to get the section of whole gastric glands. When the paraffin was solidified, tissues were sectioned (5 µm) using automated rotatory microtome machine. The sections were then floated on

water bath at 45°C. Tissue sections were then mounted on gelatin-coated slides and left to dry on hotplate at 60°C (20 minutes) and stored for further use.

2.4.3 Immuno-staining on stomach tissues

For immuno-peroxidase staining, sections were deparaffinized (incubated in xylene twice for 5 mins each), rehydrated in decreasing alcohol series (100% twice, 95%, 90%, 70%, 50%) for 3 mins each and incubated in 3% H₂O₂ (in methanol) for 30 mins to block endogenous peroxidases by incubating in 1% BSA. Then the sections were incubated for 1 hour or overnight with primary antibody against AhR (Santa Cruz Biotechnology, USA), mouse monoclonal anti H,K-ATPase β -subunit (Medical and Biological Laboratories Co., Woburn, MA, USA) and anti-BrdU (Medical and Biological Laboratories Co., Nagoya, Japan) followed by washing with PBS (3 times for 5 mins each) and incubation in biotinylated secondary antibody for 1 hour. Then the sections were washed with PBS. The substrate extravidine peroxidase conjugate (Sigma, St. Louis, MO, USA) was added for 1 hr. Then, DAB was added after washing with PBS and color development was monitored with the microscope. Sections were then washed with distilled water, dehydrated with increasing grades of alcohol series (70%, 90% and 100% twice), 3 mins each and incubated in xylene twice for 5 mins each. Sections were finally mounted with dibutylphthalate polystyrene xylene (DPX) (Sigma-Aldrich) and visualized with Olympus light microscope.

2.4.4 Lectin histochemistry

For lectin histochemistry, sections were deparaffinized, rehydrated, washed with PBS and blocked by incubating in 1% BSA for 1 hour. Then sections were incubated in rhodamine conjugated UEA-1 for 1 hour followed by washing with PBS

(3 times, 5 mins each). Then the tissue sections were incubated in the second lectin *Griffonia simplicifolia* II (GSII) conjugated with Alexa Flour 488 (Thermo-Fisher Scientific, USA) and washed thrice with PBS for 5 mins each. Sections were imaged by confocal microscope. It is established that UEA-1 binds to fucose-rich surface mucous cells and GSII is specific for N-Acetyl-D-glucosamine-rich mucous neck cells in the tissues. After washing, sections were mounted with fluoro-shield mounting medium 4',6-diamidino-2-phenylindole (DAPI) (Abcam, Cambridge, UK)

2.4.5 Quantitative analysis of labelling intensity

The images of the tissues were taken using the Olympus DP70 microscope. The labelling intensities of UEA-1 and GSII lectins were calculated using the Fiji ImageJ software. Images were taken at 40x magnification. The corpus area next to the fundus was selected for analysis. The images obtained from control and dioxin-treated tissues were compared side by side using ImageJ densitometric software for analysis. Then, the images were converted to 8-bit, and pixel density was calculated. The percentage of staining intensity obtained was taken to reflect the amount of mucus in the cells analyzed. Data were presented as Mean \pm S.E.

Cells immuno-stained with antibodies against H,K-ATPase were quantified using the same software. Images were taken at 20x magnification. The corpus area next to the fundus was selected for counting the cells per glands. The targeted labelled cells were counted using the software and the number of glands were counted manually. The periodic acid Schiff counterstaining was separated using color deconvolution from the DAB staining. The data are represented the number of labelled cells per glands. It was calculated by dividing the total of labelled cells by the total

number of glands examined. Data was expressed as the mean number of cells per gland \pm S.E.

2.4.6 Statistical Analysis

Student's t-test was used for statistical analysis. The changes were compared between control and dioxin-treated stomach tissues. The results were shown with error bars indicating the mean \pm standard errors (S.E). P-value < 0.05 was considered as statistically significant.

Chapter 3: Results

In this study, two types of 3D organoid models were generated. The first model was from the mGS cell line which is representative for the gastric progenitor cells. The second 3D organoid model was generated from freshly isolated neonatal mouse gastric glands. These organoid models were characterized using immunohistochemistry, electron microscopy and then utilized to study the role of AhR in gastric stem cell biology.

3.1 Generation of mGS cell-derived organoids

This study suggests that the mGS cells were capable of forming 3D organoids using hanging drop method for approximately 5-6 days prior to transferring them on non-adherent surface (1.5% agarose-coated 96-well plates) for further growth. Organoid growth was monitored using phase contrast microscope.

In hanging drop, the cells in the media initiate to migrate towards the inverted tip of the media drop due to the gravitational force and then the cells clumped together (Figure 9A). By day 3, the clumped cells proliferated and formed 3D organoids with a proper circular 3D shape (Figure 9B). At day 6, organoids grew larger in size with diameter of approximately 50 μm (Figure 9C).

At day 7, organoids were transferred on agarose coated 96-well plate (Figure 10A). Growth of the organoids were monitored every day. By day 17, organoids grew in size approximately up to 100 μm (Figure 10B). After a month, the organoids were healthy and maintained increasing in growth with diameter exceeding 300 μm (Figure 10C). Organoids can be maintained for months on agarose-coated culture plates.

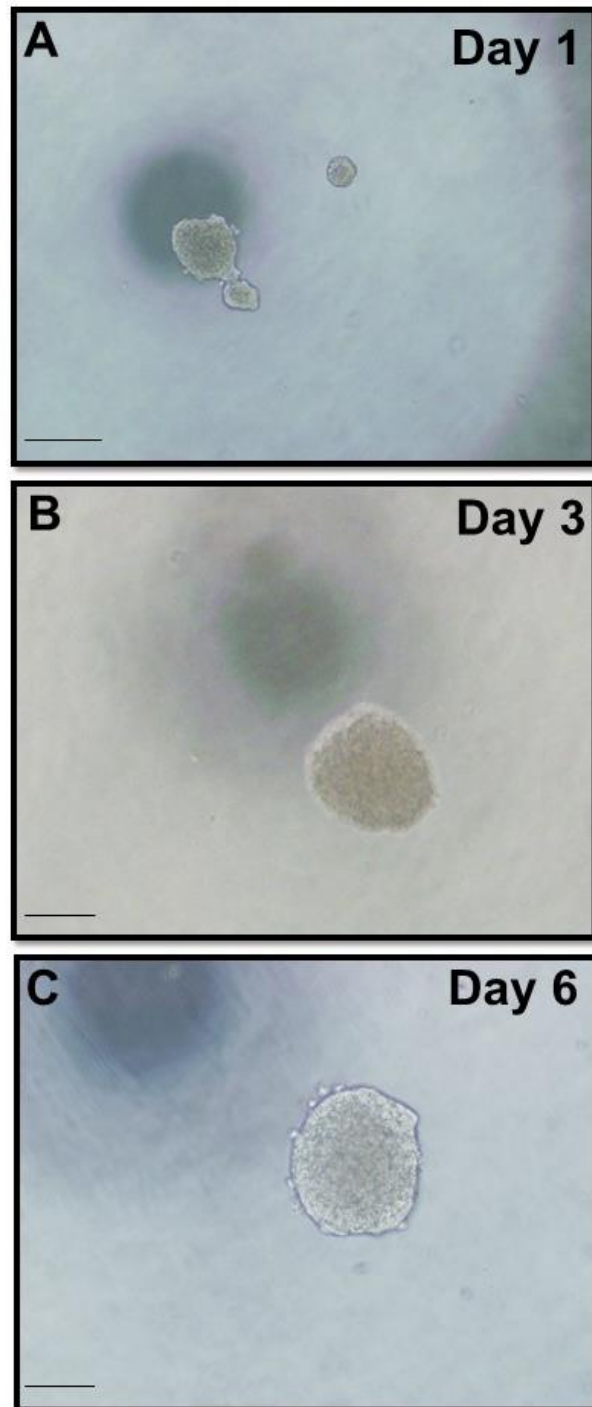


Figure 9: Phase contrast images of mGS cells forming organoids by hanging drop. A) mGS cells started clumping together at the bottom by day 1. B) At day 3, the cell clumps proliferate and organize themselves into 3D organoid. C) Cells in the organoid proliferated further and grew larger in size (50 μm). Bar=50 μm .

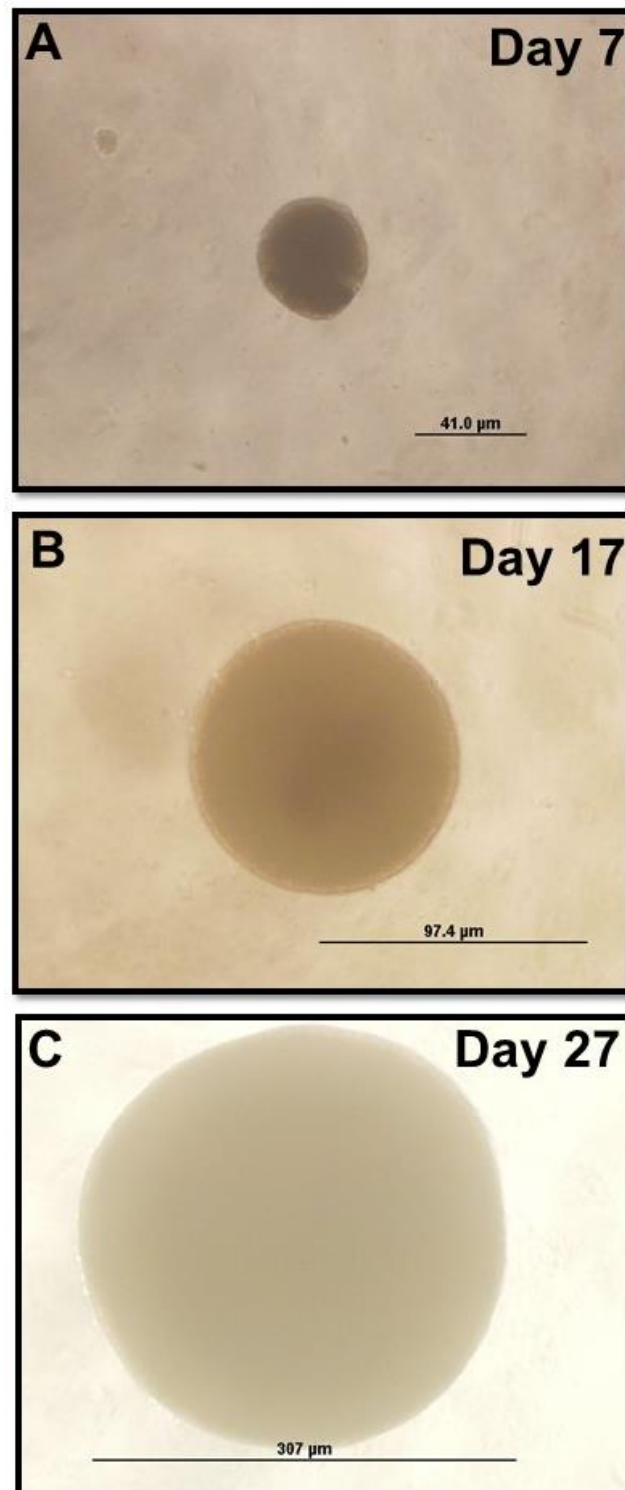


Figure 10: Phase contrast images of mGS cell-derived organoids on non-adherent surface. A) A single 7 days old organoid (diameter 40 μm) was transferred to agarose coated 96-well plate for proper media supply for growth and development. B) At day 17, organoid grew bigger in size indicating active cell proliferation (diameter 97 μm). C) At day 27, the diameter of the organoid was enlarged to approximately 307 μm . Bar represents the diameters of the organoid at different days.

To label the organoids and test for the viability of cells and whether any cells have degenerated at three days, organoids were incubated with calcein (for live cells) (Figure 11A). Calcein staining showed that the organoid was having proliferating cells on the periphery leaving a gap at the center (Figure 11B, 11C). Calcein/propidium iodide staining on 4 weeks old organoid indicated that live and healthy proliferating cells were well-organized at the periphery surrounding dead or dying cells at the center creating a cavity inside indicating continuous cell proliferation with accumulated dead cells at the center of the organoids (Figure 11D).

Cell structure and viability in the organoid was further confirmed by electron microscopic examination on a 4 weeks old organoid (Figure 12A). Cells on the periphery had euchromatin, nucleus with large nucleus to cytoplasm ratio while cells (Figure 12B) at center were condensed with dark nuclei (features of dead or dying cells) (Figure 12C). Some of the cells in the periphery contains mucous granule-like structures which could be a sign of early differentiation (Figure 12B).

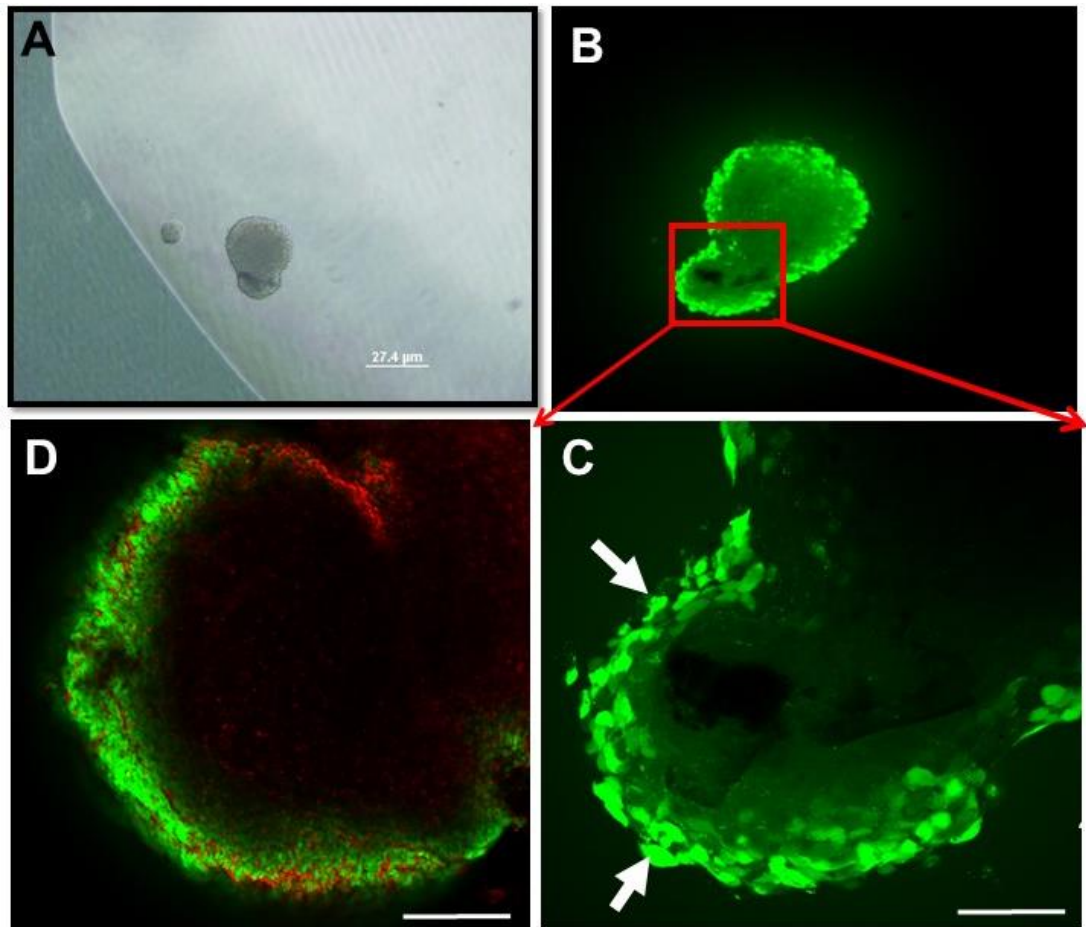


Figure 11: Phase contrast and confocal images of live and dead cells present in mGS cell-derived organoids. A) Organoid at day 3 in hanging drop (diameter 27.4 μm). B) Most of the cells in 3 days old organoid were live but more prominent at the periphery detected by calcein staining (green). C) Higher magnification (40x) of calcein staining of 3 days old organoid. D) 4 weeks old organoid stained with calcein (green) and PI (red). Organoids showed dead cells at the center having live cells at the periphery surrounding a cavity inside.

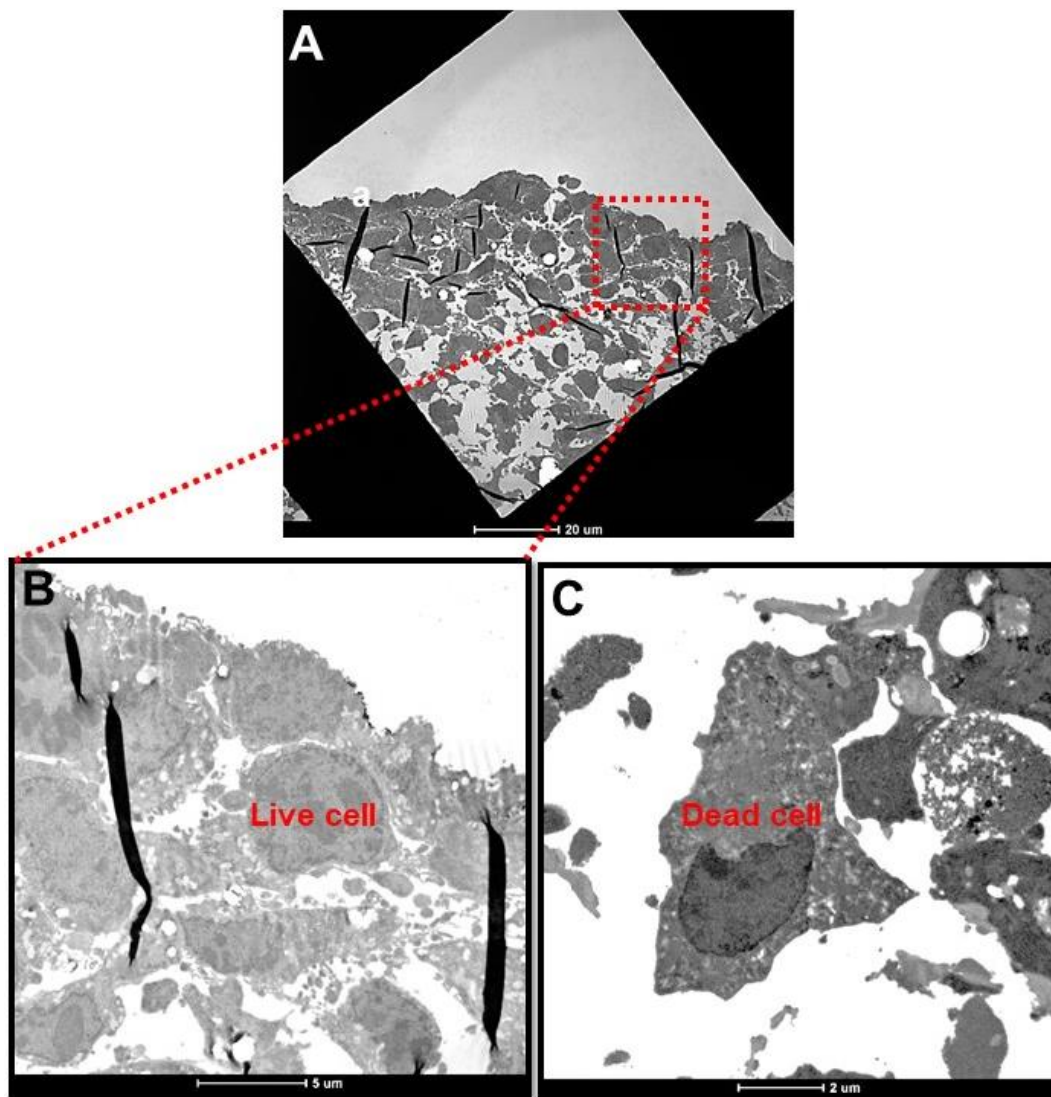


Figure 12: Electron microscopic images of a 4 weeks old organoid derived from mGS cells. A) A 4 weeks old organoid, having live and healthy cells at the periphery and dying or dead cells at the center. B) Higher magnification of a live cell at the periphery. Some of them have secretory granules that could be a sign of early differentiation towards mucous cell lineage. C) A dying cell with a pale, condensed cytoplasm and nucleus.

3.2 Generation of organoids from neonatal mouse gastric glands

In this study, the second model of 3D organoids were developed from freshly isolated stomach glands of neonatal mice using matrigel method. These neonatal glands are different from the adult mouse glands. Neonatal gastric glands are comparatively shorter in length than adult mouse and usually populated mostly by

immature progenitor cells with few mucous cells. Therefore, this study aimed to test whether these immature glands have the ability to form 3D organoids and also to test whether involvement of progenitor cells are involved in the development of these organoids.

These 3D organoids were formed with a lumen at the center by day 1 and were maintained up to day 10. The organoids grew larger in size and in some of them, there were appearance of budding. Present study showed that progenitor cells from neonatal gastric glands developed organoids within the matrigel (Figure 13).

3.2.1 Tracking BrdU-labelled proliferating cells in the organoids

Following BrdU injection, it gets incorporated into the DNA of the proliferating cells during the s-phase of the cell cycle. BrdU immuno-staining of neonatal mouse stomach showed that the glands were mostly made up of progenitor proliferating cells throughout the glands (Figure 14A). To test whether organoids were formed by the proliferating progenitor cells, BrdU-labelled cells in the organoids were tracked on day 2, day 3 and day 4. Organoids were processed for paraffin sectioning and BrdU labeling.

BrdU-labelled cells were detected at day 2 (Figure 14B), day 3 (Figure 14C) and day 4 (Figure 14D) respectively. This identification of BrdU labeled cells at day 2 and day 3 in organoids indicated that progenitor cells were involved in the development of gastric organoids. At day 4, the cells at the organoid center were also found to be BrdU-labelled. This finding suggested that the lifespan of the proliferating progenitor cells in the wall of organoids was less than four days (Figure 14D).

3.2.2 Cellular characterization of primary organoids

3.2.2.1 Morphological analysis

Firstly, the organoids were stained with hematoxylin and PAS to detect any mucus production in the organoids. PAS staining of the 4 days old organoid showed the presence of some mucus in the lumen and at the brush border of the cells characterizing their differentiation towards surface mucous cells (Figure 15A). To further confirm differentiation, organoids were stained the with UEA-1 lectin specific for surface mucous cells, and also with WGA lectin which labels membranes of gastric epithelial cells. Both lectin stainings were positive (Figure 15B, 16B).

Cells of the gastric organoids were also studied to test their possible differentiation by using immunohistochemistry. The organoids were firstly tested for epithelial cell junction. E-cadherin was found to be expressed in the cells, confirming that they were typical gastric epithelial cells connected to each other by cell junction proteins (Figure 16A). Moreover, cells were tested for H,K-ATPase expression by immunohistochemistry. Some cells showed little expression of H,K-ATPase, indicating that some progenitor cells have partially differentiated into pre-parietal cells which may later differentiate into parietal cells (Figure 16C). However, cells were tested negative for markers of other differentiated cell types including chromogranin A specific for endocrine cells (Figure 16D), pepsinogen specific for zymogenic cells (Figure 16E), and GS lectin for neck cells showed moderate staining in some cells (Figure 16F).

3.2.2.2 Expression analysis of gastric epithelial-specific genes during organoid development

Organoids at day 2, day 4 and day 10 were collected for RT-qPCR analysis, to study expression patterns of genes specific for different cell lineages in the gastric glands throughout their development process. Data revealed that at day 2, organoids expressed genes specific for surface mucous cells (Muc5AC, TFF1). However, expressions of Muc5AC and TFF1 showed gradual decrease at day 4 and highly downregulated at day 10. This may imply that some surface mucous cells were generated in the organoids from the stem/progenitor cells and later were degenerated (Figure 17). This could be supported by the fact that these cells have a short lifespan.

Moreover, at day 2, MUC6, specific for neck mucous cells did not show any expression, while at day 4, it is upregulated and highly upregulated at day 10. TFF2 (also specific for neck mucous cells) showed very low level of expression at day 2 which highly upregulated at day 4 and day 10. These findings indicated that cells at day 4 and 10 started differentiating towards mucous neck cells (Figure 17).

Genes expressed in parietal cells (H,K-ATPase) and endocrine cells (chromogranin A) were also detected at day 2, but were highly downregulated at day 4 and day 10, which indicated that some H,K-ATPase and chromogranin A producing cells were also present along with the progenitor cells during early stages of organoid development (Figure 17).

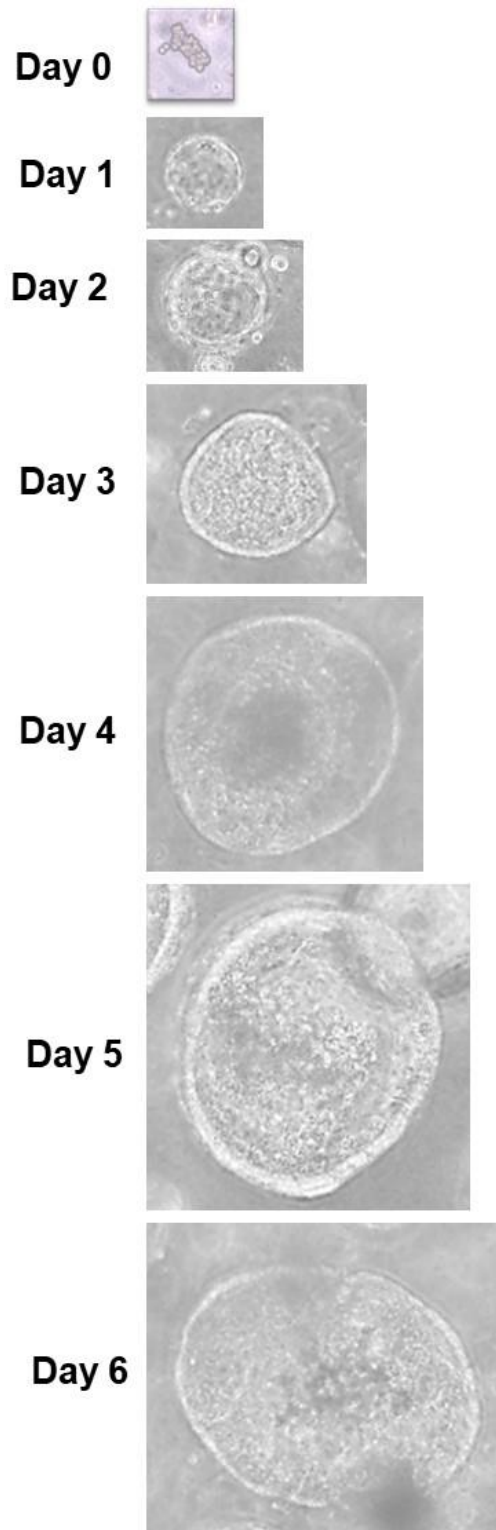


Figure 13: Phase contrast images of organoids from neonatal gastric glands. A short neonatal gland with few cells seeded in matrigel at day 0. By day 1, organoid was formed from the neonatal glands with a prominent outer layer of cells having lumen at the center. Cells of the organoid proliferated, and the organoid grew in size, some cells started to bud outwards. Figure showing organoid upto day 6. Organoids were maintained up to day 10. Bar=200 μm .

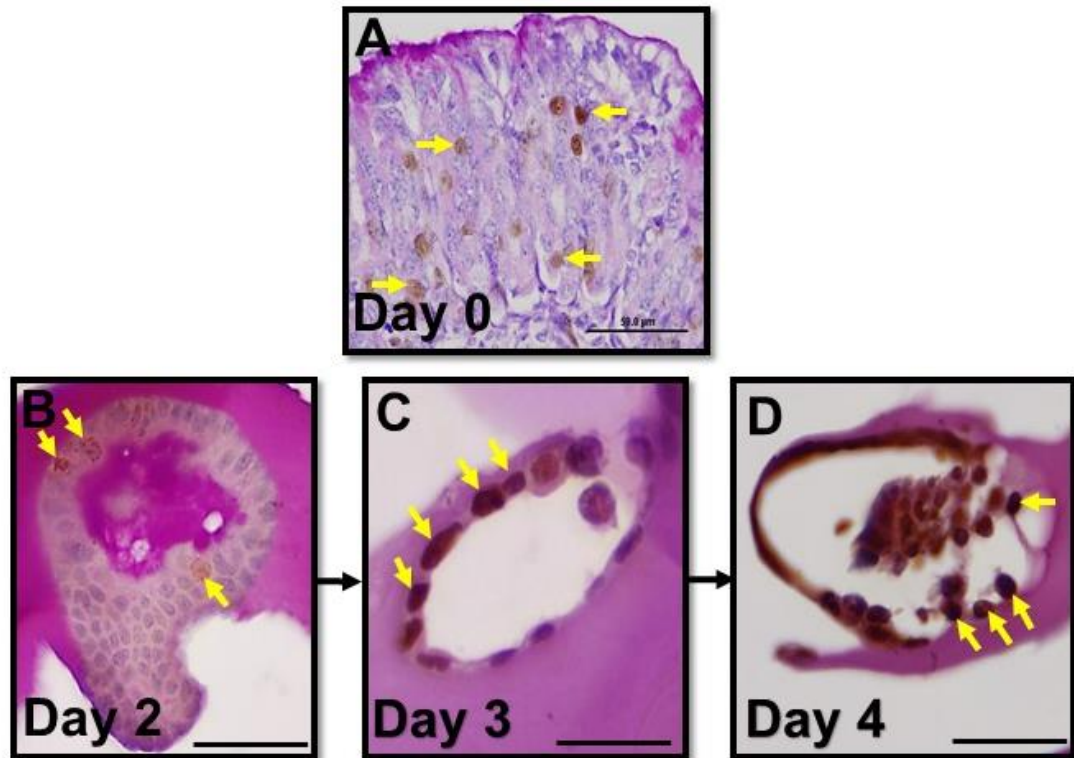


Figure 14: Tracking BrdU-labelled cells in the organoids. A) BrdU-labelled cells, scattered throughout the gland of the neonatal mouse stomach (yellow arrows pointing on BrdU-labelled cells), indicating that most of the cells are proliferating. Organoids were grown from BrdU injected neonatal gastric glands, which showed positive BrdU staining (yellow arrows) at B) day 2, C) day 3 and D) day 4, respectively, indicating the involvement of proliferating progenitor cells in the organoid development. At day 4, the dead cells at the center also were BrdU positive which suggested that the lifespan of the proliferating cells was approximately 4 days. Bar=100 μ m.

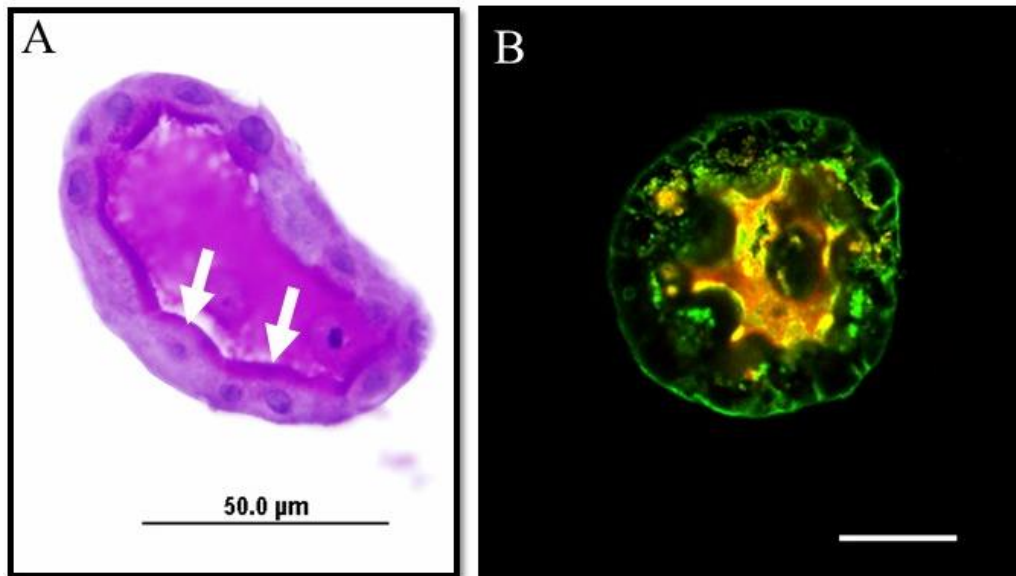


Figure 15: PAS staining and lectin histochemistry images of gastric organoids. A) Periodic acid Schiff staining on a 4 days old organoid showed that it contained mucus in the lumen and at the brush border (white arrows) which detected surface mucous cells. Hematoxylin stained the nucleus (purple). B) Organoids showed positive staining for WGA lectin (green) specific for cell membrane and UEA-1 lectin (red) for surface mucus cells. Most of the UEA-1 staining was observed at the center, an indication of the presence of mucus in the lumen. Bar=50 μm.

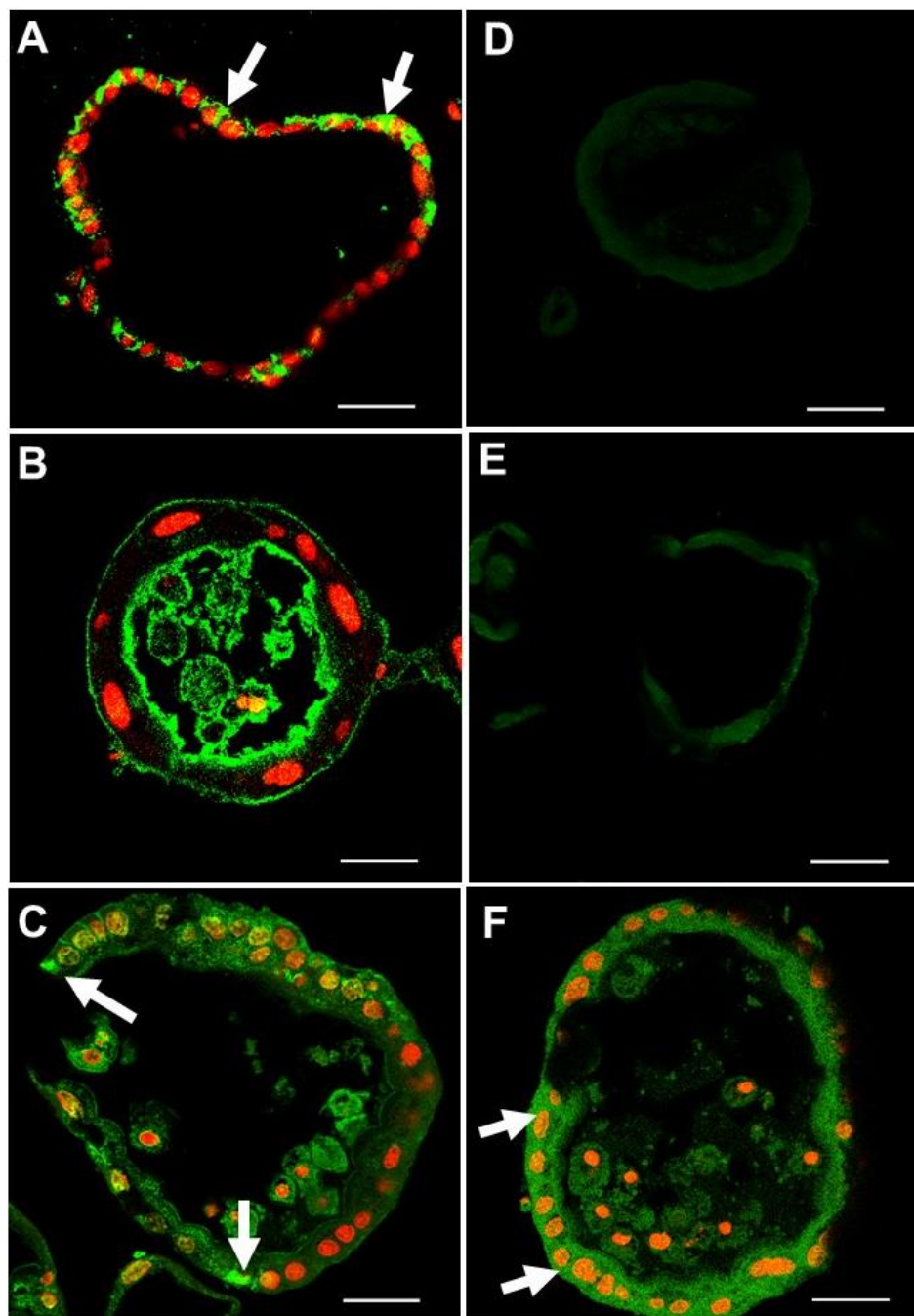


Figure 16: Immunohistochemical and lectin histochemical analysis of gastric organoids. A) E-cadherin, a cell junction marker, specific for gastric epithelial cells were detected between the junctions of the cells (white arrows). B) WGA specific for cell membrane showed positive staining. C) Some cells showed little expression of H,K-ATPase (white arrows), indicating that some progenitor cells were H,K-ATPase positive pre-parietal cells. Furthermore, D) chromogranin A for endocrine cells and E) pepsinogen for zymogenic cells did not show any expression. F) GSII lectin specific for neck cells showed moderate staining (white arrows) in some cells. PI was used as a nuclear stain (red) for E-cadherin, H,K-ATPase, WGA and GSII staining. Bar=50 μ m.

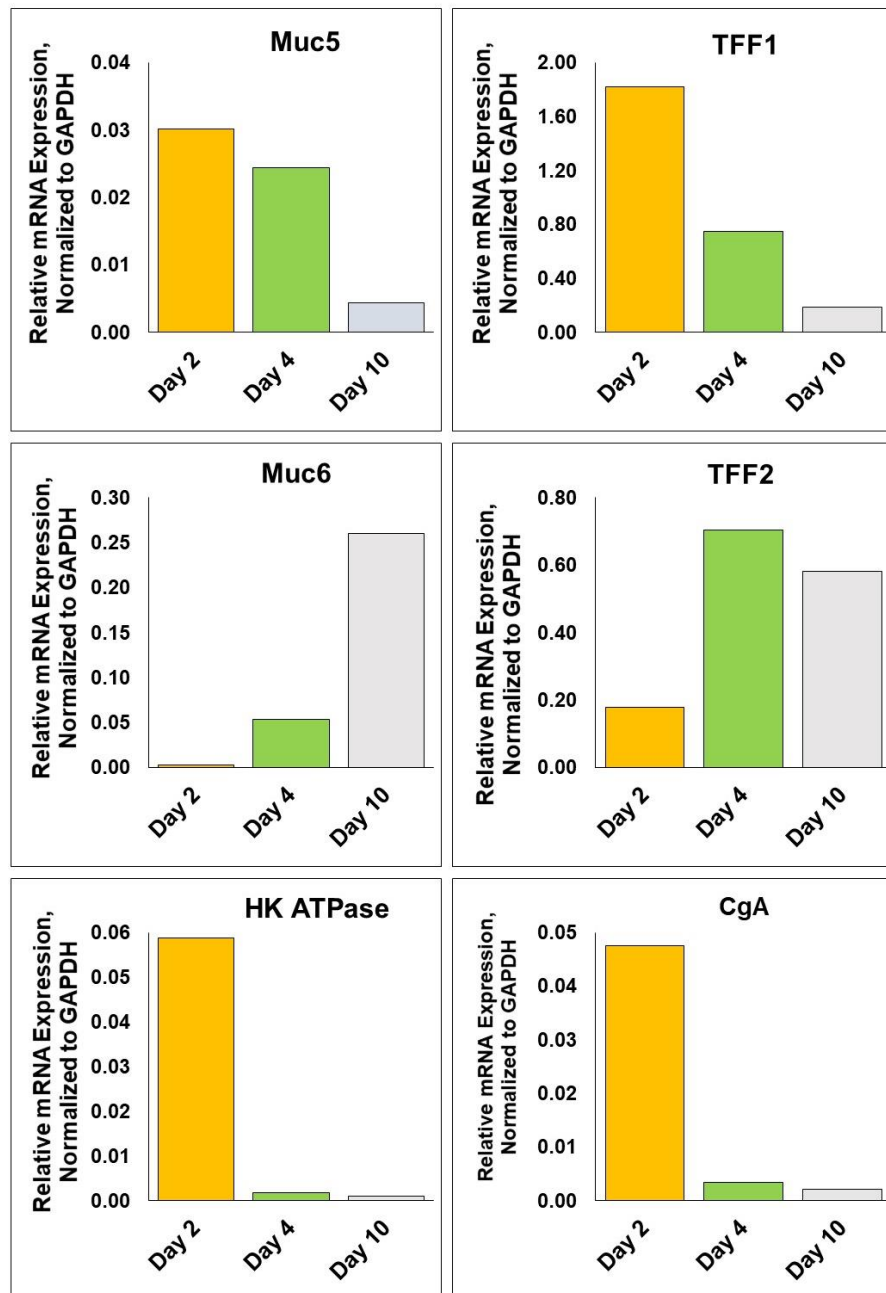


Figure 17: RT-qPCR analysis of gastric epithelial cell lineage specific genes at different stages of gastric organoid development (days 2, 4 and 10). At day 2, organoids expressed genes of surface mucous cells (Muc5AC, TFF1), whereas, at day 4 and day 10, Muc5AC and TFF1 expressions were gradually downregulated. Genes specific for neck mucous cells (MUC6 and TFF2) showed no or low expression levels at day 2 and upregulated at day 4. Genes expressed in parietal cells (H,K-ATPase) and endocrine cells (chromogranin A) were detected at day 2, but were downregulated at day 4 and day 10.

3.3 Use of organoid models to study role of AhR activation on stem cells

Before using gastric organoids to investigate the effects of dioxin activated AhR on gastric stem cells, it was necessary to define the expression of AhR in gastric epithelial cells and tissues.

3.3.1 AhR expression in mGS cells

To test whether AhR is expressed in stem cells, it was thought initially to try the AhR antibodies on mGS cells. Immunofluorescence staining showed that AhR was expressed in mGS cells. The staining was mostly located in nucleus with less intense staining in cytoplasm (Figure 18). These findings justified the needs to characterize AhR expression in stomach tissue.

3.3.2 AhR expression in neonatal mouse stomach

Neonatal stomach glands are not compartmentalized. They are short and mostly populated by proliferating progenitor cells along with few poorly differentiated surface mucous cells, neck mucous cells and parietal cells. They have no zymogenic cells, as these glands are not fully matured yet.

Immunohistochemistry revealed that AhR expression was detected all throughout the glands from the surface near to the lumen to the bottom, mostly nuclear with few cytoplasmic expressions (Figure 19A, Figure 19B). This indicated that AhR was expressed in progenitor cells in its activated form, therefore it may have a role in the proliferation and on differentiation of the progenitor cells.

Moreover, some neonatal mice were injected with BrdU and the localization of pattern of BrdU-labelled proliferating cells was compared with those expressing AhR. Immunohistochemistry revealed that BrdU-labelled cells were scattered

throughout the neonatal glands from surface to the bottom towards the muscularis mucosa (Figure 20A). When compared with location of the AhR-expressing cells, it was found to be very similar to the location of BrdU-labelled cells (Figure 20B). However, as BrdU only labels the cells at the S-phase of the cell cycle and injection was for two hrs only, there was a possibility that not all the progenitor proliferating cells showed BrdU labeling but expressed AhR. This could explain why AhR-labelled cells appeared more numerous than BrdU-labelled cells.

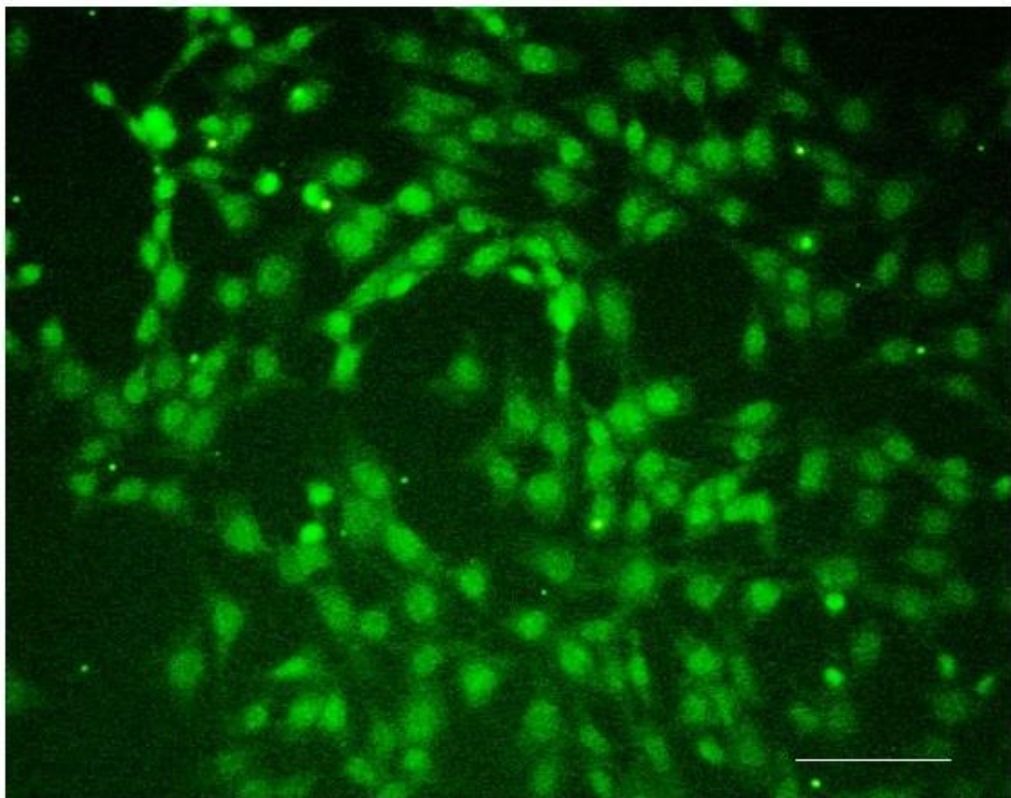


Figure 18: AhR expression in mGS cells. Immunofluorescence staining confirmed that AhR was expressed in mGS cells (green), both in nucleus and in cytoplasm. Bar=100 μ m.

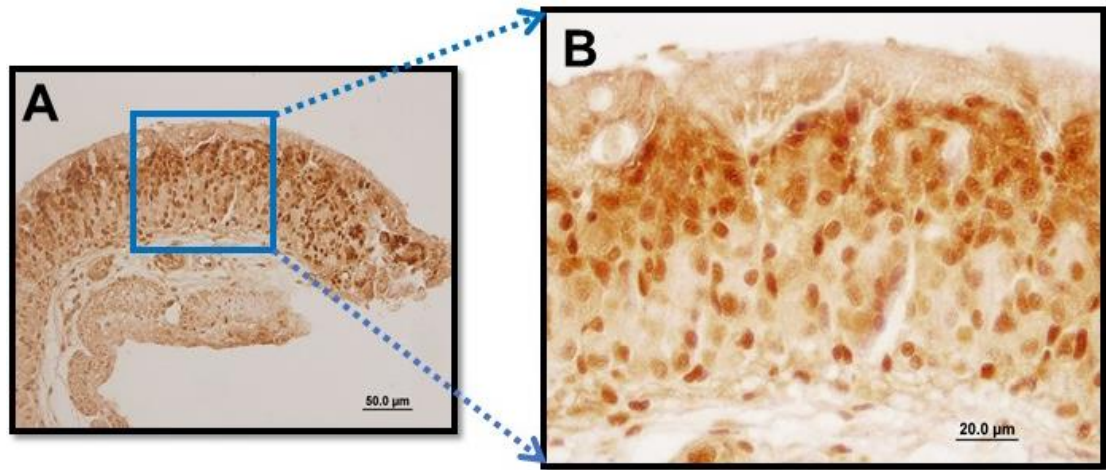


Figure 19: AhR expression in neonatal gastric glands. A) AhR expression was detected scattered throughout the glands from the surface to the bottom, mostly nuclear with few cytoplasmic expressions. Bar=50 μm . B) higher magnification (40x) image of nuclear AhR expression. Bar=20 μm .

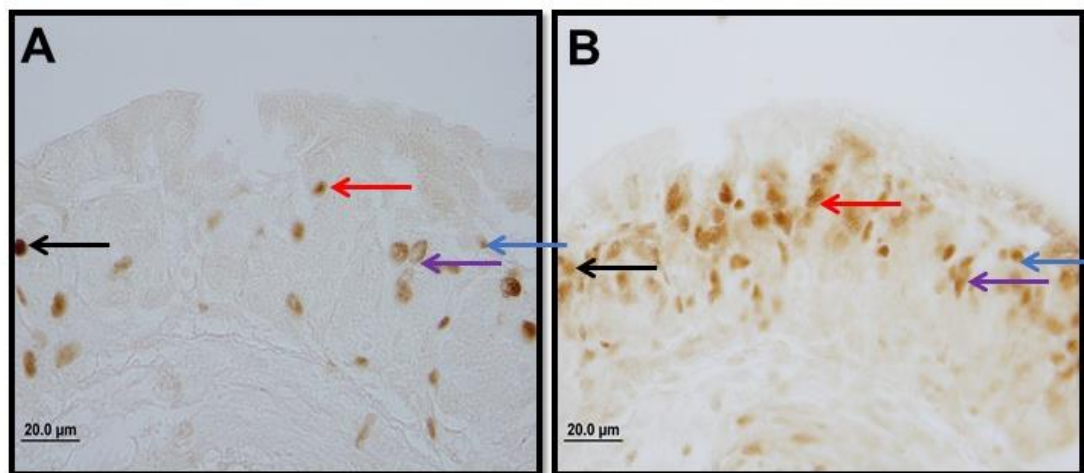


Figure 20: Comparison between cellular localization of BrdU and AhR expressions in two adjacent tissue sections obtained from neonatal stomach. A) BrdU-labelled proliferating cells appear scattered throughout the neonatal glands (arrows). B) AhR expression was also detected distributed all over the glands and in some places both the stains localized at similar cellular nuclear locations (arrows). Different colored arrows represented different locations where both BrdU and AhR were expressed. Bar=20 μm .

3.3.3 AhR expression in gastric organoids

This study also showed that AhR was expressed in gastric organoids using immunohistochemistry. Both nuclear and cytoplasmic AhR were detected in the gastric organoids (Figure 21).

3.3.4 Effects of dioxin treatment on primary gastric organoids

In this study, gastric organoids were used to test the effects of dioxin mediated AhR activation on gastric stem cell proliferation and differentiation which may later hint about its role in gastric stem cell biology and cancer development. For this purpose, considering the source (neonatal gastric glands), primary gastric organoids were chosen because these organoids showed differentiation and mimicked *in vivo* conditions of epithelial progenitors.

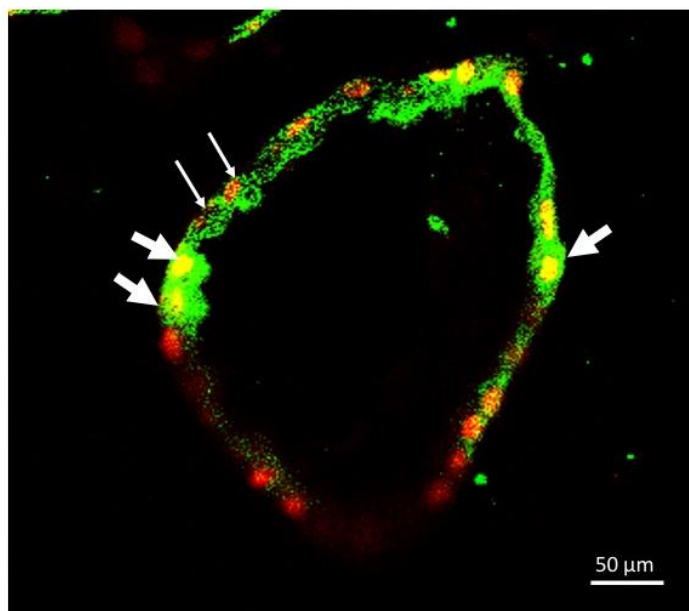


Figure 21: AhR expression in gastric organoids. Both nuclear and cytoplasmic AhR (green) were detected in some cells of the 3D primary organoids (white arrows). PI stained the nucleus (red). Bar=50 μm.

Primary organoids were treated with dioxin (0.1 nM and 1 nM) when the organoids were 2 days old. Organoid growth was monitored using phase contrast microscope. In control organoids, cells were healthy, organoids grew larger by second day (day 0 of dioxin treatment) and started accumulating dead cells by fourth day (day 2 of treatment) (Figure 22A, 22B, 22C). With dioxin treatment (0.1 nM and 1 nM), organoid growth was morphologically similar to control at day 2 (treatment day 0), as no change was expected right after the treatment (Figure 22D, Figure 22G). At day 3 (treatment day 1) and day 4 (treatment day 2), organoids did not show any morphological changes in both the dioxin treated organoids (Figure 22E, 22H, 22F, 22I).

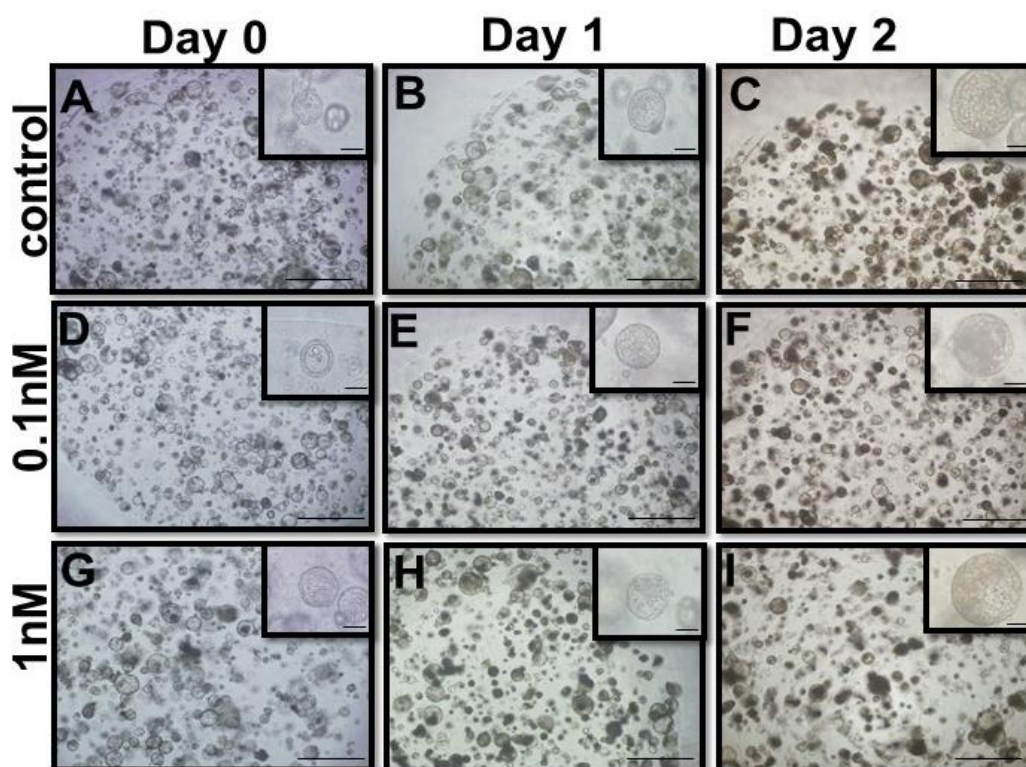


Figure 22: Phase contrast images of dioxin-treated gastric organoids at different treatment days. A) In control organoids, cells were healthy, organoids grew larger by second and B) third day (treatment day 0 and 1) and accumulated few dead cells by C) fourth day (day 2 of treatment). At Day 2 (treatment day 0), in both 0.1 nM and 1nM, no change was expected (D, G). At Day 3 (treatment day 1) and Day 4 (treatment day 2), organoid growth was morphologically similar to control for both the dioxin concentration (E, F, H, I). Bar=100 μ m.

4 days old organoids after two days of dioxin treatment were collected for analysis. Organoids treated with higher concentration of dioxin were selected for histological analysis.

Firstly, cell viability tests for both control and treated organoids showed calcein staining in cytoplasm of live cells and propidium iodide in nuclei of dead cells. In control organoid, almost all the cells were alive with few dead cells (Figure 23A). In the treated organoids, cells were alive and healthy at the periphery but with more dead cells than in control (Figure 23B). This finding indicated that dioxin activated AhR was possibly increasing the cell proliferation rate in the organoids, so the cells were dividing faster and the dead cells were accumulating at the center more than the normal ones.

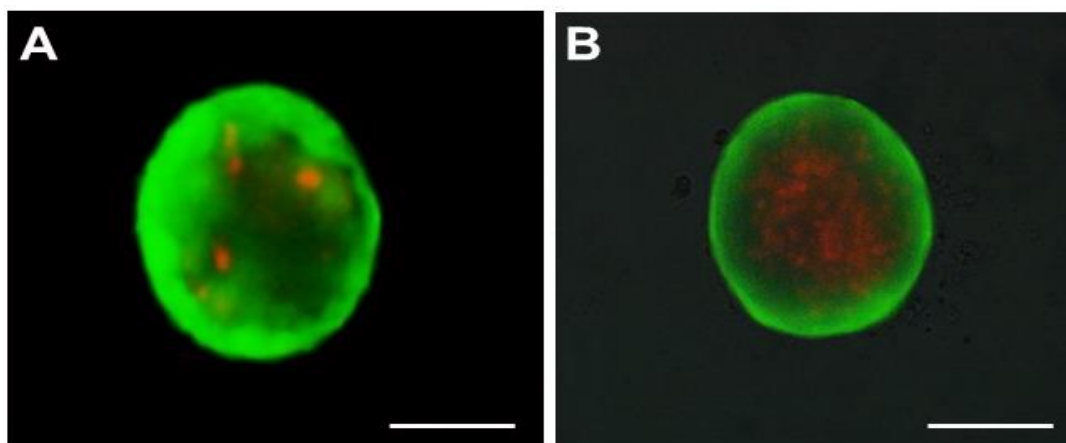


Figure 23: Celcein/PI staining images of dioxin-treated organoids. A) Control organoid had mostly live, healthy cells (green) and very few dead cells (red) at the center. B) Treated organoids had live cells (green) mostly at the periphery and more dead cells (red) at the center than to the untreated ones. Bar=100 μ m.

Moreover, dioxin-treated organoids were incubated with UEA-1 lectin to test the role of dioxin activated AhR on surface mucous cell differentiation. In control organoid, UEA-1 staining detected the mucus layer in apical cytoplasm of cells and some positive staining were also observed at the center (Figure 24A). In contrast, UEA-1 staining was more intense in the dioxin-treated organoids and most of the dead cells at the center also found to be UEA-1-labelled (Figure 24B). This can be an indication that AhR increases the mucous secretion and cell differentiation towards the surface mucous cells.

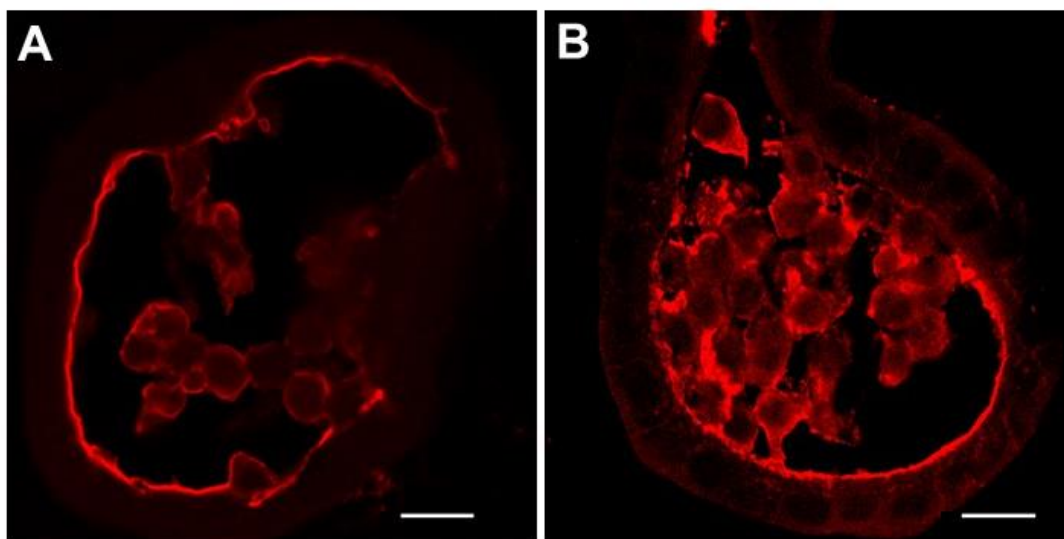


Figure 24: Lectin histochemical images of dioxin-treated organoids. A) UEA-1 lectin stained the mucus brush border (red) in the control organoid with some moderate staining at the center. B) Dioxin-treated organoids showed more intense UEA-1 staining compared to the control with a greater number of dead cells in the lumen. Most of the dead cells at the center also found to be UEA-1-labelled. Bar=50 μ m.

Furthermore, dioxin treated organoids were also tested for any effects on differentiation towards H,K-ATPase expressing cells using immunohistochemistry. In control organoids, few specific areas in the cell cytoplasm were detected for H,K-ATPase (Figure 25A). Compared to the control, dioxin-treated organoids showed more and intense staining of H,K-ATPase (Figure 25B). This could be an indication that

AhR may have a role in enhancing cell differentiation towards H,K-ATPase producing cells.

3.3.5 Effects of dioxin treatment on gene expression patterns of primary gastric organoids

Following morphological analysis, RT-qPCR was performed with the total RNA from dioxin-treated (0.1 nM and 1 nM) and un-treated gastric organoids, to analyze the gene expression patterns in dioxin-treated organoids. Organoids at day 2 were treated with dioxin, (0.1 nM and 1 nM) and collected at day 4 for RT-qPCR analysis.

mRNA for CYP1A1 (a typical AhR target gene) was chosen as a functional marker of AhR activation. CYP1A1 mRNA was detected with specific primers in the total RNA prepared from the dioxin treated organoids with and was not detected in the control organoids. CYP1A1 expression is increased with the increasing concentration of dioxin. These results suggested that the AhR was functional and activated by dioxin (Figure 26A).

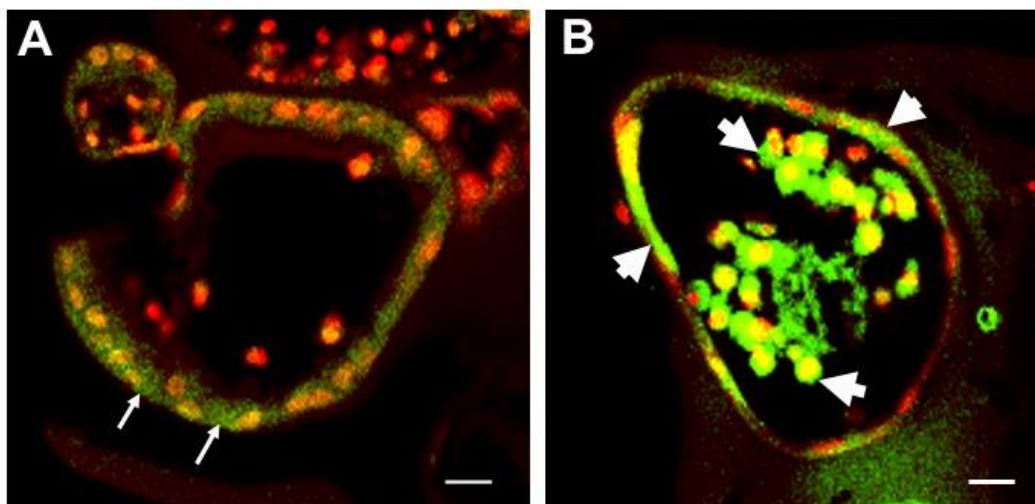


Figure 25: H,K-ATPase staining images of dioxin-treated organoids. A) Control organoids showed one or two spots (white arrows) in the cytoplasm where H,K-ATPase expression was detected. B) Dioxin-treated organoids showed more and intense staining (white arrows) of H,K-ATPase even at the center. PI stained the nucleus (red). Bar=50 μ m.

Expression of AhR was also measured in the treated organoids. There was a decrease in AhR expression level with increased concentration of dioxin treatment, but the change was not statistically significant (Figure 26B).

Firstly, using specific primers RT-qPCR was done to reveal the mRNA expression levels of gastric-specific genes (Muc5AC and TFF1 specific for surface mucous cells, MUC6 and TFF2 for mucous neck cells and H,K-ATPase specific for parietal cells) in dioxin-treated and control gastric organoids to test whether AhR has any role on cell differentiation. Muc5AC and TFF1 showed higher expression in dioxin-treated organoids compared to the control organoids. Muc5AC showed higher expression in 0.1 nM concentration of dioxin and TFF1 expression was higher in 1 nM dioxin treatment. This data altogether supported the result from lectin-histochemical analysis of the treated organoids that activated AhR increased cell differentiation towards mucous cells, but the change was not statistically significant (Figure 26B).

In addition, mRNA expression of MUC6 (specific for mucous neck cells) was significantly reduced in both the concentration of dioxin treatment compared to control organoids, while TFF2 (also specific for mucous neck cells) expression was slightly decreased in 0.1 nM and increased in 1 nM treatment. Data for TFF2 was not statistically significant. These data indicated that activated AhR decreased cell differentiation towards mucous neck cells (Figure 26B).

Additionally, H,K-ATPase showed higher expression in the treated organoids than the control ones, which corresponded to the data from immunostaining analysis. Data was analyzed and the change did not show statistical significance. Chromogranin A expression was also studied, which did not show any significant change in the treated organoids when compared to the control (Figure 26B).

Next, primers specific for stem cell markers (Lrig1, RUNX1, Troy, Oct-4 and CD 44) were used to study role of AhR activation on stem cell regulation (Figure 26B).

Lrig1 expressions in organoids were reduced in both the concentration of dioxin treatment with significant reduction in 0.1nM concentration. Dioxin treatment also showed significant reduction in CD44 expression for both the treatment conditions. These findings indicated that AhR activation decreased proliferation of Lrig1 and CD44+ stem cells and increased cellular differentiation.

RUNX1 expression did not show any change in 0.1 nM, but highly expressed in 1 nM treatment, though data was not statistically significant. Furthermore, the expression of Troy was also slightly increased in both the treated organoids, however the change was not significant. Thus, AhR activation did not show any significant change in RUNX1+ and Troy+ stem cells.

Lastly, Dioxin-activated AhR showed increase in Oct-4 expression (marker for self-renewal of stem cells) in both the dioxin concentrations, with significant increase in 0.1 nM treatment, which indicated that AhR activation enhanced self-renewal process in the progenitor cells present in the gastric organoids.

3.4 Effects of dioxin treatment on gastric mucosa

AhR is generally found to be expressed in many organs and only upon activation by specific ligands it is functional. Dioxin was a commonly used ligand by researchers for AhR activation for research purposes. It activates AhR and helps in transcription of metabolic enzymes depending on specific functions.

This study also tested effects of AhR activation *in vivo*. To activate AhR, mice were injected with dioxin (50 µg/kg) for 3 consecutive days and one day later sacrificed. Stomach tissues from control (n=3) and dioxin-treated (n=3) were then analyzed by lectin histochemistry and immunohistochemistry. Tissues were embedded as 3 individual pairs each having one control and one treated, positioned side by side to each other.

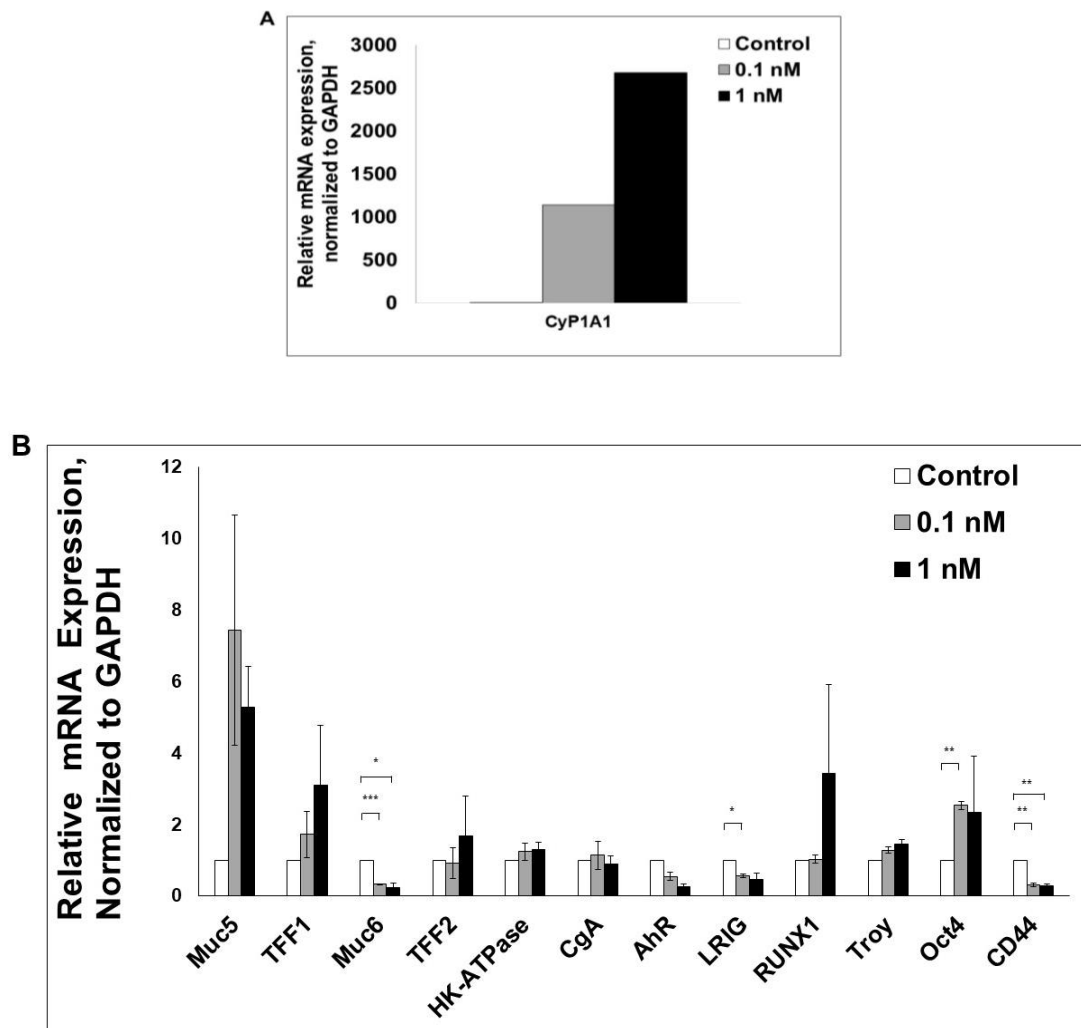


Figure 26: Effects of dioxin-activated AhR on mRNA expressions of gastric cell specific markers and gastric stem cell markers. A) Increase in CYP1A1 expression in the dioxin-treated organoids confirmed AhR activation. B) Expression of AhR was reduced in treated organoids. Surface mucous cell specific-Muc5AC and TFF1 showed higher expression in 0.1 nM and 1 nM dioxin treatment. MUC6 (specific for mucous neck cells) expression was significantly reduced in both the concentration of dioxin-treated organoids and TFF2 (also specific for mucous neck cells) expression decreased in 0.1 nM and increased in 1 nM treatment. Furthermore, H,K-ATPase expression was higher in the treated organoids than the control ones. Chromogranin A expression did not show any significant change in the treated organoids. Stem cell marker, Lrig1 expression was downregulated in both treatments with significant reduction in 0.1 nM. Moreover, CD44 expression (stem cell marker) was also significantly downregulated in both the dioxin treatment conditions and RUNX1 (stem cell marker) expression didn't show any change in 0.1 nM but upregulated in 1 nM treatment. Expression of Troy (stem cell marker) was also upregulated in dioxin-treated organoids. Lastly, Oct-4 expression (marker for stem cell self-renewal) was increased in both the concentrations of dioxin treatment, with significant increase in 0.1 nM treatment. Data were biological replicates of independent experiments. Bars represent the SEM. The asterisks indicate the significance of change in gene expression between the control and dioxin-treated organoids, * $p < 0.05$, ** $p < 0.01$, *** $p < 0.001$.

3.4.1 Characterization of AhR expression in stomach tissues

To test effects of dioxin activated AhR on stomach, it is important to test the expression of this receptor in stomach tissues. In this study, AhR expression was detected using immunohistochemistry in adult mice and rat stomach tissues.

3.4.1.1 AhR expression in adult mouse stomach

AhR expression was studied to test whether it is expressed in normal adult gastric glands. Stomach glands in mice are tubular and consist mostly of matured differentiated cells unlike the neonatal glands.

In the corpus glands, AhR was found to be expressed in nucleus, mostly in the middle of the glands with moderate cytoplasmic expressions (Figure 27A, 27B). This concluded that AhR was not only limited to progenitor cells but also expressed in differentiated cells, which was an indication that it may have a role in stem cell differentiation process.

3.4.1.2 AhR expression in rat stomach

In addition, this study also tested AhR expression levels in rat stomach (BrdU injected). BrdU-labelled cells were mostly located at the isthmus region (Figure 28A). Expression of AhR in rat stomach glands is nearly similar to expression in adult mouse glands and mostly expressed in the neck area near the base, localized both in cytoplasm and nucleus and few localized in the isthmus region (Figure 28B, 28C).

3.4.2 Effects of dioxin activated AhR *in vivo*

The last objective of this study was to test the effects of dioxin activated AhR *in vivo*. 21 days old mice were given daily injections of dioxin for three consecutive

days and sacrificed on the fourth day. The stomachs were then studied using immunohistochemistry and lectin histochemistry.

3.4.2.1 Detection of activated AhR expression in mouse liver

Firstly, liver tissue was examined to detect activated nuclear AhR as a positive control because it was well established that the liver is a target organ for dioxin. Both the control and dioxin-treated liver were processed together, embedded in same block, mounted on same slide and exposed to immunolabelling simultaneously.

The liver is mostly made up of hepatocytes with round nucleus with one or two nucleoli. Immunohistochemistry confirmed that in control liver, AhR expression was visible in both cytoplasm and nucleus but the intensity was weak (Figure 29A). In the treated liver, AhR-labelled nuclei were more in number and intensity was also higher than in the control tissue (Figure 29B). This finding was an indication that AhR was activated by dioxin treatment.

3.4.2.2 Detection of activated AhR expression in mouse stomach

AhR activation was tested in the stomach tissues using immunohistochemistry. Data in control stomach showed that, AhR expression was localized in both cytoplasm and nucleus of epithelial cells mostly in the middle region of the gland (Figure 30A). In the treated stomach, a similar pattern was observed but nuclear AhR expression was detected with higher intensity and more in numbers than the control tissue (Figure 30B), indicating that AhR was activated in the stomach by dioxin treatment. Data was supported by RT-qPCR showing significant increase in CYP1A1 gene expression (Figure 30C).

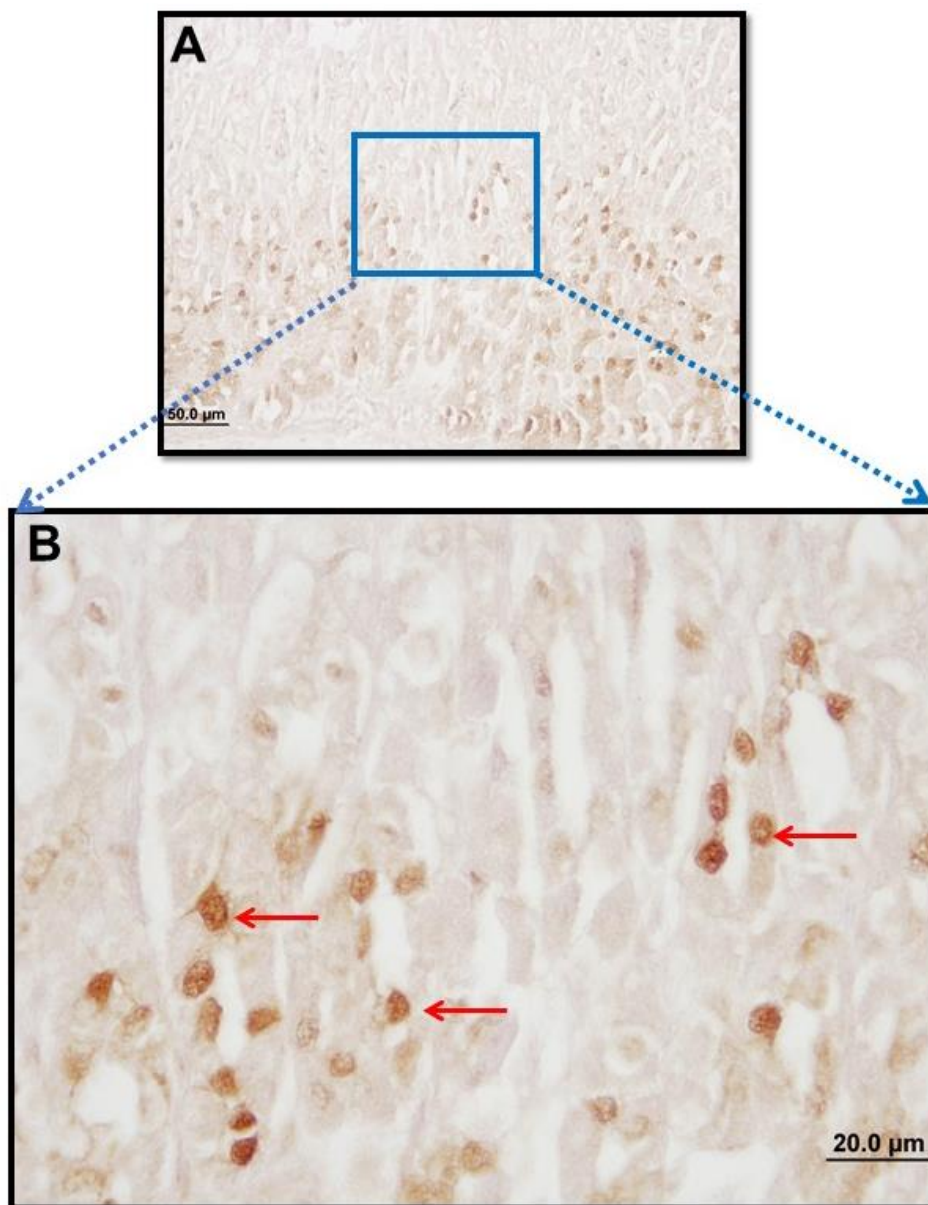


Figure 27: AhR expression in adult mouse stomach. A) Immunohistochemistry study showed that nuclear AhR expression was expressed in corpus glands mostly in the area above the base of the glands. Few cytoplasmic AhR was also detected. B) Higher magnification image of nuclear AhR expression (red arrows pointing towards nuclear AhR stain).

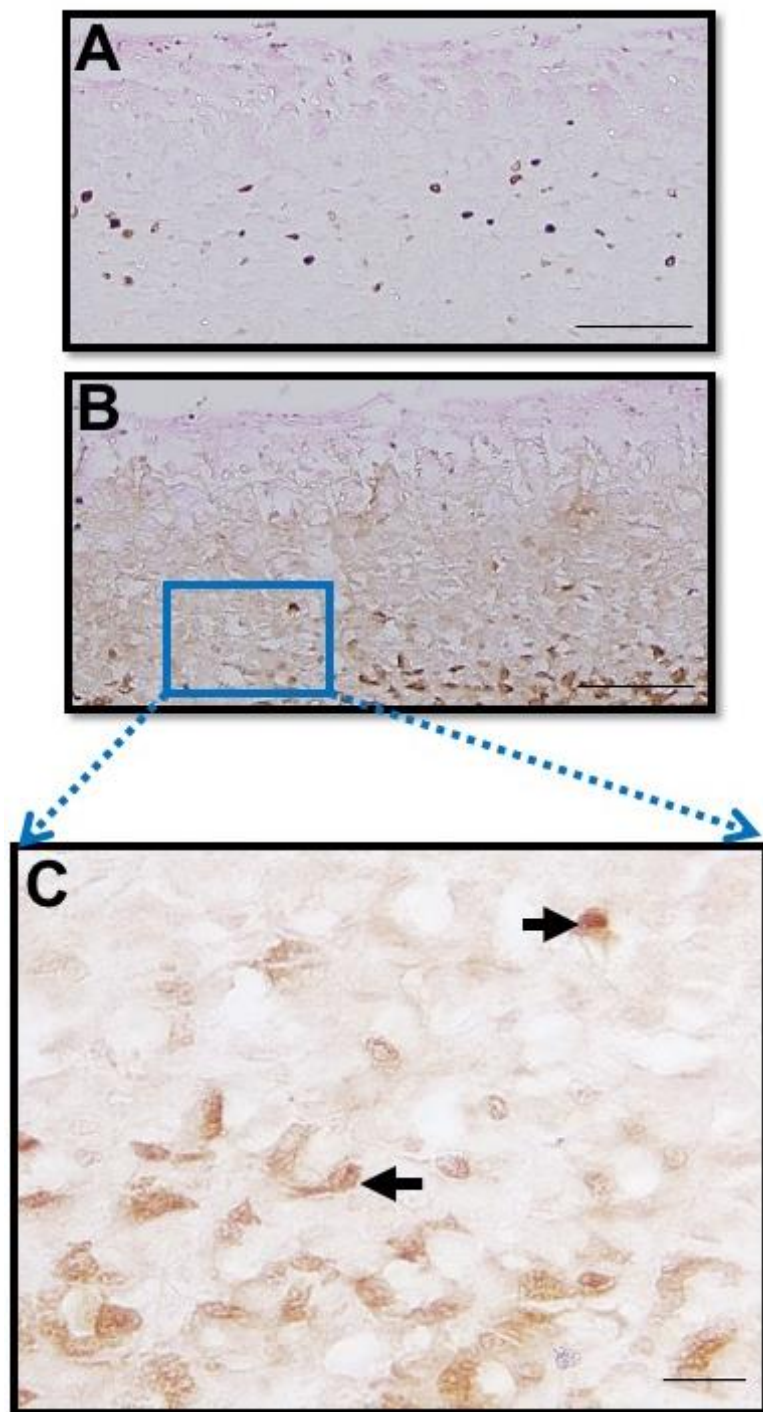


Figure 28: Immuno-labelling images of BrdU and AhR expression in rat stomach. A) BrdU-labelled proliferating cells (brown) were detected at the isthmus region. Bar=100 μ m. B) Cytoplasmic and nuclear AhR (Brown) was found in the neck area near the base, few cells with AhR expression were also detected near the isthmus region. Bar=100 μ m. C) higher magnification image of AhR expression. Bar=20 μ m.

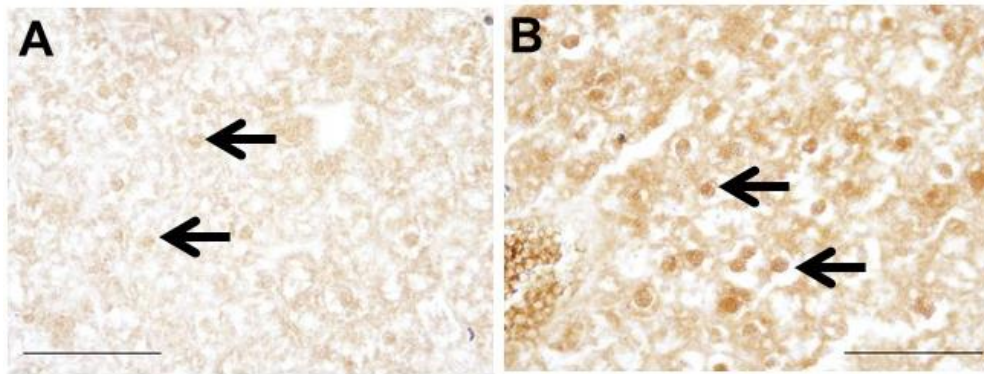


Figure 29: Dioxin-treated AhR activation in mouse liver. A) In control liver, both cytoplasmic and nuclear AhR expression (pointed with arrows) were visible but the intensity was less. B) In the treated liver, the number of nuclear AhR (pointed with arrows) was more and the intensity was also higher than the control tissue. Bar=100 μ m.

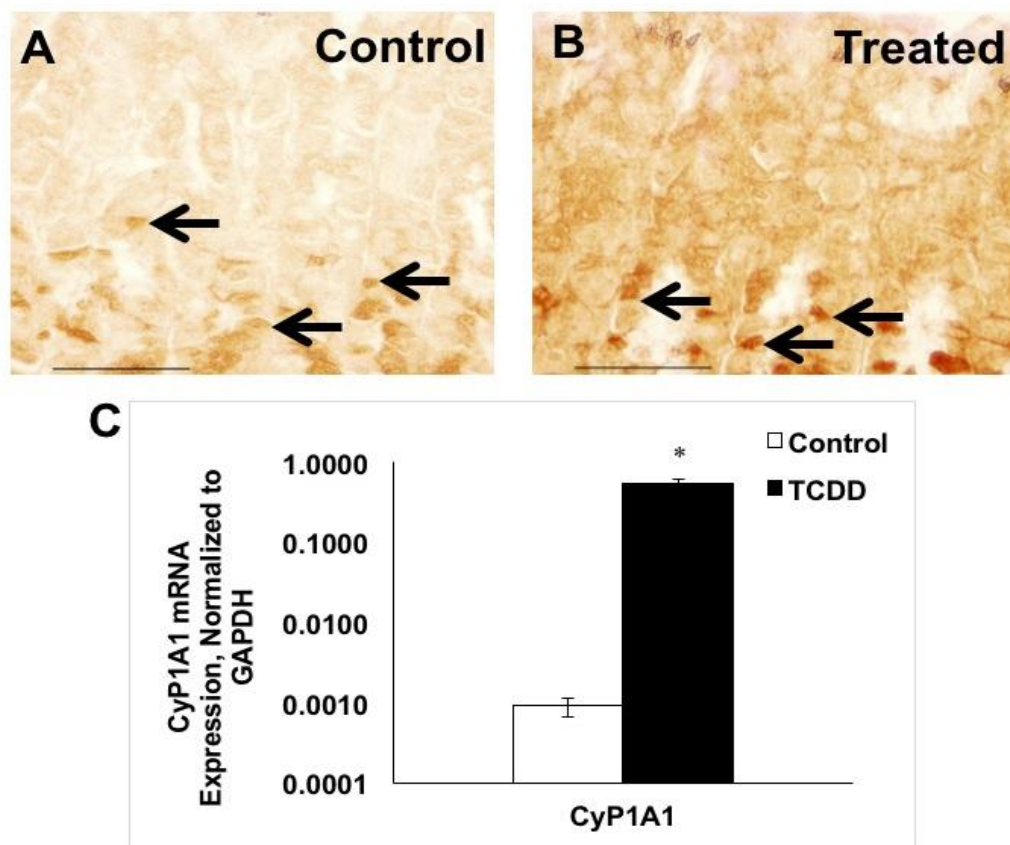


Figure 30: Dioxin-treated AhR activation in mouse stomach. A) Control stomach tissues showing AhR expression in cytoplasm and nucleus (arrows) in the middle region of the gland. B) In the treated stomach, highly intense nuclear AhR stain (arrows) was detected in the similar area compared to the control tissue (arrows).C) CyP1A1 expression was significantly increased. Bar=100 μ m.

3.4.2.3 Characterization of mucous cells in control and dioxin treated stomach

Lectin histochemistry was used to study the effects of AhR on surface mucous cells and neck cells. UEA-1 lectin was used for surface mucous cells, and GSII lectin was used for neck cells. In control stomach, UEA-1 stained the cells at the epithelial lining and the luminal surface (Figure 31A). GSII stained epithelial cells in the middle of the glands which correspond to the neck cells at the neck region (Figure 31C). The treated stomach showed a reduction in the intensity of UEA-1 staining of surface mucus cells (Figure 31B). The GSII labeling in dioxin-treated stomach also showed a decrease in the staining intensity (Figure 31D). To quantify the data, statistical analysis was done for the staining intensities to compare between the control and treated stomachs (Figure 31E, 31F). Therefore, with the recent data it was not possible to detect significant effects for AhR on surface mucous cells and neck cells.

3.4.2.4 Characterization of parietal cells in control and dioxin treated stomach

Immunohistochemistry was used to examine whether dioxin activated AhR has any effects on the parietal cells using antibody against H,K-ATPase. Immunostaining intensity of parietal cells was analyzed. In control stomach, H,K-ATPase parietal cells were detected throughout the gland from pit region (near to lumen) to base (near to muscle layer) (Figure 32A). There was a reduction in the labelling intensity of parietal cells exposed to dioxin (Figure 32B). The data was statistically analyzed, which showed that AhR may not have significant but moderate effects on parietal cells (Figure 32C).

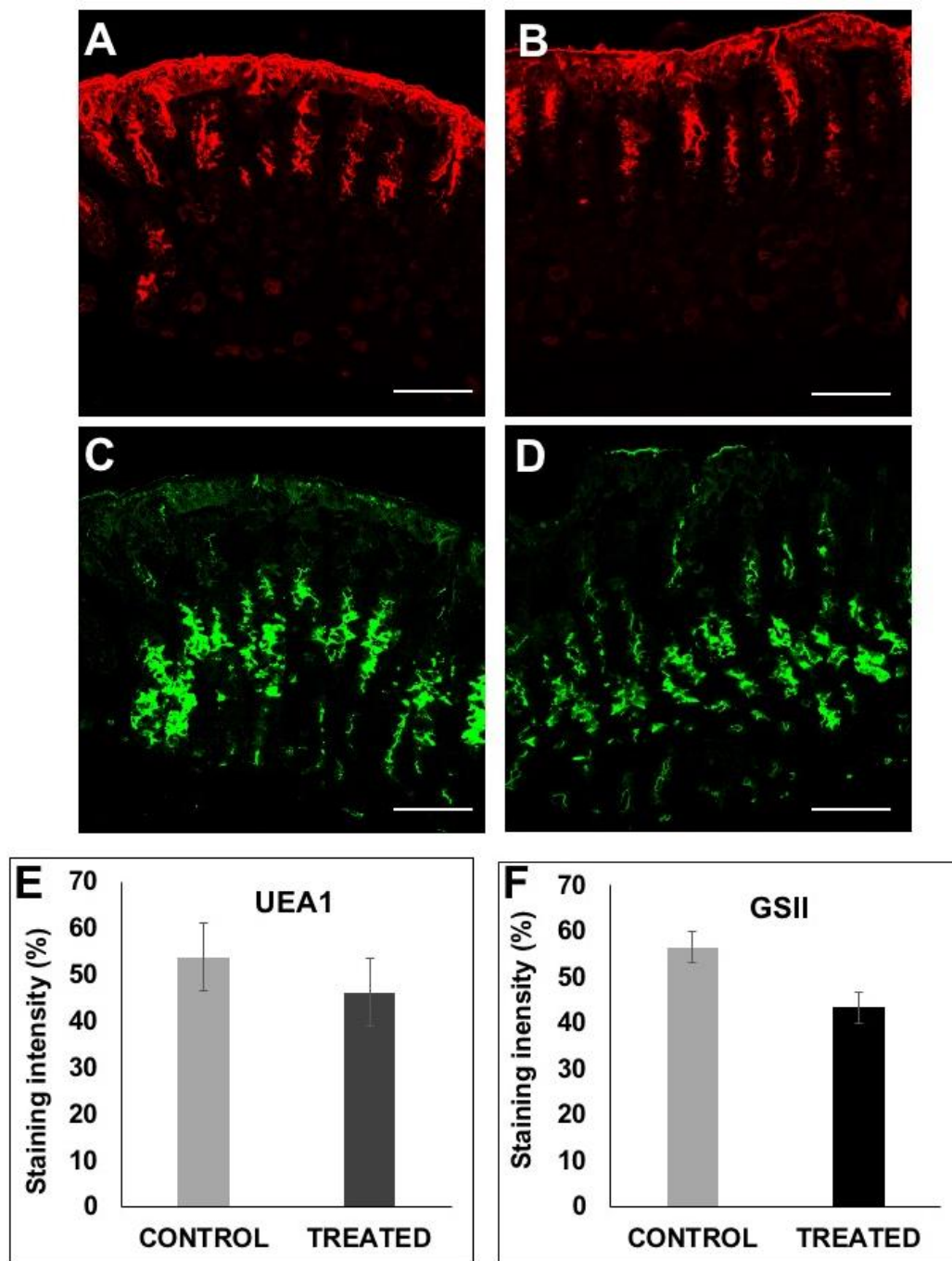


Figure 31: Effects of dioxin treatment on mucous cells. A), C) In the control stomach, rhodamine-conjugated UEA-1 lectin detected surface mucous cells (red), and fluorescein isothiocyanate-conjugated GSII lectin detected neck mucous cells (green) in the gastric mucosa. B), D) In the treated stomach, there was a reduction in the intensity of UEA-1 staining and the GSII staining respectively. The graphs E and F showed the percentages of labelling intensity of UEA-1 and GSII in control and treated stomach respectively. Data was presented as mean \pm SEM. Bar=50 μ m.

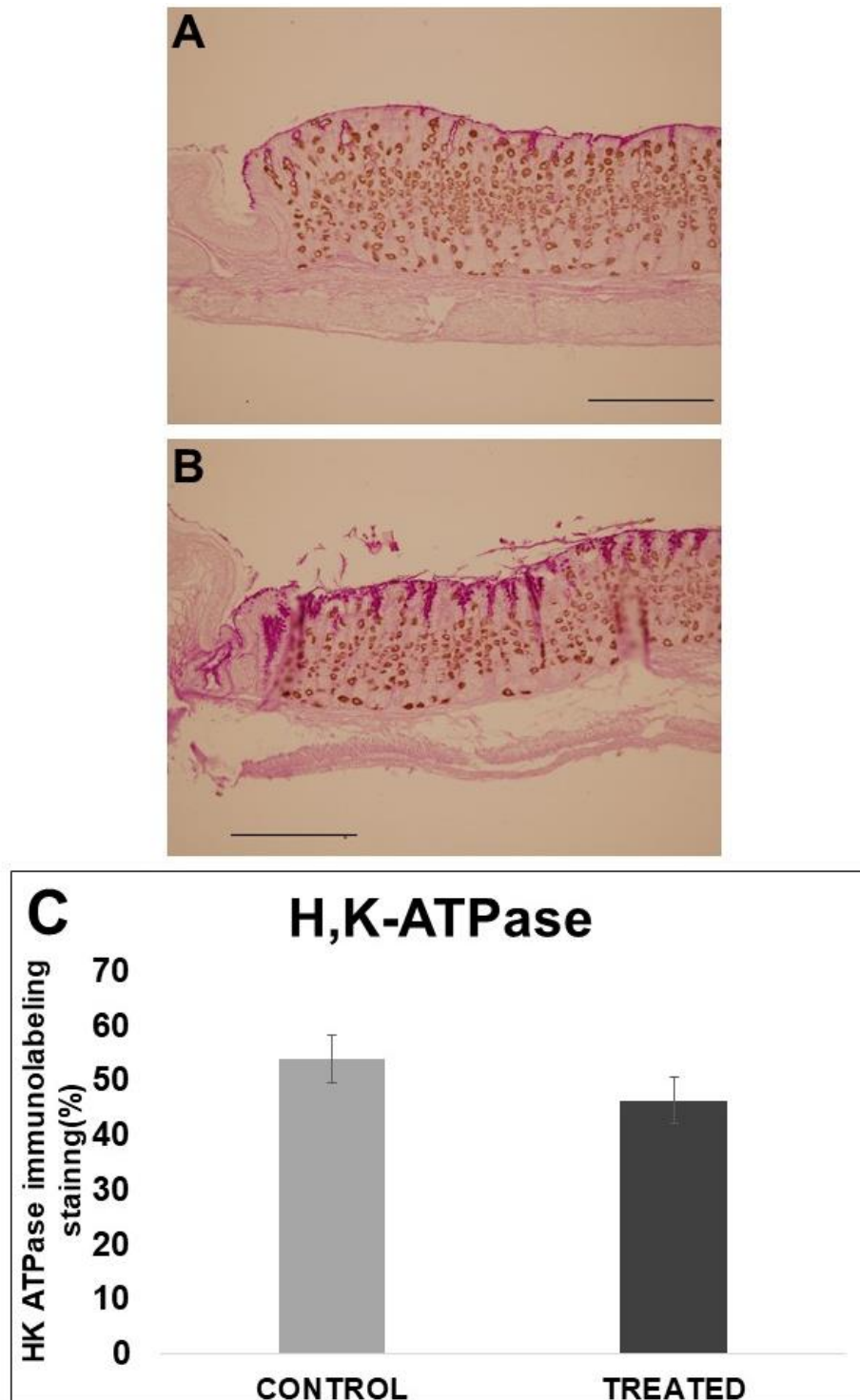


Figure 32: Effects of dioxin treatment on parietal cells. A) In control stomach, H,K-ATPase+ parietal cells (brown color) were detected throughout the gland from pit region to base. Tissues were counterstained with PAS. B) In the treated stomach, the number of parietal cells was similar to control, but the labelling intensity showed moderate reduction. Bars=100 μ m. C) The graph showed the staining intensity differences between H,K-ATPase+ cells in control and treated stomachs. Data are presented as mean \pm SEM.

Chapter 4: Discussion

In this study, two novel types of organoid models were developed: one from the mGS cells and the other from neonatal stomach glands. These models will be an addition to the available models used by scientists previously to study gastric stem cells and their role in the differentiation of gastric epithelial cells and gastric cancer development.

Following their characterization, gastric organoids were used to study effects of dioxin activated AhR on gastric stem cells, which will also open a door in research on gastric cancer development as gastric stem cells and AhR are believed to be involved in carcinogenesis. This idea was based on some previous studies demonstrating upregulation of AhR in cancer tissues and augmentation of stem cells during cancer development. It is still questionable how the factors are involved and whether the effects are cancer driven or inhibitory.

4.1 Gastric organoids from mGS cells

The mGS cells are cloned immortal cells developed from a mouse model with amplified progenitor cells. These cells have some important morphological and molecular characteristic features similar to gastric progenitor cells. They have large nucleus-to-cytoplasm ratio, nucleus with reticulated nucleoli and abundant euchromatin, cytoplasm containing many free ribosomes, a few small cisternae rough endoplasmic reticulum, scanty mitochondria, and undeveloped Golgi apparatus. Furthermore, these cells express some stem cell markers such as Notch3, Oct-4, CD44 and DCLK1 (Al-Marzoqee et al., 2012; Giannakis et al., 2008). Thus, these cells can be a good alternative source to study stem cells. Previously, these cells were characterized in two-dimensional culture. However, recently, demands on 3D cell

culture models for stem cell research is increasing because of its high efficiency towards mimicking *in vivo* conditions and for possible use in tissue engineering. Recently, a study on the mGS cells were cultured on 3D electrospun microfibrinous polycaprolactone scaffolds and maintained for upto 9 days. This culture conditions supported their differentiation into surface mucous cells (Pulikkot et al., 2014). In the present study, the mGS cells were used to develop organoids which were maintained for upto 6 months.

In this study, two protocols were used to develop organoids from mGS cells. First one is hanging drop method. mGS cells were seeded in hanging drops of RPMI media and cells aggregated towards the bottom of the media drop and formed a small mass of cells. Cells were then transferred on agarose-coated 96-well plates for further growth. This technique is known as force floating technique. Within a month, the organoids grew larger in size with diameter of 400 μm . Organoids were maintained on agarose for upto four months and they grew even larger. Furthermore, cell viability tests and electron microscopic analysis on mGS cell-derived organoids indicated that the organoids were structured into live, healthy proliferating cells in the periphery with dead or degenerating cells at the center. Some of the cells on the periphery contained mucous granule-like structures, indicating sign of early differentiation. mGS cells were also capable of forming 3D organoids while seeded in matrigel. Therefore, using these 3D organoids could be another beneficial *in vitro* model for studying gastric stem cells. They are reproducible and made of cells easily accessible. They develop in conventional media without a need for growth factors.

4.2 Gastric organoids from neonatal mouse gastric glands

The second organoid model was developed from freshly isolated stomach glands of 4-day old neonatal mice using matrigel technique. Neonatal stomach glands are mostly composed of proliferating progenitor cells with few poorly differentiated surface mucous cells, neck mucous cells and parietal cells and they lack zymogenic cells (Karam & Leblond 1995).

The first 3D primary gastrointestinal organoid models were established from intestinal glands (Sato & Clevers, 2013) using the matrigel technique along with a mix of growth factors including R-spondin-1, noggin, and FGF-10. Using a similar protocol, stomach organoids were developed from corpus glands of the gastric mucosa (Barker et al., 2010; Stange et al., 2013). These previously established models of organoids were reported using only adult mouse stomach. The present study was designed to develop gastric organoid models from “neonatal” glands as these glands are mostly made up of immature progenitor cells. This 3D model will be helpful for future studies on gastric stem cell dynamics and differentiation pathways based on the fact that neonatal gastric glands mostly consist of progenitor cells.

Immature glands were isolated from neonatal mouse and seeded in matrigel in the presence of growth factors important for stem cell proliferation and differentiation during stomach development. Cells from glands organized themselves into spherical organoids with a lumen at the center by day one and they were maintained up to day 10. Cell viability tests on these organoids showed that almost all the cells in the organoids were live with only few dead cells at the center.

To demonstrate that organoids originate mostly from stem/progenitor cells, some of the organoids were grown from BrdU-injected neonatal mice. This could help

to track the proliferating progenitor cells during the organoid development. Immunohistochemistry revealed that organoids were having BrdU-labelled cells even up to day 4, which was an indication of continuous proliferation of progenitor cells while progressing towards differentiation. Some of the BrdU labelled cells were also present at the center in the lumen of the organoids, which indicates the short lifespan of progenitor cells as previously shown in the mouse stomach (Karam, 1993). These findings provide an evidence for the generation of the organoids from progenitor stem cells as suggested by previous studies. (Barker et al., 2010)

Furthermore, UEA-1 lectin histochemistry confirmed the presence of surface mucous cells and H,K-ATPase synthesizing cells were also detected using immunohistochemistry in 3D primary organoids. This data was supported by RT-qPCR analysis on organoids at day 2. 2-day old organoids showed mRNA expressions of surface mucous cell specific Muc5AC and TFF1 as well as parietal cell specific H,K-ATPase, which is an indication that stem cells differentiated to surface mucous cells and H,K-ATPase producing cells by day 2. The expressions of Muc5AC and TFF1 were comparatively higher than that of day 8 and day 10. This data suggested that because of the short lifespan of surface mucous cells some cells that are generated at day 2 started to degenerate during the later days. There is also a possibility that some cells were probably there from day 0 in the glands while they were extracted, but it is very unlikely that the differentiated cells will survive in the culture for two days. H,K-ATPase and CgA expressions were low at day 4 and 10. This could be an indication that cells were initially differentiated towards H,K-ATPase producing cells and endocrine cells, but the culture conditions were not suitable for the survival for these cells. Another reason for these findings can be supported by the idea proposed by some previous studies that some differentiated cells were already there from day 0, along

with the proliferating progenitor cells (Burkitt, Duckworth, Williams, & Pritchard, 2017), though it is not expected that the differentiated cells from the glands will survive.

Organoids at day 4 and day 10 showed expressions of MUC6 and TFF2 (specific for neck mucous cells), which was undetectable and low respectively at day 2. Thus, the progenitor stem cells in the organoids were also differentiated towards the mucous neck cells. Cells in the organoids were also tested for pepsinogen expression, which was very low or undetectable.

These organoid models can be used to assess detailed early differentiation steps towards mucous cells and parietal cells.

4.3 Effects of AhR activation on gastric stem cells and gastric cancer *in vivo* and *in vitro*

In the present study, the effects of dioxin-activated AhR on gastric stem cells were tested using organoids and *in vivo* using mouse. As a first step, AhR expression was tested in gastric epithelial cells, tissues and organoids.

Immunohistochemical analysis revealed that AhR was found to be expressed in the mGS cells, mouse and rat stomach tissues and also in gastric organoids. Both nuclear and cytoplasmic AhR were detected.

AhR is a well-known factor for its role in pathogenesis of cancer development. Recently, researchers also tested variations in the expression level of cytoplasmic and activated nuclear AhR in the human gastric cancer tissues. One of such study showed that AhR expression is inhibited in the presence of *H. pylori* in *H. pylori*-related gastric cancer (Zhu et al., 2018). Therefore, this study also tested the expression levels of AhR

in human tissues of different conditions starting from normal to gastritis to tumor tissues respectively. In this study, gastric mucosal tissues were collected from the pyloric region of patients at Tawam Hospital undergoing endoscopy (n=89) for the examination of recurrent upper gastrointestinal symptoms, or gastrectomy (n=3) for adenocarcinoma. All patients gave written informed consent prior to the study. Following the endoscopic or surgical procedures, biopsies or cancer tissues (taken from 3 areas: tumor, tumor edge and from the safe margin) were processed for immunohistochemistry (Al-Marzoqee et al., 2012). For the AhR expression study, 3 sets of tissues were chosen from 3 different patients for each condition (normal, gastritis, tumor, safe margin).

Immunohistochemistry revealed that with the increasing progression of gastric cancer, the level of AhR expression increased. In normal tissues, the AhR expression was very low or undetectable (Figure 33A), while in gastritis tissues mild expression of nuclear AhR was detected in the pit area of the glands (Figure 33B). In the safe margin region, which is most likely the nearby area to the tumor, AhR expression (both nuclear and cytoplasmic) was increased (Figure 33C). Moreover, the staining intensity of nuclear AhR was higher in tumor tissues and localized in both basal and epical surface (Figure 33D). These data supported the previous evidences on the role of AhR expression and its involvement in gastric cancer development. These data can also be co-related with the results from a previous study on the same tissues that showed upregulation of self-renewal gene Oct-4 in the similar areas during the progression of the cancer (Al-Marzoqee et al., 2012), indicating that AhR plays a role in the stem cell self-renewal.

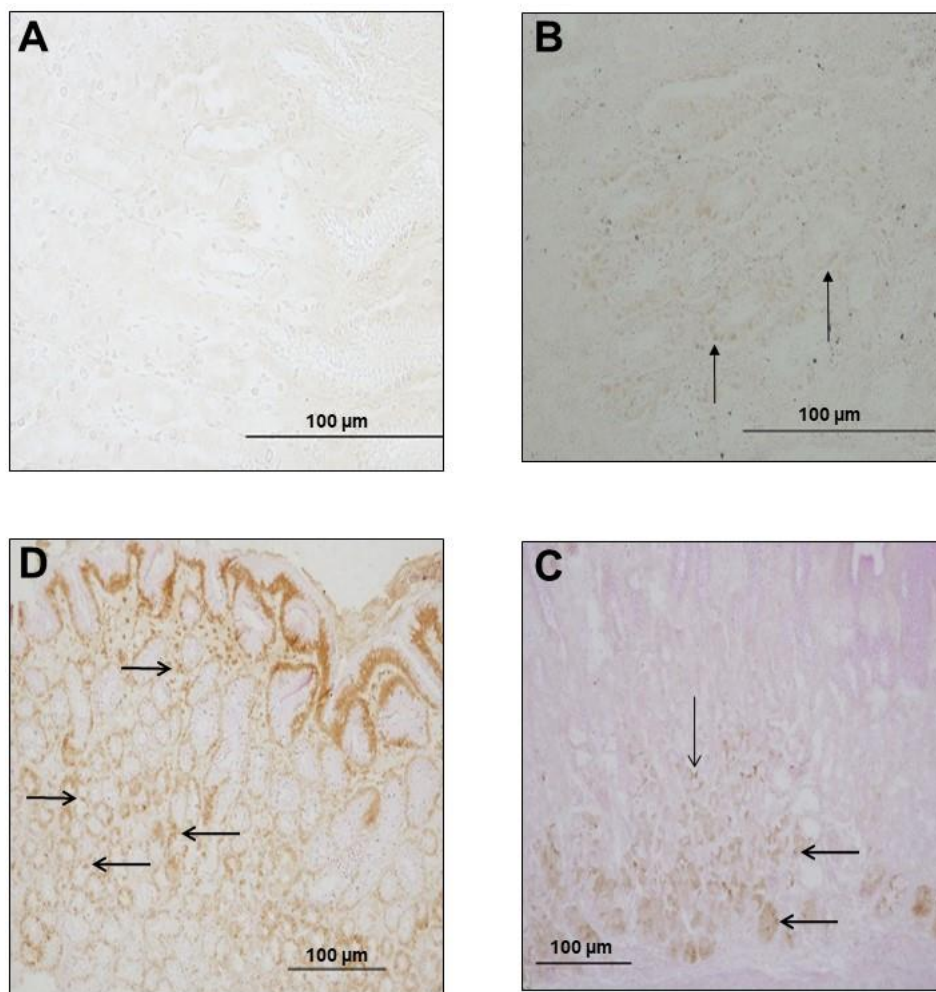


Figure 33: AhR expression in human tissues (normal, gastritis and tumor). A) AhR expression was very low or undetectable in the normal tissues. B) In gastritis tissues, mild expression of nuclear AhR was observed in the pit area of the glands (arrows). C) In the safe margin region, nuclear and cytoplasmic AhR expression were detected (arrows). D) Compared to other regions, tumor area showed highly intense expression of nuclear AhR (arrows). Bar=100 μ m.

4.3.1 Effects of AhR activation on gastric organoids

AhR mRNA is normally expressed in many human tissues with high expressions in liver, pancreas, lungs, spleen, placenta and relatively low in brain, skeletal muscles and heart (Jiang et al., 2010; Spence et al., 2011). Both protein and mRNA AhR expressions have also been reported in placentas of mouse and rabbits. as

well as in fetal tissues (high expressions in lungs, liver, kidneys, pancreas, testicles, esophagus, thymus glands, retinas, and epithelial cells and comparatively low levels in the heart, brain, choroids, thoracic aorta, and sclera) (Jiang et al., 2010). The distribution of intracellular AhR expressions changes significantly with age. AhR has been studied mainly in the environmental toxicological field because of its role in mediating xenobiotic metabolism and environmental responses (Yi et al., 2018).

Recently, studies also started investigating the involvement of activated AhR in maintenance of stem cell homeostasis, which was first suggested by Singh et al., (2019). Their study showed that, the AhR expression was vital for the proper maintenance of quiescence in HSCs and AhR down-regulation was needed for “escape” from quiescence state and subsequent proliferation of HSCs. Another study on skin stem cells proposed that activated AhR altered stem cell proliferation and differentiation towards the epidermal pathway at the expense of hair follicle and sebaceous gland cells (Arnold & Watt, 2001; Panteleyev & Bickers, 2006). Adding to it, previous studies have also revealed that AhR was an important regulatory factor in neural development, indicated by expression of both AhR and ARNT genes in the embryonic neuroepithelium as well as neural stem cells. Studies on AhR-KO mice proposed that AhR was important for development and/or maintenance of this neuronal population. Together, these studies supported the positive contribution of AhR activation in neurogenesis through regulation of neural stem cells and neuronal precursor cells (Abbott et al., 1995; Abbott & Probst, 1995; Collins et al., 2008; Williamson et al., 2005).

Using different mouse models, scientists also suggested that AhR play a significant role in intestinal homeostasis. The study discovered that AhR influenced

the regeneration of intestinal epithelial cells (IECs) upon injury and removal of AhR in IECs resulted in uncontrollable cell proliferation and reduced differentiation. Whereas, ligand-bound activated AhR restored ISC's homeostasis maintaining the niche and was also able to block tumorigenesis (Metidji et al., 2018). These findings supported the need for studying role of AhR in stomach stem cell homeostasis, as stomach and intestine are inter-connected through common developmental pathways and there is lack of information on its role on gastric stem cell regulation and tissue development. Therefore, this study focused on studying the role of AhR on gastric stem cells using organoids.

Two days incubation of gastric organoids with dioxin induced AhR activation as indicated by upregulation of its target gene, cytochrome p450. This was associated with upregulation of Muc5AC and TFF1 (specific for surface mucous cells) and parietal cell specific-H,K-ATPase, indicated by lectin histochemistry and PCR. Following, dioxin treatment significantly decreased the cell differentiation towards neck mucous cells, indicated by significant down regulation of MUC6 mRNA expressions. Therefore, dioxin-activated AhR plays an important role in differentiation directions of progenitor proliferating cells towards mucous neck cells.

This study tested role of dioxin-activated AhR on gastric stem cells using RT-qPCR. mRNA expressions of various stem cell markers (Lrig1, RUNX1, Troy, Oct-4 and CD44) were examined in dioxin-treated organoids. Dioxin treatment significantly reduced the Lrig1 expression, which can be an indication that dioxin treatment reduced the proliferation of Lrig1+ cells. Moreover, RUNX1 and Troy expressions were upregulated in the treated organoids. Though the change was not statistically significant.

Moreover, present data showed that AhR activation enhanced self-renewal process in the progenitor cells indicated by the significant upregulation of the Oct-4 gene in the gastric organoids. This data was supported by information from previous studies demonstrating that Oct-4 is involved in the self-renewal of undifferentiated embryonic stem cells by investigating the target genes using genomic scale location analysis (chromatin immunoprecipitation coupled with DNA microarrays) (Laurie et al., 2005). Thus, in the present study, Oct-4 was used as a marker for self-renewal process for stem cells.

Following, CD44+ (a marker for gastric stem cells) expressions were significantly downregulated in dioxin-treated organoids compared to the control. Thus, dioxin-activated AhR reduced number of CD44+ cells in the gastric organoids.

These findings indicated that the gastric organoid established in this study is a useful model to study cell proliferation and differentiation and require future analysis on this AhR to study its regulatory role on gastric stem cell control and differentiation studies.

4.3.2 Role of AhR activation *in vivo*

Dioxin-dependent effects of AhR were first identified in skin and liver cancers (Barouki et al., 2007; Ikuta et al., 2013). Thus, in this study, AhR activation was first confirmed by detecting activated AhR expression in liver. According to AhR functional pathway, activated AhR should be detected in the nucleus as it acts as a transcription factor. Immunohistochemistry revealed more nuclear AhR expression in the dioxin-treated liver, which confirmed the activation AhR in liver. Then stomach

was also examined for AhR activation, which was confirmed by intense nuclear AhR staining and increased CYP1A1 gene expression in the dioxin treated stomach.

Present study investigated the role of activated AhR on surface mucous cells, neck cells and parietal cells. lectin histochemical analysis for surface mucous cells and neck cells showed that dioxin mediated AhR activation reduced the intensity of the stains. In addition, it also reduced the intensity of H,K-ATPase staining in the parietal cells. Though the effects were not significant, data from mucous neck cells somehow correlated with significant data from the organoid experiment. These findings indicated that dioxin-activated AhR has a significant role in gastric stem cell regulation and differentiation.

Following the present provided data, more future experiments can be conducted using organoid models as these mimic *in vivo* conditions. These organoid models are more suitable than animal models for experimental purposes as less animals can be used or harmed specially when considered to be tested by injecting harmful agents.

Chapter 5: Conclusion

In this study, two types of gastric organoids were developed. For the first one, mGS cells were used with hanging drop method and the second was from neonatal stomach glands using matrigel. Organoids grow in size with time. Cell labeling showed that both organoids maintain live cells at the periphery and dying cells at the center. Cells of primary organoids differentiate to form mucus-secreting cells. Organoids were used to test the role of AhR on gastric stem cells. AhR activation with dioxin enhanced the capability of stem cells for self-renewal and reduced their differentiation towards mucus-secreting neck cells (Figure 34). Reduction in mucus-secreting neck cells correlated with results of dioxin injection into mice and with the upregulation of AhR during gastric carcinogenesis.

This study provides novel findings regarding the generation of two new types of gastric organoids and also new insights into involvement of AhR in stem cell regulation which could provide some explanation for its role in gastric cancer progression. These data will be useful not only for gastric cell biologists and molecular biologists, but also for gastroenterologists and gastrointestinal surgeons making decisions regarding diagnosis and staging of gastric cancer, the most fatal and second most common cancer among gastrointestinal tumors.

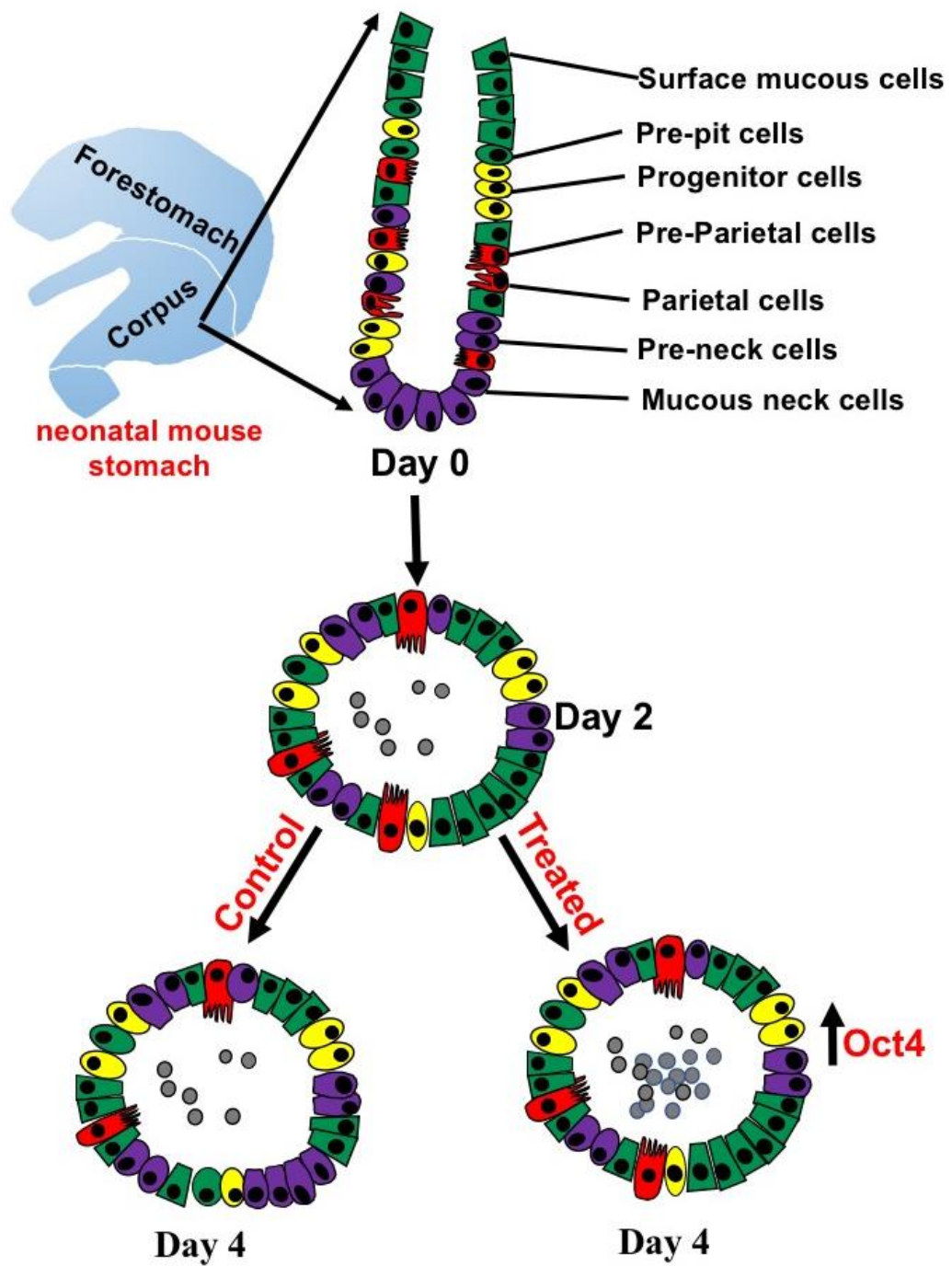


Figure 34: Illustration of overall findings on role of AhR on gastric organoids. Dioxin-activated AhR increased cell self-renewal and decreased cell differentiation in the gastric organoids towards mucous neck cells.

Chapter 6: Future Prospective

Organoids are novel representative models that mimic *in vivo* conditions and can be used for studying stem cells either involved in organ development or in pathogenesis of various diseases. Therefore, these models open up great possibilities in the field of biomedical research for modelling diseases, regenerative medicine, testing new therapeutic approaches and other biological studies.

In this study, the first organoid model from mGS cells will be a useful model to study the cell renewal process, as the cells continuously proliferate in the organoid with live and healthy cells organized at the periphery and dead cells accumulated at the center. These models can also be used for long term research purposes as these organoids can be maintained for many months.

Moreover, this study is the first to generate organoids from neonatal gastric glands. It would be interesting to compare the characteristic features of these organoids with ones from adult glands as the neonatal glands consist mostly of stem/progenitor cells.

Most of the cells detected in the neonatal gland-derived organoids at day 4 were mucous cells. However, some possible strategies can be tested further to drive the differentiation towards parietal cells which may include: 1) co-culturing the organoids with immortal mesenchymal stem cells or freshly isolated bone-marrow mesenchymal stem cells, 2) co-culturing with fibroblasts, 3) extracting parietal cells from adult glands and seeding them with neonatal glands, these adult parietal cells could be the source of factors that drive differentiation into parietal cells as previously suggested and 4) adding BMP or GSK3 β inhibitor CHIR99021 to induce H,K-ATPase

gene expression. All the above-mentioned conditions could be directly or indirectly involved in stem cell differentiation.

These gastric organoids can also be used to model overexpression or knockdown of stem cell-specific genes to study effects on cell proliferation and differentiation. They can also be used to model gastric cancer and study stem cell role in cancer development, as previous evidences suggest their possible involvement in carcinogenesis. Finally, these organoids will be useful to model microbial infections (bacterial and viral) and testing potential drugs or compounds involved in their repair capacity.

References

- Abbott, B. D., Birnbaum, L. S., & Perdew, G. H. (1995). Developmental expression of two members of a new class of transcription factors: I. Expression of aryl hydrocarbon receptor in the C57BL/6N mouse embryo. *Dev. Dyn.*, *204*(2), 133-143. doi:10.1002/aja.1002040204
- Abbott, B. D., & Probst, M. R. (1995). Developmental expression of two members of a new class of transcription factors: II. Expression of aryl hydrocarbon receptor nuclear translocator in the C57BL/6N mouse embryo. *Dev. Dyn.*, *204*(2), 144-155. doi:10.1002/aja.1002040205
- Al-Marzooqee, F., Khoder, G., Al-Awadhi, H., John, R., Beg, A., Vincze, A., Karam, S. et al. (2012). Upregulation and inhibition of the nuclear translocation of Oct-4 during multistep gastric carcinogenesis. *Inter. J. of Oncology*, *41*(5), 1733-1743. doi:10.3892/ijo.2012.1608
- Allan, L. L., & Sherr, D. H. (2005). Constitutive activation and environmental chemical induction of the aryl hydrocarbon receptor/transcription factor in activated human B lymphocytes. *Mol. Pharmacol.*, *67*(5), 1740-1750. doi:10.1124/mol.104.009100
- Andersson, P., McGuire, J., Rubio, C., Gradin, K., Whitelaw, M. L., Pettersson, S., Poellinger, L. et al. (2002). A constitutively active dioxin/aryl hydrocarbon receptor induces stomach tumors. *Proc. Natl. Acad. Sci. USA*, *99*(15), 9990-9995. doi:10.1073/pnas.152706299
- Ang, T. L., & Fock, K. M. (2014). Clinical epidemiology of gastric cancer. *Singapore Med. J.*, *55*(12), 621-628. doi:10.11622/smedj.2014174
- Arnold, I., & Watt, F. M. (2001). c-Myc activation in transgenic mouse epidermis results in mobilization of stem cells and differentiation of their progeny. *Curr. Biol.*, *11*(8), 558-568. doi:10.1016/s0960-9822(01)00154-3
- Arnold, K., Sarkar, A., Yram, M. A., Polo, J. M., Bronson, R., Sengupta, S., Hochedlinger, K. et al. (2011). Sox2(+) adult stem and progenitor cells are important for tissue regeneration and survival of mice. *Cell Stem Cell*, *9*(4), 317-329. doi:10.1016/j.stem.2011.09.001
- Avramopoulos, D., Cox, T., Blaschak, J., Chakravarti, A., & Antonarakis, S. (1992). Linkage mapping of the aml1 gene on human chromosome 21 using a dna polymorphism in the 3' untranslated region. *Genomics*, *14*(2), 506-507. doi:10.1016/s0888-7543(05)80253-8
- Barker, N., Huch, M., Kujala, P., van de Wetering, M., Snippert, H. J., van Es, J. H., Clevers, H. et al. (2010). Lgr5(+ve) stem cells drive self-renewal in the

- stomach and build long-lived gastric units in vitro. *Cell Stem Cell*, 6(1), 25-36. doi:10.1016/j.stem.2009.11.013
- Barker, N., van Es, J. H., Kuipers, J., Kujala, P., van den Born, M., Cozijnsen, M., Clevers, H. et al. (2007). Identification of stem cells in small intestine and colon by marker gene *Lgr5*. *Nature*, 449(7165), 1003-1007. doi:10.1038/nature06196
- Barouki, R., Coumoul, X., & Fernandez-Salguero, P. M. (2007). The aryl hydrocarbon receptor, more than a xenobiotic-interacting protein. *FEBS Lett.*, 581(19), 3608-3615. doi:10.1016/j.febslet.2007.03.046
- Bartfeld, S., Bayram, T., van de Wetering, M., Huch, M., Begthel, H., Kujala, P., Clevers, H. et al. (2015). In vitro expansion of human gastric epithelial stem cells and their responses to bacterial infection. *Gastroenterology*, 148(1), 126-136.e126. doi:10.1053/j.gastro.2014.09.042
- Bjerknes, M., & Cheng, H. (2002). Multipotential stem cells in adult mouse gastric epithelium. *Am. J. Physiol. Gastrointest. Liver Physiol.*, 283(3), 767-777. doi:10.1152/ajpgi.00415.2001
- Boyer, Lee, T., Cole, M., Johnstone, S., Levine, S., Zucker, J., Young, et al. (2005). Core Transcriptional Regulatory Circuitry in Human Embryonic Stem Cells. *Cell*, 122(6), 945-957. doi:10.1016/j.cell.2005.08.020
- Braunstein, E. M., Qiao, X. T., Madison, B., Pinson, K., Dunbar, L., & Gumucio, D. L. (2002). Villin: A marker for development of the epithelial pyloric border. *Dev. Dyn.*, 224(1), 90-102. doi:10.1002/dvdy.10091
- Burkitt, M., Duckworth, C., Williams, J., & Pritchard, D. (2017). Helicobacter Pylori-Induced Gastric Pathology: Insights From in Vivo and Ex Vivo Models. *Disease Models & Mechanisms*, 10(2), 89-104 . doi:10.1242/dmm.027649
- Chen, M., Yokomizo, T., Zeigler, B., Dzierzak, E., & Speck, N. (2009). RUNX1 Is Required for the Endothelial to Haematopoietic Cell Transition but Not Thereafter. *Nature*, 457(7231), 887-891 doi:10.1038/nature07619
- Collins, L. L., Williamson, M. A., Thompson, B. D., Dever, D. P., Gasiewicz, T. A., & Opanashuk, L. A. (2008). 2,3,7,8-Tetracholorodibenzo-p-dioxin exposure disrupts granule neuron precursor maturation in the developing mouse cerebellum. *Toxicol. Sci.*, 103(1), 125-136. doi:10.1093/toxsci/kfn017
- Danjo, T., Eiraku, M., Muguruma, K., Watanabe, K., Kawada, M., Yanagawa, Y., Sasai, Y. et al. (2011). Subregional specification of embryonic stem cell-derived ventral telencephalic tissues by timed and combinatory treatment with extrinsic signals. *J. Neurosci.*, 31(5), 1919-1933. doi:10.1523/jneurosci.5128-10.2011

- de Lau, W., Barker, N., Low, T. Y., Koo, B. K., Li, V. S., Teunissen, H., Clevers, H. et al. (2011). Lgr5 homologues associate with Wnt receptors and mediate R-spondin signalling. *Nature*, *476*(7360), 293-297. doi:10.1038/nature10337
- Defetos, L. (1991). Chromogranin A: Its Role in Endocrine Function and as an Endocrine and Neuroendocrine Tumor Marker. *Endocrine Rev.*, *12*(2), 141-155. doi:10.1210/edrv-12-2-181
- Denison, M. S., & Nagy, S. R. (2003). Activation of the aryl hydrocarbon receptor by structurally diverse exogenous and endogenous chemicals. *Annu. Rev. Pharmacol. Toxicol.*, *43*, 309-334. doi:10.1146/annurev.pharmtox.43.100901.135828
- Diaz-Diaz, C. J., Ronnekleiv-Kelly, S. M., Nukaya, M., Geiger, P. G., Balbo, S., Dator et al., (2016). The aryl hydrocarbon receptor is a repressor of inflammation-associated colorectal tumorigenesis in mouse. *Ann. Surg.*, *264*(3), 429-436.. doi:10.1097/sla.0000000000001874
- Dorrell, C., Tarlow, B., Wang, Y., Canaday, P. S., Haft, A., Schug, J., Grompe, M. et al. (2014). The organoid-initiating cells in mouse pancreas and liver are phenotypically and functionally similar. *Stem Cell Res.*, *13*(2), 275-283. doi:10.1016/j.scr.2014.07.006
- Ehrmann, R. L., & Gey, G. O. (1956). The growth of cells on a transparent gel of reconstituted rat-tail collagen. *J. Natl. Cancer Inst.*, *16*(6), 1375-1403. doi:10.1093/jnci/16.6.1375
- Eiraku, M., Watanabe, K., Matsuo-Takasaki, M., Kawada, M., Yonemura, S., Matsumura, M., Sasai, Y. et al. (2008). Self-organized Formation of Polarized Cortical Tissues From ESCs and Its Active Manipulation by Extrinsic Signals. *Cell Stem Cell*, *3*(5), 519-532. doi:10.1016/j.stem.2008.09.002
- Ema, M., Ohe, N., Suzuki, M., Mimura, J., Sogawa, K., Ikawa, S., & Fujii-Kuriyama, Y. (1994). Dioxin binding activities of polymorphic forms of mouse and human arylhydrocarbon receptors. *J. Biol. Chem.*, *269*(44), 27337-27343 Retrieved from: <https://pubmed.ncbi.nlm.nih.gov/7961644/>
- Farook, V. S., Alkhalaf, M., & Karam, S. M. (2008). Establishment of a gastric epithelial progenitor cell line from a transgenic mouse expressing the simian virus 40 large T antigen gene in the parietal cell lineage. *Cell Prolif.*, *41*(2), 310-320. doi:10.1111/j.1365-2184.2008.00522.x
- Fatehullah, A., Tan, S. H., & Barker, N. (2016). Organoids as an in vitro model of human development and disease. *Nature Cell Biology*, *18*(3), 246-254. doi:10.1038/ncb3312

- Fell, H. B., & Robison, R. (1929). The growth, development and phosphatase activity of embryonic avian femora and limb-buds cultivated in vitro. *Biochem. J.*, 23(4), 767-784. doi:10.1042/bj0230767
- Fukaya, M., Isohata, N., Ohta, H., Aoyagi, K., Ochiya, T., Saeki, N., Sasaki, H. et al. (2006). Hedgehog signal activation in gastric pit cell and in diffuse-type gastric cancer. *Gastroenterology*, 131(1), 14-29. doi:10.1053/j.gastro.2006.05.008
- Giannakis, M., Chen, S. L., Karam, S. M., Engstrand, L., & Gordon, J. I. (2008). Helicobacter pylori evolution during progression from chronic atrophic gastritis to gastric cancer and its impact on gastric stem cells. *Proc. Natl. Acad. Sci. USA*, 105(11), 4358-4363. doi:10.1073/pnas.0800668105
- Guasch, G., & Fuchs, E. (2005). Mice in the world of stem cell biology. *Nature Genetics*, 37(11), 1201-1206. doi:10.1038/ng1667
- Han, M. E., & Oh, S. O. (2013). Gastric stem cells and gastric cancer stem cells. *Anat. Cell Biol.*, 46(1), 8-18. doi:10.5115/acb.2013.46.1.8
- Hanby, A. M., Poulsom, R., Singh, S., Elia, G., Jeffery, R., & Wright, N. (1993). Spasmolytic Polypeptide Is a Major Antral Peptide: Distribution of the Trefoil Peptides Human Spasmolytic Polypeptide and pS2 in the Stomach. *Gastroenterology*, 105(4), 1110-1116. doi:10.1016/0016-5085(93)90956-d
- Hashimoto, T., Schlessinger, D., & Cui, C. Y. (2008). Troy binding to lymphotoxin-alpha activates NF kappa B mediated transcription. *Cell Cycle*, 7(1), 106-111. doi:10.4161/cc.7.1.5135
- Hayakawa, Y., Fox, J. G., & Wang, T. C. (2017). The Origins of Gastric Cancer From Gastric Stem Cells: Lessons From Mouse Models. In *Cell Mol. Gastroenterol. Hepatol.* 3(3), 331-338. doi:10.1016/j.jcmgh.2017.01.013
- Helander, H. F. (1995). Inhibiting gastric H(+)-K(+)-ATPase activity by omeprazole promotes degeneration and production of parietal cells. *Am. J. Physiol.*, 268(2), G387-388. doi:10.1152/ajpgi.1995.268.2.G387
- Hill, D. R., & Spence, J. R. (2017). Gastrointestinal Organoids: Understanding the Molecular Basis of the Host-Microbe Interface. *Cell Mol. Gastroenterol. Hepatol.*, 3(2), 138-149. doi:10.1016/j.jcmgh.2016.11.007
- Hohenberger, P., & Gretschel, S. (2003). Gastric cancer. *Lancet*, 362(9380), 305-315. doi:10.1016/s0140-6736(03)13975-x
- Horrison, R., G. (1906). Observations on the living developing nerve fiber. *The Anatomical Record*, 1(5), 116-128. doi:10.3181/00379727-4-98

- Houghton, J., Stoicov, C., Nomura, S., Rogers, A. B., Carlson, J., Li, H., Wang, T. C. et al. (2004). Gastric cancer originating from bone marrow-derived cells. *Science*, *306*(5701), 1568-1571. doi:10.1126/science.1099513
- Huch, M., Dorrell, C., Boj, S. F., van Es, J. H., Li, V. S., van de Wetering, M., Clevers, H. et al. (2013). In vitro expansion of single Lgr5+ liver stem cells induced by Wnt-driven regeneration. *Nature*, *494*(7436), 247-250. doi:10.1038/nature11826
- Huch, M., Gehart, H., van Boxtel, R., Hamer, K., Blokzijl, F., Verstegen, M. M., Clevers, H. et al. (2015). Long-term culture of genome-stable bipotent stem cells from adult human liver. *Cell*, *160*(1-2), 299-312. doi:10.1016/j.cell.2014.11.050
- Ikuta, T., Kobayashi, Y., Kitazawa, M., Shiizaki, K., Itano, N., Noda, T., Kawajiri, K. et al. (2013). ASC-associated inflammation promotes cecal tumorigenesis in aryl hydrocarbon receptor-deficient mice. *Carcinogenesis*, *34*(7), 1620-1627. doi:10.1093/carcin/bgt083
- Ikuta, T., Namiki, T., Fujii-Kuriyama, Y., & Kawajiri, K. (2009). AhR protein trafficking and function in the skin. *Biochem. Pharmacol.*, *77*(4), 588-596. doi:10.1016/j.bcp.2008.10.003
- Ishimoto, T., Oshima, H., Oshima, M., Kai, K., Torii, R., Masuko, T., Nagano, O. et al. (2010). CD44+ Slow-Cycling Tumor Cell Expansion Is Triggered by Cooperative Actions of Wnt and Prostaglandin E2 in Gastric Tumorigenesis. *Cancer Science*, *101*(3), 673-678. doi:10.1111/j.1349-7006.2009.01430.x
- Ivascu, A., & Kubbies, M. (2006). Rapid generation of single-tumor spheroids for high-throughput cell function and toxicity analysis. *J. Biomol. Screen.*, *11*(8), 922-932. doi:10.1177/1087057106292763
- Jensen, K. B., & Watt, F. M. (2006). Single-cell expression profiling of human epidermal stem and transit-amplifying cells: Lrig1 is a regulator of stem cell quiescence. *Proc. Natl. Acad. Sci. USA*, *103*(32), 11958-11963. doi:10.1073/pnas.0601886103
- Jiang, Y., Wang, K., Fang, R., & Zheng, J. (2010). Expression of Aryl Hydrocarbon Receptor in Human Placentas and Fetal Tissues. *In J. Histochem. Cytochem* *58*(8), 679-685. doi: 10.1369/jhc.2010.955955
- Johnson, L. R. (1988). Regulation of gastrointestinal mucosal growth. *Physiol. Rev.*, *68*(2), 456-502. doi:10.1152/physrev.1988.68.2.456
- Jørgensen, K., Diamant, B., Jørgensen, K., & Thim, L. (1982). Pancreatic Spasmolytic Polypeptide (PSP): III. Pharmacology of a New Porcine Pancreatic

Polypeptide With Spasmolytic and Gastric Acid Secretion Inhibitory Effects. *Regulatory Peptides*, 3(3-4), 231-243. doi:10.1016/0167-0115(82)90128-8

- Karam, S. M. (1993). Dynamics of epithelial cells in the corpus of the mouse stomach. IV. Bidirectional migration of parietal cells ending in their gradual degeneration and loss. *Anat. Rec.*, 236(2), 314-332.. doi:10.1002/ar.1092360205
- Karam, S. M., & Alexander, G. (2001). Blocking of histamine H2 receptors enhances parietal cell degeneration in the mouse stomach. *Histol. Histopathol.*, 16(2), 469-480. doi:10.14670/hh-16.469
- Karam, S. M., Ansari, H. R., Al-Dhaheri, W. S., & Alexander, G. (2004). Retinol enhances differentiation of the gastric parietal cell lineage in developing rabbits. *Cell Physiol. Biochem.*, 14(4-6), 333-342. doi:10.1159/000080343
- Karam, S. M., Hassan, W. M., & John, R. (2005). Expression of retinoid receptors in multiple cell lineages in the gastric mucosae of mice and humans. *J Gastroenterol. Hepatol.*, 20(12), 1892-1899. doi:10.1111/j.1440-1746.2005.04064.x
- Karam, S. M., John, R., Alpers, D. H., & Ponery, A. S. (2005). Retinoic acid stimulates the dynamics of mouse gastric epithelial progenitors. *Stem Cells*, 23(3), 433-441. doi:10.1634/stemcells.2004-0178
- Karam, S. M., & Leblond, C. P. (1992). Identifying and counting epithelial cell types in the "corpus" of the mouse stomach. *Anat. Rec.*, 232(2), 231-246. doi:10.1002/ar.1092320208
- Karam, S. M., & Leblond, C. P. (1993). Dynamics of epithelial cells in the corpus of the mouse stomach. I. Identification of proliferative cell types and pinpointing of the stem cell. *Anat. Rec.*, 236(2), 259-279. doi:10.1002/ar.1092360202
- Karam, S. M., Li, Q., & Gordon, J. I. (1997). Gastric epithelial morphogenesis in normal and transgenic mice. *Am. J. Physiol.*, 272(5), G1209-1220. doi:10.1152/ajpgi.1997.272.5.G1209
- Karam, S. M., Tomasetto, C., & Rio, M. C. (2004). Trefoil factor 1 is required for the commitment programme of mouse oxyntic epithelial progenitors. *Gut*, 53(10), 1408-1415. doi:10.1136/gut.2003.031963
- Kelm, J. M., Timmins, N. E., Brown, C. J., Fussenegger, M., & Nielsen, L. K. (2003). Method for generation of homogeneous multicellular tumor spheroids applicable to a wide variety of cell types. *Biotechnol. Bioeng.*, 83(2), 173-180. doi:10.1002/bit.10655

- Khurana, S., Riehl, T., Moore, B., Fassan, M., Rugge, M., Romero-Gallo, J., Mills, J. et al. (2013). The Hyaluronic Acid Receptor CD44 Coordinates Normal and Metaplastic Gastric Epithelial Progenitor Cell Proliferation. *The Journal of Biological Chemistry*, 288(22), 16085–16097. doi:10.1074/jbc.M112.445551
- Kim, D., & Dressler, G. R. (2005). Nephrogenic factors promote differentiation of mouse embryonic stem cells into renal epithelia. *J Am Soc Nephrol*, 16(12), 3527-3534. doi:10.1681/asn.2005050544
- Kleinman, H. K., & Martin, G. R. (2005). Matrigel: basement membrane matrix with biological activity. *Semin. Cancer Biol.*, 15(5), 378-386. doi:10.1016/j.semcancer.2005.05.004
- Kolluri, S. K., Jin, U. H., & Safe, S. (2017). Role of the aryl hydrocarbon receptor in carcinogenesis and potential as an anti-cancer drug target. *Arch. Toxicol.*, 91(7), 2497-2513. doi:10.1007/s00204-017-1981-2
- Laurie A. B., Tong I. L., Megan F. C., Sarah E. J., Stuart S. L., Jacob P. Z., Richard A. Y. et al. (2005). Core Transcriptional Regulatory Circuitry in Human Embryonic Stem Cells. *Cell*, 122(6), 947-956. doi:10.1016/j.cell.2005.08.020
- Lancaster, M. A., & Knoblich, J. A. (2014). Organogenesis in a dish: modeling development and disease using organoid technologies. *Science*, 345(6194), 1247125. doi:10.1126/science.1247125
- Lancaster, M. A., Renner, M., Martin, C. A., Wenzel, D., Bicknell, L. S., Hurles, M. E., Knoblich, J. A. et al. (2013). Cerebral organoids model human brain development and microcephaly. *Nature*, 501(7467), 373-379. doi:10.1038/nature12517
- Lefebvre, O., Wolf, C., Kédinger, M., MPChenard, Tomasetto, C., Chambon, P., & Rio, M. (1993). The Mouse One P-domain (pS2) and Two P-domain (mSP) Genes Exhibit Distinct Patterns of Expression. *The Journal of Cell Biology*, 122(1), 191-198. doi:10.1083/jcb.122.1.191
- Li, M. L., Aggeler, J., Farson, D. A., Hatier, C., Hassell, J., & Bissell, M. J. (1987). Influence of a reconstituted basement membrane and its components on casein gene expression and secretion in mouse mammary epithelial cells. *Proc. Natl. Acad. Sci. USA*, 84(1), 136-140. doi:10.1073/pnas.84.1.136
- Li, Q., Jia, Z., Wang, L., Kong, X., Guo, K., Tan, D., Xie, K. et al. (2012). Disruption of Klf4 in villin-positive gastric progenitor cells promotes formation and progression of tumors of the antrum in mice. *Gastroenterology*, 142(3), 531-542. doi:10.1053/j.gastro.2011.11.034
- Li, Q., Karam, S. M., & Gordon, J. I. (1995). Simian virus 40 T antigen-induced amplification of pre-parietal cells in transgenic mice. Effects on other gastric

epithelial cell lineages and evidence for a p53-independent apoptotic mechanism that operates in a committed progenitor. *J. Biol. Chem.*, 270(26), 15777-15788. doi: 10.1074/jbc.270.26.15777

- Li, Q., Karam, S. M., & Gordon, J. I. (1996). Diphtheria toxin-mediated ablation of parietal cells in the stomach of transgenic mice. *J. Biol. Chem.*, 271(7), 3671-3676. Retrieved from: <https://pubmed.ncbi.nlm.nih.gov/8631979/>
- Lin, R. Z., & Chang, H. Y. (2008). Recent advances in three-dimensional multicellular spheroid culture for biomedical research. *Biotechnol. J.*, 3(9-10), 1172-1184. doi:10.1002/biot.200700228
- Matsuo, J., Shunichi, K., Akihiro, Y., Cai P. K., Zakir M. H., Dede L. H., et al. (2017). Identification of Stem Cells in the Epithelium of the Stomach Corpus and Antrum of Mice. *Gastroenterology*, 152(1), 218-231. doi:10.1053/j.gastro.2016.09.018
- McCracken, K. W., Aihara, E., Martin, B., Crawford, C. M., Broda, T., Treguier, J., et al. Wells, J. M. (2017). Wnt/beta-catenin promotes gastric fundus specification in mice and humans. *Nature*, 541(7636), 182-187. doi:10.1038/nature21021
- McCracken, K. W., Cata, E. M., Crawford, C. M., Sinagoga, K. L., Schumacher, M., Rockich, B. E., Wells, J. M. et al. (2014). Modelling human development and disease in pluripotent stem-cell-derived gastric organoids. *Nature*, 516(7531), 400-404. doi:10.1038/nature13863
- Metidji, A., Omenetti, S., Crotta, S., Li, Y., Nye, E., Ross, E., Stockinger, B. et al. (2018). The Environmental Sensor AHR Protects from Inflammatory Damage by Maintaining Intestinal Stem Cell Homeostasis and Barrier Integrity. In *Immunity*, 49(353-362 e355). 353-362. doi: 10.1016/j.immuni.2018.07.010
- Mills, J. C., Syder, A. J., Hong, C. V., Guruge, J. L., Raaii, F., & Gordon, J. I. (2001). A molecular profile of the mouse gastric parietal cell with and without exposure to *Helicobacter pylori*. *Proc. Natl. Acad. Sci. USA*, 98(24), 13687-13692. doi:10.1073/pnas.231332398
- Mizuno, T., & Ishizuya, A. (1982). Electron microscopic study of in vitro differentiation of the small intestinal endoderm in young bird embryo in the presence or absence of mesenchyme. *C. R. Seances Soc. Biol. Fil.*, 176(4), 580-584. Retrieved from: <https://pubmed.ncbi.nlm.nih.gov/6217880/>
- Modlin, I. M., Kidd, M., Latich, I., Zikusoka, M. N., & Shapiro, M. D. (2005). Current status of gastrointestinal carcinoids. *Gastroenterology*, 128(6), 1717-1751. doi:10.1053/j.gastro.2005.03.038
- Moscona, A. A. (1959). Tissues from dissociated cells. *Sci. Am.*, 200(5), 132-134 Retrieved from: www.jstor.org/stable/24940306

- Murray, I. A., Patterson, A. D., & Perdew, G. H. (2014). Aryl hydrocarbon receptor ligands in cancer: friend and foe. *Nat. Rev. Cancer*, *14*(12), 801-814. doi:10.1038/nrc3846
- Murray, I. A., & Perdew, G. H. (2017). Ligand activation of the Ah receptor contributes to gastrointestinal homeostasis. *Curr. Opin. Toxicol.*, *2*, 15-23. doi:10.1016/j.cotox.2017.01.003
- Nebert, D. W. (2017). Aryl hydrocarbon receptor (AHR): "pioneer member" of the basic-helix/loop/helix per-Arnt-sim (bHLH/PAS) family of "sensors" of foreign and endogenous signals. *Prog. Lipid. Res.*, *67*, 38-57. doi:10.1016/j.plipres.2017.06.001
- Nilsson, J., Vallbo, C., Guo, D., Golovleva, I., Hallberg, B., RHenriksson, & Hedman, H. (2001). Cloning, Characterization, and Expression of Human LIG1. *Biochemical and Biophysical Research Communications*, *284*(5), 1155-1161. doi:10.1006/bbrc.2001.5092
- Nomura, A., Stemmermann, G. N., Chyou, P. H., Kato, I., Perez-Perez, G. I., & Blaser, M. J. (1991). Helicobacter pylori infection and gastric carcinoma among Japanese Americans in Hawaii. *N. Engl. J. Med.*, *325*(16), 1132-1136. doi:10.1056/nejm199110173251604
- Nomura, S., Settle, S. H., Leys, C. M., Means, A. L., Peek, R. M., Jr., Leach, S. D., Goldenring, J. R. et al. (2005). Evidence for repatterning of the gastric fundic epithelium associated with Menetrier's disease and TGFalpha overexpression. *Gastroenterology*, *128*(5), 1292-1305. doi:10.1053/j.gastro.2005.03.019
- Oh, J. D., Karam, S. M., & Gordon, J. I. (2005). Intracellular Helicobacter pylori in gastric epithelial progenitors. *Proc. Natl. Acad. Sci. USA*, *102*(14), 5186-5191. doi:10.1073/pnas.0407657102
- Okamoto, H, O., A, O., M, S., M, M., & H, H. (1990). A novel octamer binding transcription factor is differentially expressed in mouse embryonic cells. *Cell*, *60*(3), 461-472. doi:10.1016/0092-8674(90)90597-8
- Panteleyev, A. A., & Bickers, D. R. (2006). Dioxin-induced chloracne--reconstructing the cellular and molecular mechanisms of a classic environmental disease. *Exp. Dermatol.*, *15*(9), 705-730. doi:10.1111/j.1600-0625.2006.00476.x
- Parsonnet, J., Friedman, G. D., Vandersteen, D. P., Chang, Y., Vogelman, J. H., Orentreich, N., & Sibley, R. K. (1991). Helicobacter pylori infection and the risk of gastric carcinoma. *N. Engl. J. Med.*, *325*(16), 1127-1131. doi:10.1056/nejm199110173251603

- Pinto, D., Gregorieff, A., Begthel, H., & Clevers, H. (2003). Canonical Wnt signals are essential for homeostasis of the intestinal epithelium. *Genes Dev.*, *17*(14), 1709-1713. doi:10.1101/gad.267103
- Poland, A., Glover, E., & Kende, AS. (1976). Stereospecific, high affinity binding of 2,3,7,8-tetrachlorodibenzo-p-dioxin by hepatic cytosol. Evidence that the binding species is receptor for induction of aryl hydrocarbon hydroxylase. *J. Biol. Chem.* *251*(16), 4936-46. Retrieved from: <https://pubmed.ncbi.nlm.nih.gov/956169/>
- Powell, A. E., Wang, Y., Li, Y., Poulin, E. J., Means, A. L., Washington, M. K., Coffey, R. J. et al. (2012). The pan-ErbB negative regulator Lrig1 is an intestinal stem cell marker that functions as a tumor suppressor. *Cell*, *149*(1), 146-158. doi:10.1016/j.cell.2012.02.042
- Puga, A., Xia, Y., & Elferink, C. (2002). Role of the aryl hydrocarbon receptor in cell cycle regulation. *Chem. Biol. Interact.*, *141*(1-2), 117-130. doi: 10.1016/s0009-2797(02)00069-8
- Pulikkot, S., Greish, Y., Mourad, A., & Karam, S. (2014). Establishment of a Three-Dimensional Culture System of Gastric Stem Cells Supporting Mucous Cell Differentiation Using Microfibrous Polycaprolactone Scaffolds. *Cell Proliferation*, *47*(6). doi:10.1111/cpr.12141
- Qiao, X. T., Ziel, J. W., McKimpton, W., Madison, B. B., Todisco, A., Merchant, J. L., Gumucio, D. L. et al. (2007). Prospective identification of a multilineage progenitor in murine stomach epithelium. *Gastroenterology*, *133*(6), 1989-1998. doi:10.1053/j.gastro.2007.09.031
- Que, J., Okubo, T., Goldenring, J. R., Nam, K. T., Kurotani, R., Morrisey, E. E., Hogan, B. L. et al. (2007). Multiple dose-dependent roles for Sox2 in the patterning and differentiation of anterior foregut endoderm. *Development*, *134*(13), 2521-2531. doi:10.1242/dev.003855
- Quintana, F. J., & Sherr, D. H. (2013). Aryl hydrocarbon receptor control of adaptive immunity. *Pharmacol. Rev.*, *65*(4), 1148-1161. doi:10.1124/pr.113.007823
- Ramsey, V. G., Doherty, J. M., Chen, C. C., Stappenbeck, T. S., Konieczny, S. F., & Mills, J. C. (2007). The maturation of mucus-secreting gastric epithelial progenitors into digestive-enzyme secreting zymogenic cells requires Mist1. *Development*, *134*(1), 211-222. doi:10.1242/dev.02700
- Richmond, O., MGHothbaddini, Allen, C., Walker, A., Zahir, S., & Powell, J. (2014). The aryl hydrocarbon receptor is constitutively active in advanced prostate cancer cells. *PloS one*, *9*(4), e95058. doi:10.1371/journal.pone.0095058

- Rizzino. (2009). Sox2 and Oct-3/4: A versatile pair of master regulators that orchestrate the self-renewal and pluripotency of embryonic stem cells. *Wiley Interdisciplinary Reviews. Systems Biology and Medicine*, 1(2), 228-236. doi:10.1002/wsbm.12
- Ronnekleiv-Kelly, S. M., Nukaya, M., Diaz-Diaz, C. J., Megna, B. W., Carney, P. R., Geiger, P. G., & Kennedy, G. D. (2016). Aryl hydrocarbon receptor-dependent apoptotic cell death induced by the flavonoid chrysin in human colorectal cancer cells. *Cancer Lett.*, 370(1), 91-99. doi:10.1016/j.canlet.2015.10.014
- Rosner, Vigano, K. et al. (1990). A pou-domain transcription factor in early stem cells and germ cells of the mammalian embryo. *Nature*, 345(6277), 686-692. doi:10.1038/345686a0
- Saito, R., Miki, Y., Hata, S., Takagi, K., Iida, S., Oba, Y., Sasano, H. et al. (2014). Aryl hydrocarbon receptor in breast cancer—a newly defined prognostic marker. *Hormones & Cancer*, 5(1), 11-21. doi:10.1007/s12672-013-0160-z
- Sato, A., & Spicer, S. S. (1980). Ultrastructural cytochemistry of complex carbohydrates of gastric epithelium in the guinea pig. *Am. J. Anat.*, 159(3), 307-329. doi:10.1002/aja.1001590306
- Sato, T., & Clevers, H. (2013). Growing self-organizing mini-guts from a single intestinal stem cell: mechanism and applications. *Science*, 340(6137), 1190-1194. doi:10.1126/science.1234852
- Sato, T., Stange, D. E., Ferrante, M., Vries, R. G., Van Es, J. H., Van den Brink, S., Clevers, H. et al. (2011). Long-term expansion of epithelial organoids from human colon, adenoma, adenocarcinoma, and Barrett's epithelium. *Gastroenterology*, 141(5), 1762-1772. doi:10.1053/j.gastro.2011.07.050
- Sato, T., van Es, J. H., Snippert, H. J., Stange, D. E., Vries, R. G., van den Born, M., Clevers, H. (2011). Paneth cells constitute the niche for Lgr5 stem cells in intestinal crypts. *Nature*, 469(7330), 415-418. doi:10.1038/nature09637
- Sato, T., Vries, R. G., Snippert, H. J., van de Wetering, M., Barker, N., Stange, D. E., Clevers, H. et al. (2009). Single Lgr5 stem cells build crypt-villus structures in vitro without a mesenchymal niche. *Nature*, 459(7244), 262-265. doi:10.1038/nature07935
- Schumacher, M. A., Aihara, E., Feng, R., Engevik, A., Shroyer, N. F., Ottemann, K. M., Zavros, Y. et al. (2015). The use of murine-derived fundic organoids in studies of gastric physiology. *J. Physiol.*, 593(8), 1809-1827. doi:10.1113/jphysiol.2014.283028
- Schweiger, P. J., Clement, D. L., Page, M. E., Schepeler, T., Zou, X., Sirokmany, G., Jensen, K. B. et al. (2018). Lrig1 marks a population of gastric epithelial cells

- capable of long-term tissue maintenance and growth in vitro. *Sci. Rep.*, 8(1), 15255. doi:10.1038/s41598-018-33578-6
- Schöler, H. R., Rupper, t. S., Suzuki, N., Chowdhury, K., & Gruss, P. (1990). New type of pou domain in germ line-specific protein oct-4. *Nature*, 344(6265), 435-439. doi:10.1038/344435a0
- Shinohara, M., Mao, M., Keeley, T. M., El-Zaatari, M., Lee, H. J., Eaton, K. A., Todisco, A. et al. (2010). Bone morphogenetic protein signaling regulates gastric epithelial cell development and proliferation in mice. *Gastroenterology*, 139(6), 2050-2060. doi:10.1053/j.gastro.2010.08.2052
- Singh, K. P., Casado, F. L., Opanashuk, L. A., & Gasiewicz, T. A. (2009). The aryl hydrocarbon receptor has a normal function in the regulation of hematopoietic and other stem/progenitor cell populations. *Biochem. Pharmacol.*, 77(4), 577-587. doi:10.1016/j.bcp.2008.10.001
- Spence, J. R., Mayhew, C. N., Rankin, S. A., Kuhar, M. F., Vallance, J. E., Tolle, K., Wells, J. M. et al. (2011). Directed differentiation of human pluripotent stem cells into intestinal tissue in vitro. *Nature*, 470(7332), 105-109. doi:10.1038/nature09691
- Spring, F. A., Dalchau, R., Daniels, G. L., Mallinson, G., Judson, P. A., Parsons, S. F., Anstee, D. J. et al. (1988). The Ina and Inb blood group antigens are located on a glycoprotein of 80,000 MW (the CDw44 glycoprotein) whose expression is influenced by the In(Lu) gene. *Immunology*, 64(1), 37-43. Retrieved from: <https://www.ncbi.nlm.nih.gov/pmc/articles/PMC1385183/>
- Stange, D. E., Koo, B. K., Huch, M., Sibbel, G., Basak, O., Lyubimova, A., Clevers, H. et al. (2013). Differentiated Troy+ chief cells act as reserve stem cells to generate all lineages of the stomach epithelium. *Cell*, 155(2), 357-368. doi:10.1016/j.cell.2013.09.008
- Stepan, V., Ramamoorthy, S., Nitsche, H., Zavros, Y., Merchant, J. L., & Todisco, A. (2005). Regulation and function of the sonic hedgehog signal transduction pathway in isolated gastric parietal cells. *J. Biol. Chem.*, 280(16), 15700-15708. doi:10.1074/jbc.M413037200
- Stockinger, B., Di Meglio, P., Gialitakis, M., & Duarte, J. H. (2014). The aryl hydrocarbon receptor: multitasking in the immune system. *Annu. Rev. Immunol.*, 32, 403-432. doi:10.1146/annurev-immunol-032713-120245
- Strangeways, T. S. P., & Honor, B. F. (1926). Experimental Studies on the Differentiation of Embryonic Tissues Growing in vivo and in vitro.--II. The Development of the Isolated Early Embryonic Eye of the Fowl when

Cultivated in vitro. *Containing Papers of a Biological Character*, 100(703) 273-283. doi:10.1098/rspb.1926.0049

- Su, J., Lin, P., & Chang, H. (2013). Prognostic Value of Nuclear Translocation of Aryl Hydrocarbon Receptor for Non-Small Cell Lung Cancer. *Anticancer Research*, 33(9). Retrieved from: <http://ar.iiarjournals.org/content/33/9/3953.full.Pdf+html>
- Suga, H., Kadoshima, T., Minaguchi, M., Ohgushi, M., Soen, M., Nakano, T., Sasai, Y. et al. (2011). Self-formation of functional adenohypophysis in three-dimensional culture. *Nature*, 480(7375), 57-62. doi:10.1038/nature10637
- Syder, A. J., Guruge, J. L., Li, Q., Hu, Y., Oleksiewicz, C. M., Lorenz, R. G., Gordon, J. I. et al. (1999). Helicobacter pylori attaches to NeuAc alpha 2,3Gal beta 1,4 glycoconjugates produced in the stomach of transgenic mice lacking parietal cells. *Mol. Cell*, 3(3), 263-274. doi: 10.1016/s1097-2765(00)80454-2
- Syder, A. J., Karam, S. M., Mills, J. C., Ippolito, J. E., Ansari, H. R., Farook, V., & Gordon, J. I. (2004). A transgenic mouse model of metastatic carcinoma involving transdifferentiation of a gastric epithelial lineage progenitor to a neuroendocrine phenotype. *Proc. Natl. Acad. Sci. USA*, 101(13), 4471-4476. doi:10.1073/pnas.0307983101
- Tai, M.-H., Chang, C.-C., Kiupel, M., Webster, J. D., Olson, L. K., & Trosko. (2005). Oct-4 expression in adult human stem cells: evidence in support of the stem cell theory of carcinogenesis. *Carcinogenesis*, 26(2), 495-502. doi:10.1093/carcin/bgh321
- Takaishi, S., Okumura, T., Tu, S., Wang, S., Shibata, W., Vigneshwaran, R., Wang, T. et al. (2009). Identification of Gastric Cancer Stem Cells Using the Cell Surface Marker CD44. *Stem cells (Dayton, Ohio)*, 27(5). doi:10.1002/stem.30
- Takebe, T., Sekine, K., Enomura, M., Koike, H., Kimura, M., Ogaeri, T., Taniguchi, H. et al. (2013). Vascularized and functional human liver from an iPSC-derived organ bud transplant. *Nature*, 499(7459), 481-484. doi:10.1038/nature12271
- Tauchi, M., Hida, A., Negishi, T., Katsuoka, F., Noda, S., Mimura, J., Yamamoto, M. et al. (2005). Constitutive expression of aryl hydrocarbon receptor in keratinocytes causes inflammatory skin lesions. *Mol. Cell. Biol.*, 25(21), 9360-9368. doi:10.1128/mcb.25.21.9360-9368.2005
- Tian, X., Jin, R. U., Bredemeyer, A. J., Oates, E. J., Blazewska, K. M., McKenna, C. E., & Mills, J. C. (2010). RAB26 and RAB3D are direct transcriptional targets of MIST1 that regulate exocrine granule maturation. *Mol. Cell Biol.*, 30(5), 1269-1284. doi:10.1128/mcb.01328-09

- Timpl, R., Rohde, H., Robey, P. G., Rennard, S. I., Foidart, J. M., & Martin, G. R. (1979). Laminin--a glycoprotein from basement membranes. *J. Biol. Chem.*, 254(19), 9933-9937. Retrieved from: <https://pubmed.ncbi.nlm.nih.gov/114518/>
- Tompkins, L. M., Li, H., Li, L., Lynch, C., Xie, Y., Nakanishi, T., Wang, H. et al. (2010). A novel xenobiotic responsive element regulated by aryl hydrocarbon receptor is involved in the induction of BCRP/ABCG2 in LS174T cells. *Biochem. Pharmacol.*, 80(11), 1754-1761. doi:10.1016/j.bcp.2010.08.016
- Tongtawee, T., Wattanawongdon, W., Simawaranon, T., Kaewpitoon, S., Kaengpenkae, S., Jintabanditwong, N., Panpimanmas, S. et al. (2017). Expression of Cancer Stem Cell Marker CD44 and Its Polymorphisms in Patients with Chronic Gastritis, Precancerous Gastric Lesion, and Gastric Cancer: A Cross-Sectional Multicenter Study in Thailand. *Biomed. Res. Int.*, 2017, 4384823. doi:10.1155/2017/4384823
- Vaidya, M., Bacchus, M., & Sugaya, K. (2018). Differential sequences of exosomal nanog dna as a potential diagnostic cancer marker. *PloS one*, 13(5), e0197782 . Accessed on, 20th march 2019. doi:10.1371/journal.pone.0197782
- Villard, P. H., Caverni, S., Baanannou, A., Khalil, A., Martin, P. G., Penel, C., Barra, Y. et al. (2007). PPARalpha transcriptionally induces AhR expression in Caco-2, but represses AhR pro-inflammatory effects. *Biochem. Biophys. Res. Commun.*, 364(4), 896-901. doi:10.1016/j.bbrc.2007.10.084
- Wang, T. C., Koh, T. J., Varro, A., Cahill, R. J., Dangler, C. A., Fox, J. G., & Dockray, G. J. (1996). Processing and proliferative effects of human progastrin in transgenic mice. *J. Clin. Invest.*, 98(8), 1918-1929. doi:10.1172/jci118993
- Watanabe, K., Kamiya, D., Nishiyama, A., Katayama, T., Nozaki, S., Kawasaki, H., Sasai, Y. et al. (2005). Directed differentiation of telencephalic precursors from embryonic stem cells. *Nat. Neurosci.*, 8(3), 288-296. doi:10.1038/nn1402
- Williamson, M. A., Gasiewicz, T. A., & Opanashuk, L. A. (2005). Aryl hydrocarbon receptor expression and activity in cerebellar granule neuroblasts: implications for development and dioxin neurotoxicity. *Toxicol. Sci.*, 83(2), 340-348. doi:10.1093/toxsci/kfi031
- Xie, G., Peng, Z., & Raufman, J. P. (2012). Src-mediated aryl hydrocarbon and epidermal growth factor receptor cross talk stimulates colon cancer cell proliferation. *Am. J. Physiol. Gastrointest. Liver Physiol.*, 302(9), G1006-1015. doi:10.1152/ajpgi.00427.2011
- Yi, T., Wang, J., Zhu, K., Tang, Y., Huang, S., Shui, X. et al. Lei, W. (2018). Aryl Hydrocarbon Receptor: A New Player of Pathogenesis and Therapy in

Cardiovascular Diseases. *Biomed. Res. Int.*, 2018, 6058784.
doi:10.1155/2018/6058784

- Yin, X., Mead, B. E., Safaei, H., Langer, R., Karp, J. M., & Levy, O. (2016). Engineering Stem Cell Organoids. *Cell Stem Cell*, 18(1), 25-38. doi:10.1016/j.stem.2015.12.005
- Zavros, Y., Eaton, K. A., Kang, W., Rathinavelu, S., Katukuri, V., Kao, J. Y., Merchant, J. L. et al. (2005). Chronic gastritis in the hypochlorhydric gastrin-deficient mouse progresses to adenocarcinoma. *Oncogene*, 24(14), 2354-2366. doi:10.1038/sj.onc.1208407
- Zhu, L., Gibson, P., Currle, D. S., Tong, Y., Richardson, R. J., Bayazitov, I. T., Gilbertson, R. J. et al. (2009). Prominin 1 marks intestinal stem cells that are susceptible to neoplastic transformation. *Nature*, 457(7229), 603-607. doi:10.1038/nature07589
- Zhu, R., Gao, C., Wang, L., Zhang, G., Zhang, W., Zhang, Z., Wang, S. et al. (2018). Involvement of aryl hydrocarbon receptor and aryl hydrocarbon receptor repressor in helicobacter pylori-related gastric pathogenesis. *J. Cancer*, 9(15), 2757-2764. doi:10.7150/jca.26083